2021 Spring

"Phase Equilibria *in* Materials"

03.23.2021

Eun Soo Park

Office: 33-313
Telephone: 880-7221
Email: espark@snu.ac.kr
Office hours: by an appointment

Equilibrium in Heterogeneous Systems

In X^0, $G_0^{\beta} > G_0^{\alpha} > G_1$ ⇒ α + β separation ⇒ unified chemical potential

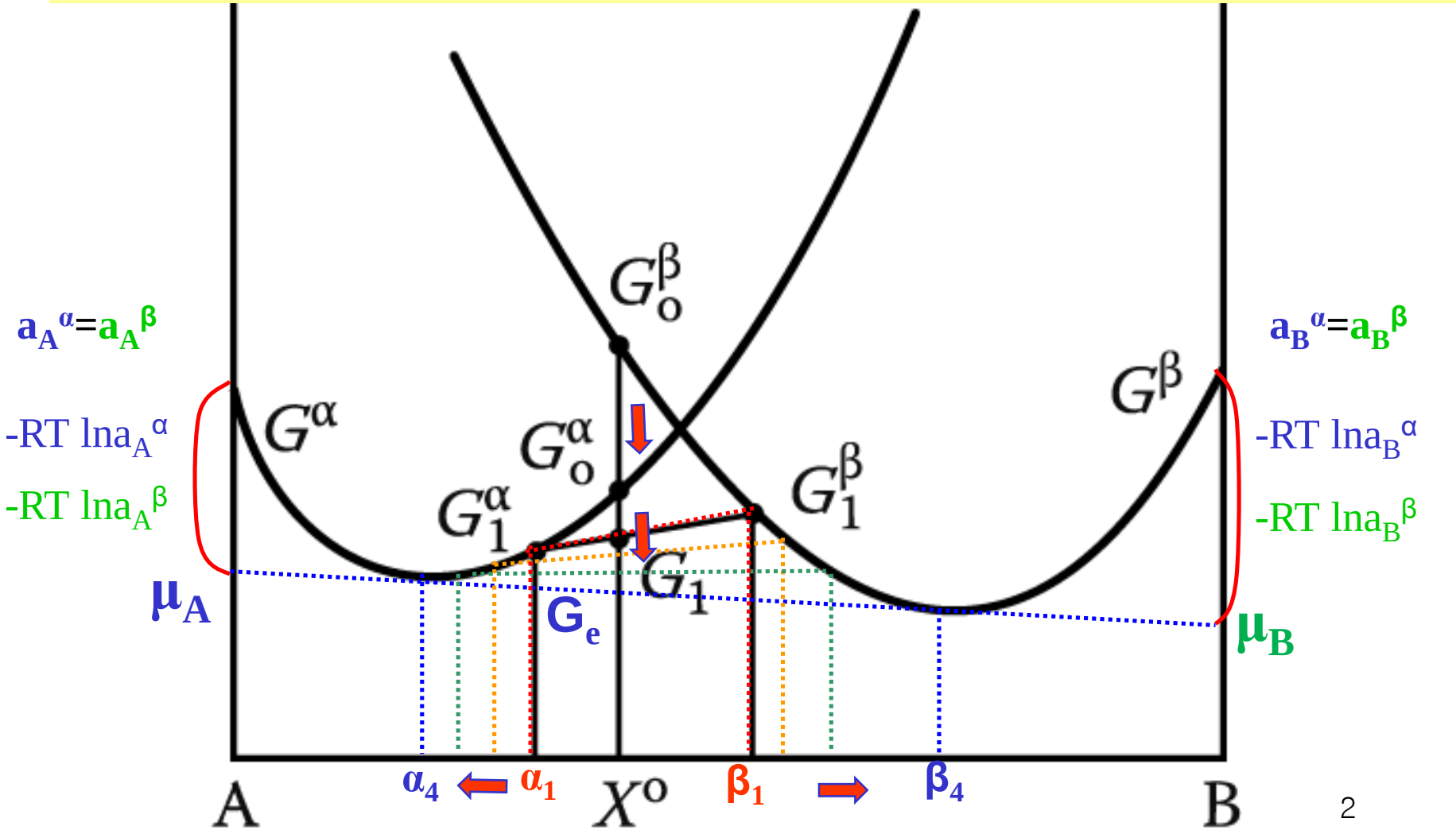

- Two-Phase Equilibrium

1) Simple Phase Diagrams

Assumption: (1) completely miscible in solid and liquid.

(2) Both are ideal soln.

(3) T_m(A) > T_m(B)

$$\Delta H^{L}_{mix} = 0 \quad \Delta H^{S}_{mix} = 0$$

Since $S^s \neq S^l$, then $dT/dX_A = 0$. Thus the condition $X^s_A = X^l_A$ is only associated with $dT/dX_A = 0$, *i.e.* with a minimum or a maximum in the line $T_A T_B$ of Fig. 22. Except for this particular case therefore $X^s_A \neq X^l_A$. There is a difference between the composition of the liquid and solid phase in the general case.

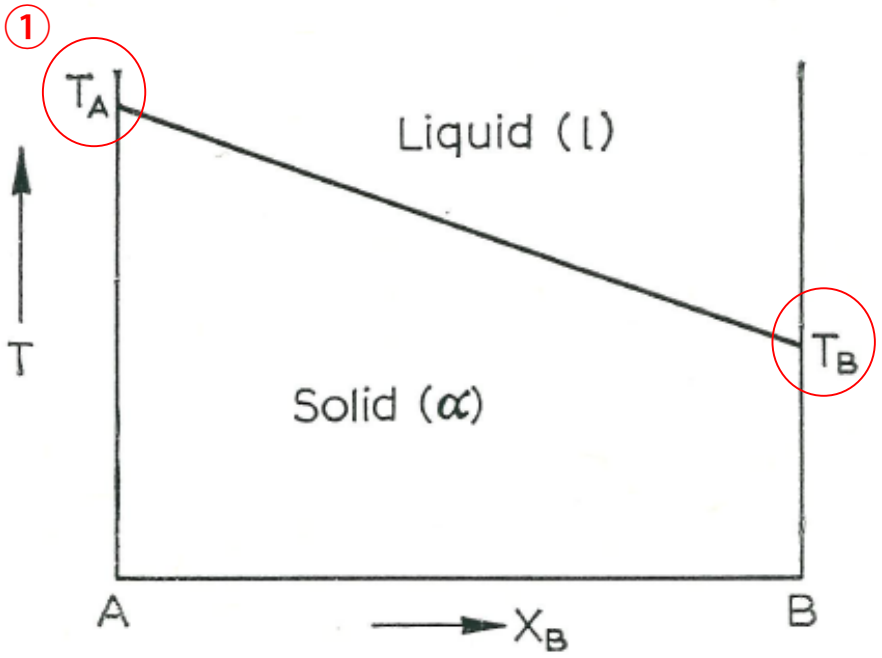

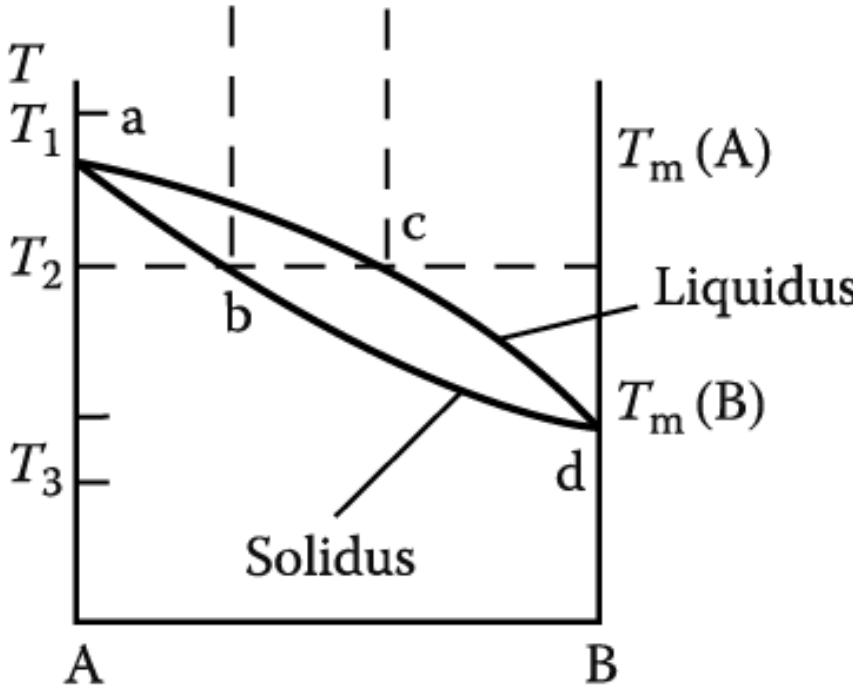

*** Consider the free energy curves for liquid and α phase at a temperature T, where $T_A > T > T_B$. The standard states are pure *solid* A and pure *liquid* B at temperature T. → Derive the free energy curves for the liquid and α phases.**

② X-T relationship in A-rich and B-rich compositions

As the temperature approaches T_A the quantities X_A^s and X_A^l will approach unity, and $1/T$ will approach $1/T_A$.

Hence near T_A:

$$\ln \frac{X_B^s}{X_B^l} = \frac{\Delta H_B}{R}\left(\frac{1}{T} - \frac{1}{T_B}\right). \qquad (103)$$

X-T relationship in A-rich composition

Similarly, if the temperature approaches T_B, $X_B^s \simeq X_B^l \to 1$ and $1/T \to 1/T_B$. Near T_B:

$$\ln \frac{X_A^s}{X_A^l} = \frac{\Delta H_A}{R}\left(\frac{1}{T} - \frac{1}{T_A}\right). \qquad (104)$$

X-T relationship in B-rich composition

Knowing ΔH_A, ΔH_B, T_A and T_B, the above two equations can be used to determine the compositions of co-existing phases at a series of temperatures, T, between T_A and T_B. → **Fig. 23*f***

Referring to Fig. 23f, if A is regarded as the solvent, for very dilute solutions of B in A we can write

$$X_A \to 1 \quad \text{and} \quad -\ln X_A \simeq X_B.$$

In terms of eqn. (104):

$$X_A^l - X_A^s = \frac{\Delta H_A}{R}\left(\frac{T_A - T}{T T_A}\right).$$

Since $X_A^l = 1 - X_B^l$ and $X_A^s = 1 - X_B^s$

$$X_B^s - X_B^l = \frac{\Delta H_A}{R}\left(\frac{T_A - T}{T T_A}\right). \tag{105}$$

As T approaches T_A (in dilute solutions of B in solvent A), the denominator on the right-hand side of eqn. (105) can be written RT_A^2. Therefore

$$X_B^s - X_B^l = \frac{\Delta H_A}{R T_A^2}(T_A - T) \tag{106}$$

or,

③ ΔH effect for G curvature
: initial slope of solidus and liquidus curve

$$\left(\frac{dX_B^s}{dT} - \frac{dX_B^l}{dT}\right)_{T=T_A} = \frac{\Delta H_A}{R T_A^2}. \tag{107}$$

Equations (106) and (107) are referred to as the Van't Hoff relation. They give the depression of the freezing point for a liquid solution in equilibrium with a solid solution. The difference in initial slopes of the solidus and liquidus curves, the slopes at $T = T_A$ and $X_A = 1$, are dependent on the latent heat of fusion of pure A (ΔH_A) but independent of the nature of the solute.

* Consider actual (or so-called regular) solutions

in which $\Delta H_m \neq 0$, but $\Delta S_m = \Delta S_{m,\text{ideal}}$

$$\Delta G_m^l = \Delta H_m^l + X_A^l \Delta G_A + RT(X_A^l \ln X_A^l + X_B^l \ln X_B^l).$$

Since

$$\Delta G_A = \Delta H_A - T\Delta S_A$$

then,

$$\Delta G_m^l = \Delta H_m^l + X_A^l \Delta H_A - X_A^l T\Delta S_A + RT(X_A^l \ln X_A^l + X_B^l \ln X_B^l).$$

The free energy curve for the solid phase is:

$$\Delta G_m^s = \Delta H_m^s - X_B^s \Delta G_B + RT(X_A^s \ln X_A^s + X_B^s \ln X_B^s)$$

or,

$$\Delta G_m^s = \Delta H_m^s - X_B^s \Delta H_B + X_B^s T\Delta S_B + RT(X_A^s \ln X_A^s + X_B^s \ln X_B^s).$$

④ Temperature effect for G variation
: role of **ΔS**

1) Simple Phase Diagrams

a) Variation of temp.: $G^L > G^s$

b) T ↓ → Decrease of curvature of G curve

(∵ decrease of $-T\Delta S_{mix}$ effect)

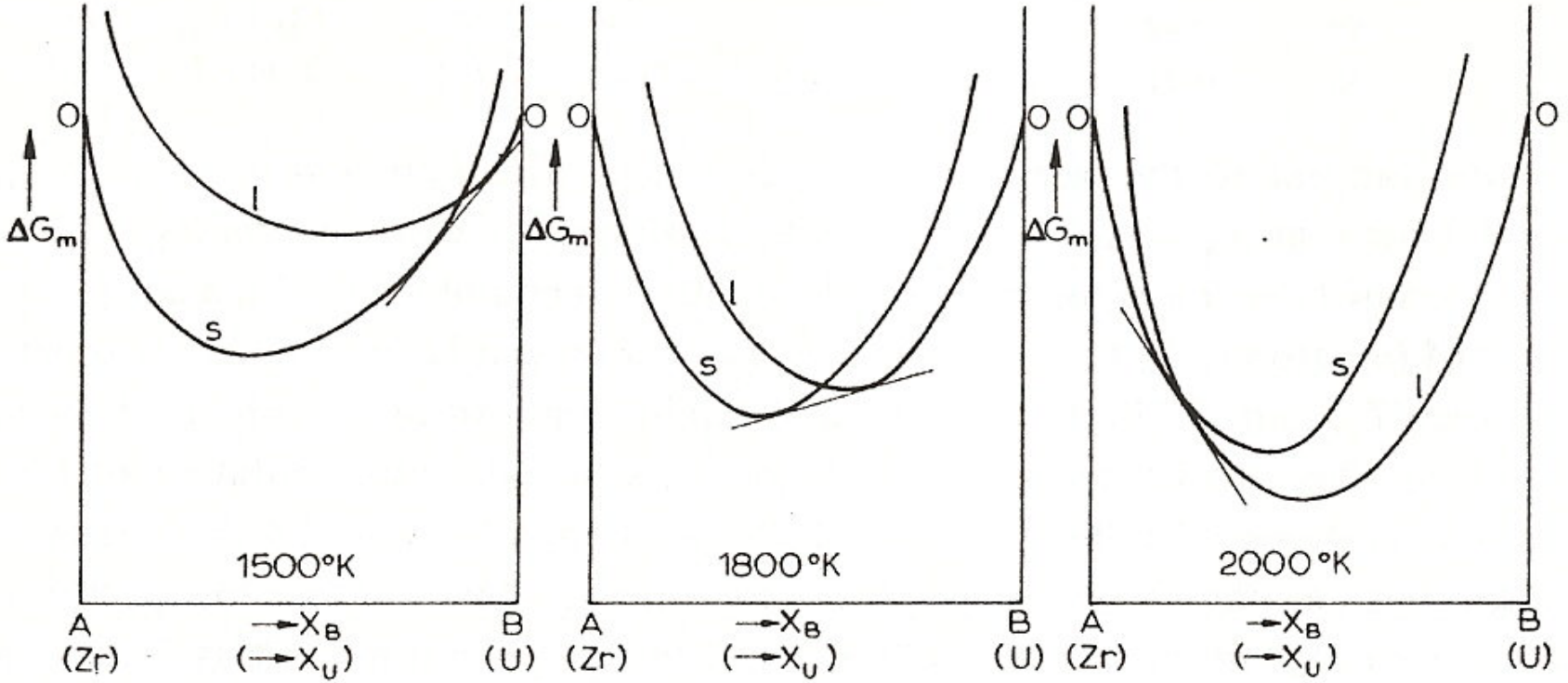

Fig. 26. Free energy curves for liquid and solid phases in the U–Zr system at 1500°, 1800° and 2000 °K.

It was assumed that $\Delta H_m^l = \Delta H_m^s$

1.5 Binary phase diagrams

1) Simple Phase Diagrams

Assumption:

(1) completely miscible in solid and liquid.

(2) Both are ideal soln.

(3) $T_m(A) > T_m(B)$

(4) $T_1 > T_m(A) > T_2 > T_m(B) > T_3$

a) Variation of temp.: $G^L > G^s$

b) T ↓ → Decrease of curvature of G curve

(∵ decrease of $-T\Delta S_{mix}$ effect)

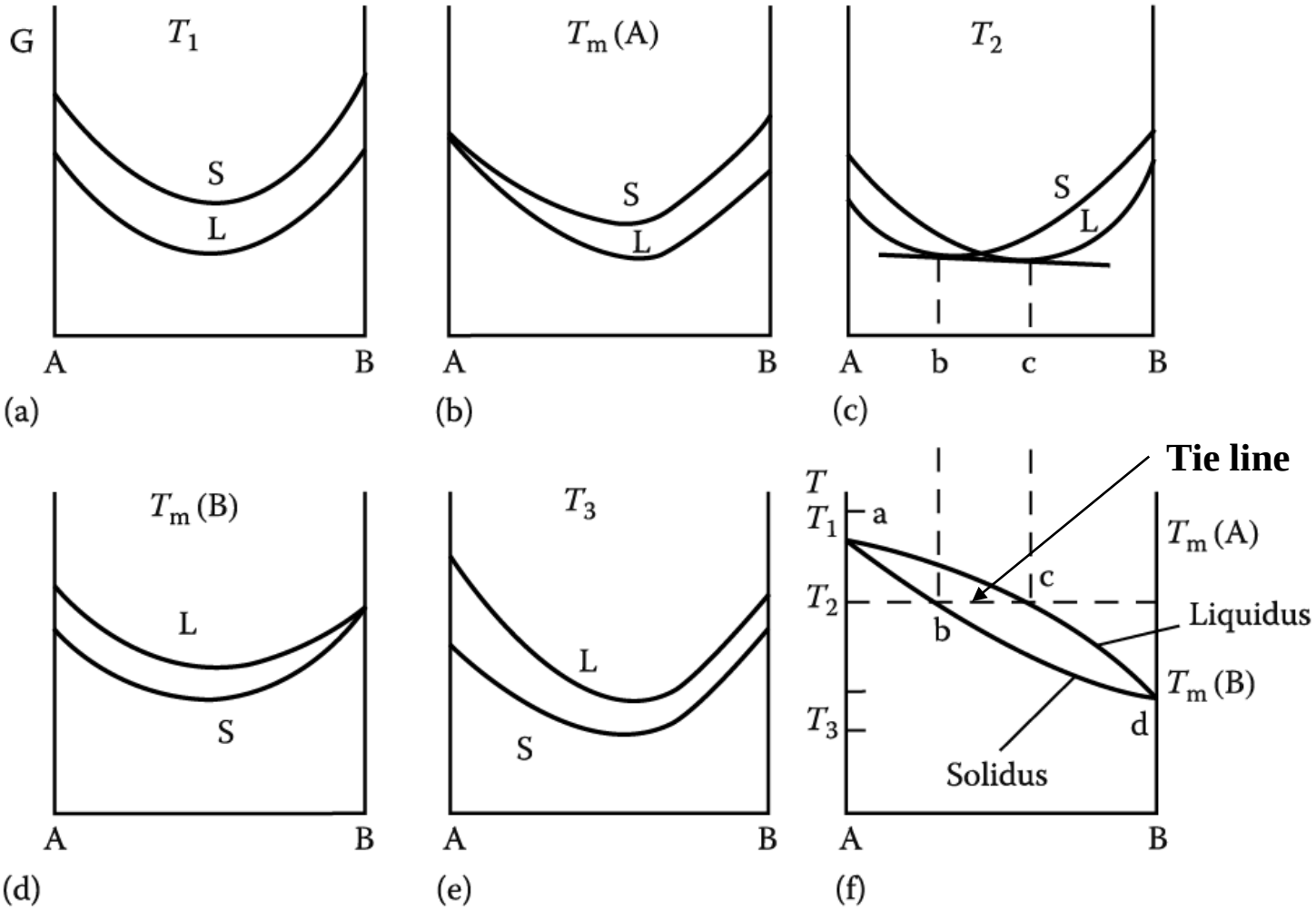

Contents for previous class

- Equilibrium in Heterogeneous Systems

$G_0^{\beta} > G_0^{\alpha} > G_0^{\alpha+\beta}$ ⇒ α + β separation ⇒ unified chemical potential

- Binary phase diagrams

1) Simple Phase Diagrams

$\Delta H_{mix}^{L} = 0 \; \Delta H_{mix}^{S} = 0$

Assume: (1) completely miscible in solid and liquid.
(2) Both are ideal soln.

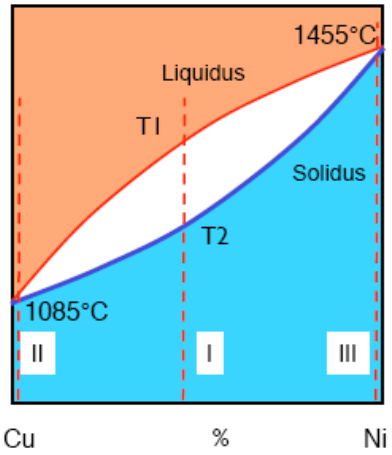

2) Variant of the simple phase diagram

$\Delta H_{mix}^{\alpha} > \Delta H_{mix}^{l} > 0$

miscibility gab

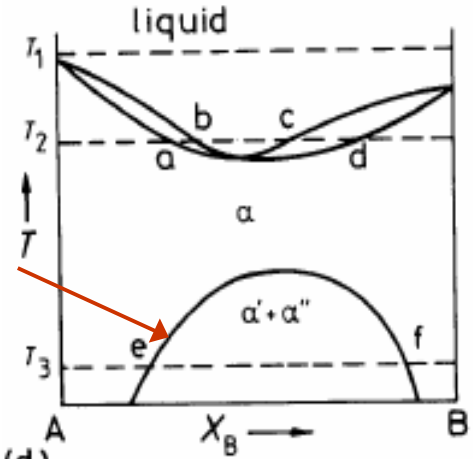

$\Delta H_{mix}^{\alpha} < \Delta H_{mix}^{l} < 0$

Ordered phase

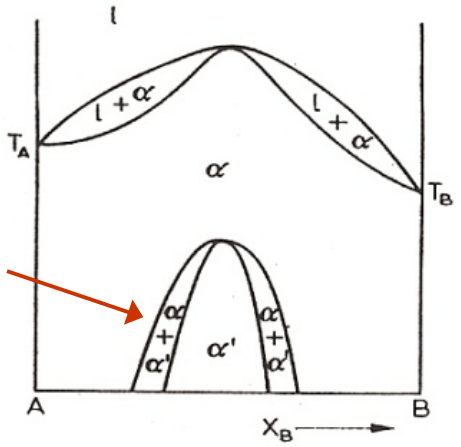

3.2.6 Pressure-Temperature-Composition phase diagram for a system with continuous series of solutions

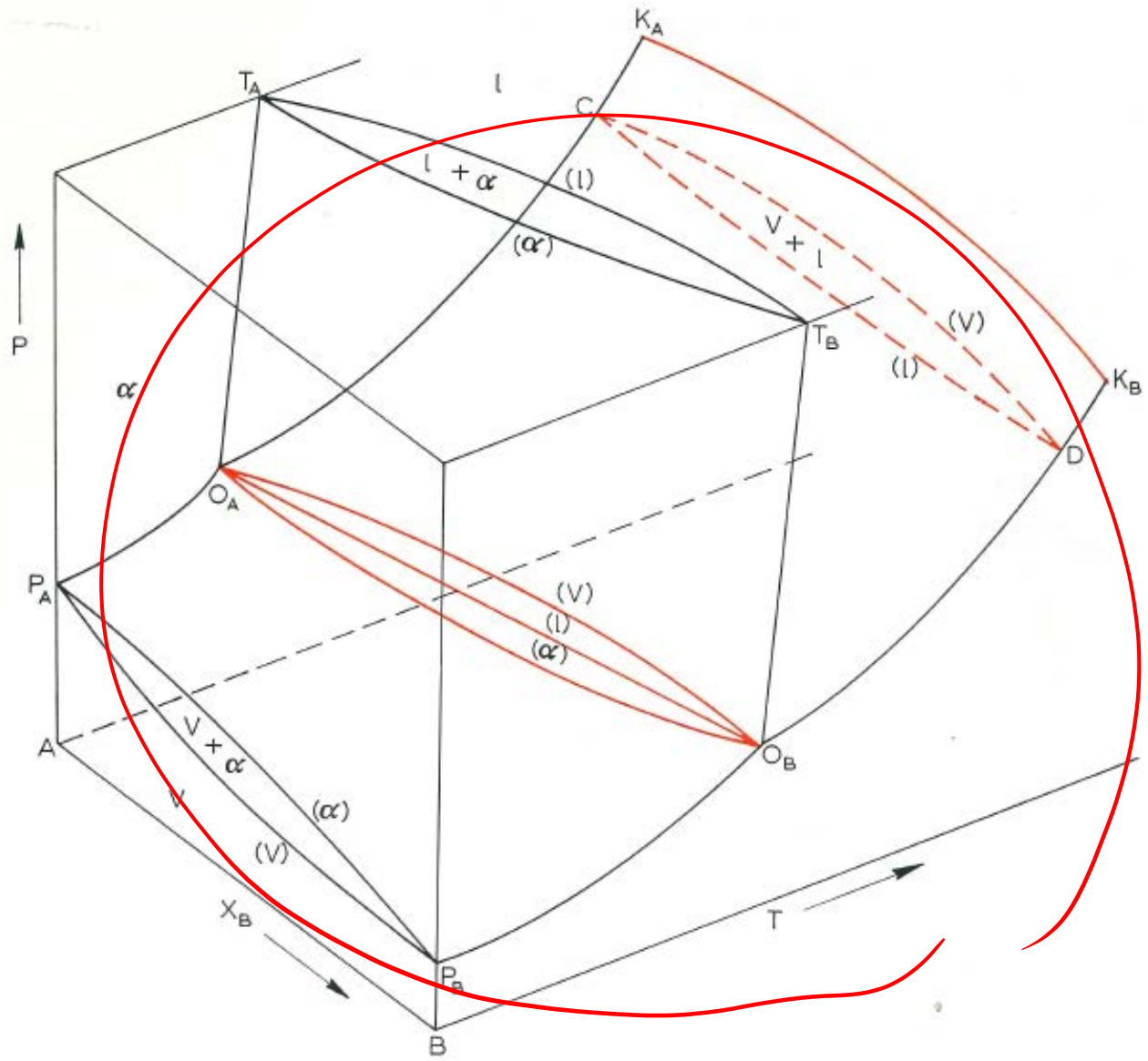

Fig. 35. Pressure–temperature–composition phase diagram for a system with continuous series of solutions

3.2.6 Pressure-Temperature-Composition phase diagram for a system with continuous series of solutions

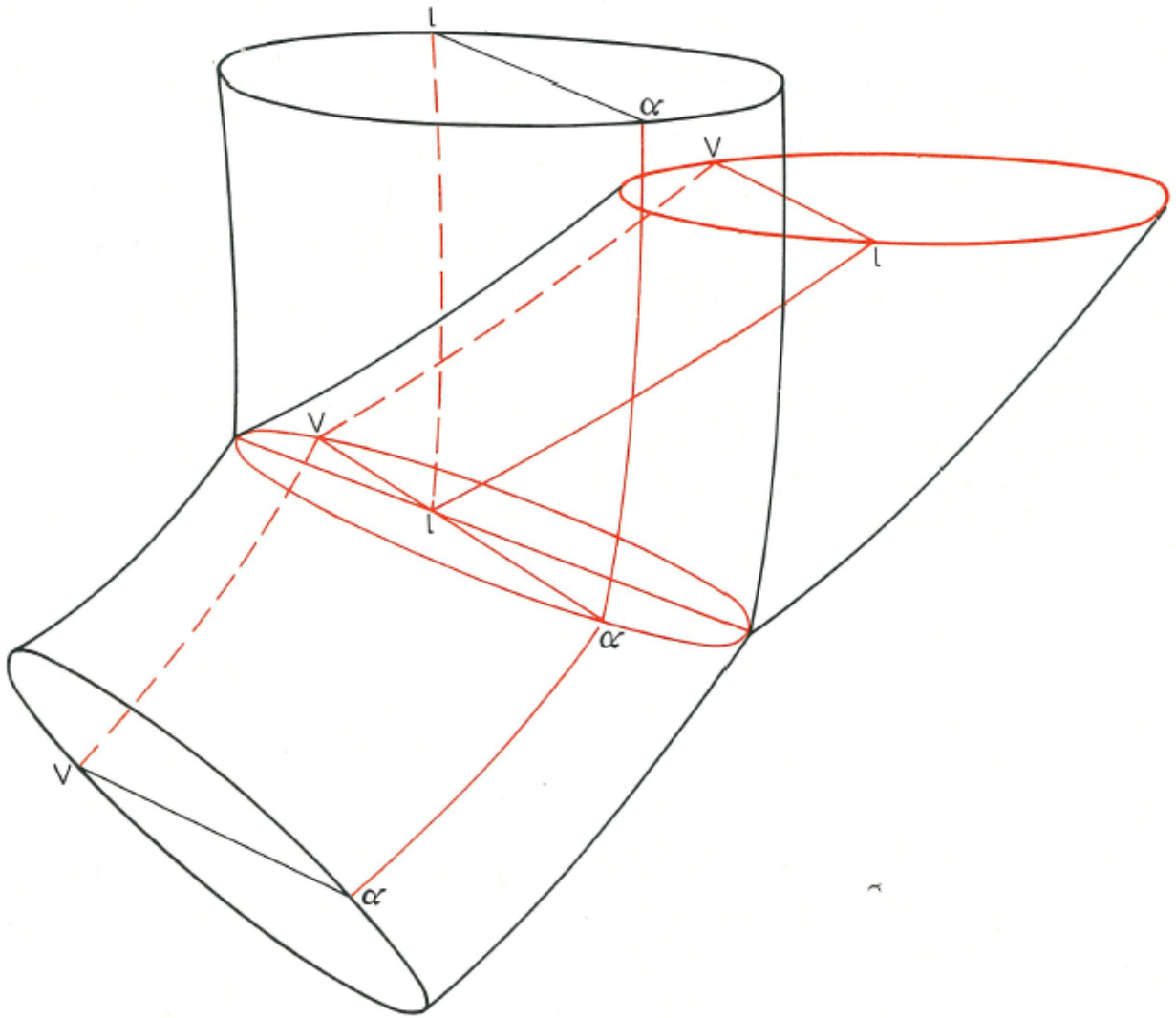

Fig. 36. Formation of a three-phase tie line *Vlα*.

3.2.6 Pressure-Temperature-Composition phase diagram for a system with continuous series of solutions

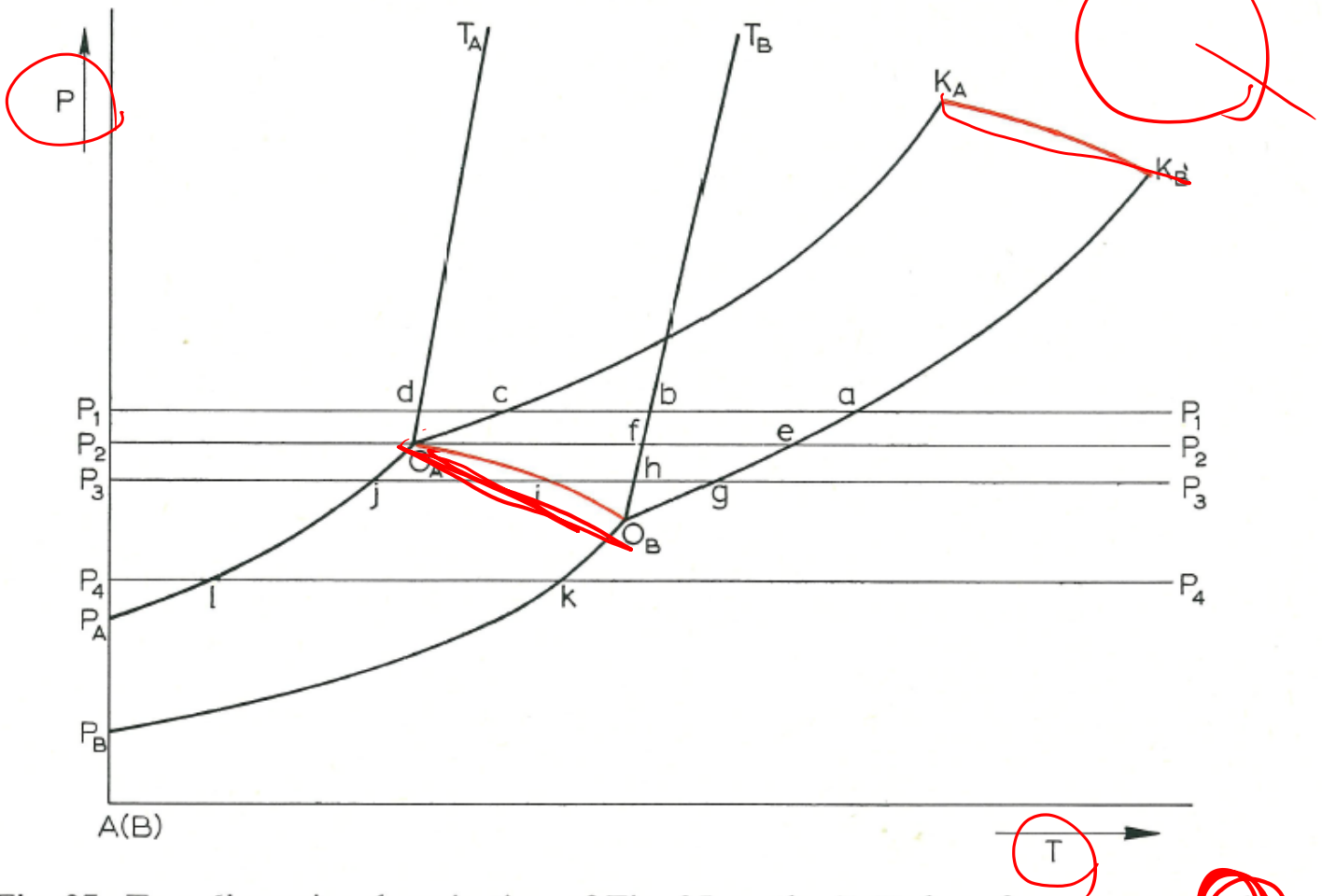

Fig. 37. Two-dimensional projection of Fig. 35 on the P–T plane for component A; $P_A O_A$ — equilibrium between V_A and α_A; $P_B O_B$ — V_B and α_B; $O_A T_A$ — l_A and α_A; $O_B T_B$ — l_B and α_B; $O_A K_A$ — V_A and l_A; $O_B K_B$ — V_B and l_B; $O_A O_B$ — V_{AB}, l_{AB} and α_{AB}; O_A — V_A, l_A and α_A; O_B — V_B, l_B and α_B; $K_A K_B$ — $V_{AB} = l_{AB}$.

3.2.6 Pressure-Temperature-Composition phase diagram for a system with continuous series of solutions

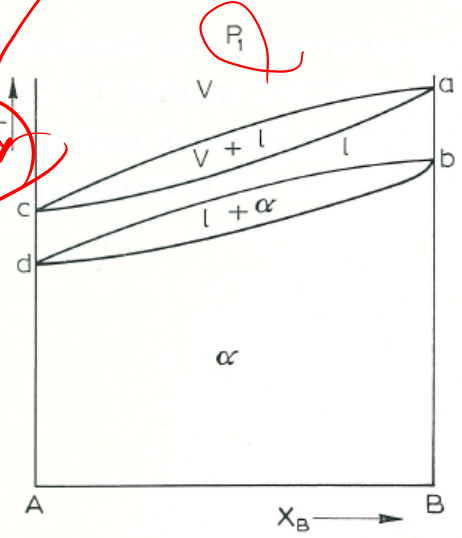

Fig. 38. *T–X* section through Fig. 35 at a pressure P_1 where $K_B > P_1 > O_A$.

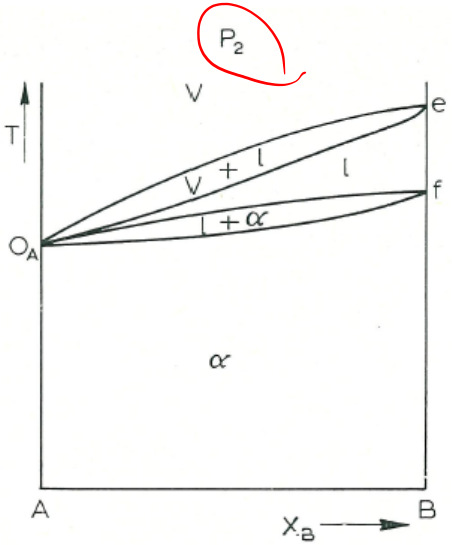

Fig. 39. *T–X* section through Fig. 35 at a pressure P_2 where $P_2 = O_A$

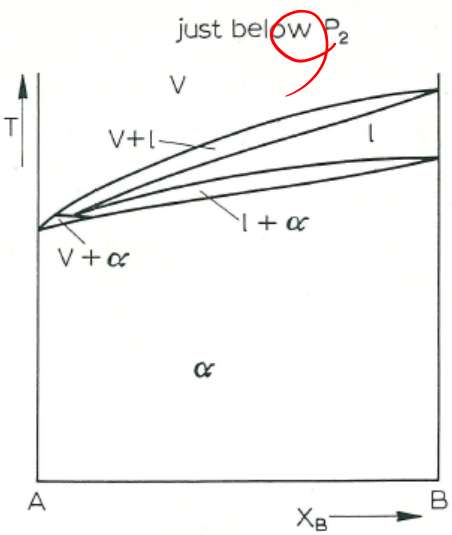

Fig. 40. *T–X* section through Fig. 35 at a pressure just below P_2.

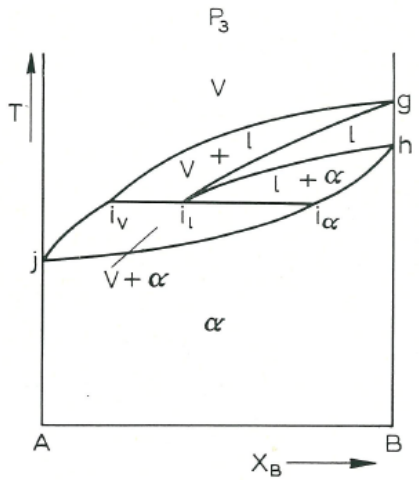

Fig. 41. *T–X* section through Fig. 35 at a pressure P_3 where $O_A > P_3 > O_B$.

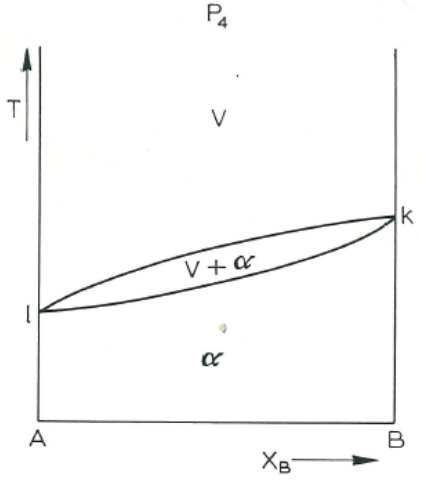

Fig. 42. *T–X* section through Fig. 35 at a pressure P_4 where $O_B > P_4 > P_B$.

Contents for today's class

CHAPTER 4
Binary Phase Diagrams

Three-Phase Equilibrium Involving Limited Solubility of the Components in the Solid State but Complete Solubility in the Liquid State

* Three-Phase Equilibrium : Eutectic Reactions

a) Structural Factor: Hume-Rothery Rules

Empirical rules for substitutional solid-solution

complete solid solution ⟷ limited solid solution

Similar atomic radii, the same valency and crystal structure

b) The eutectic reaction

c) Limiting forms of eutectic phase diagrams

d) Retrogade solidus curves

* Simple Eutectic Systems

$$\Delta H_{mix}^{\alpha} > \Delta H_{mix}^{l} > 0$$

- **Three-Phase Equilibrium Involving Limited Solubility of the Components in the Solid State but Complete Solubility in the Liquid State**

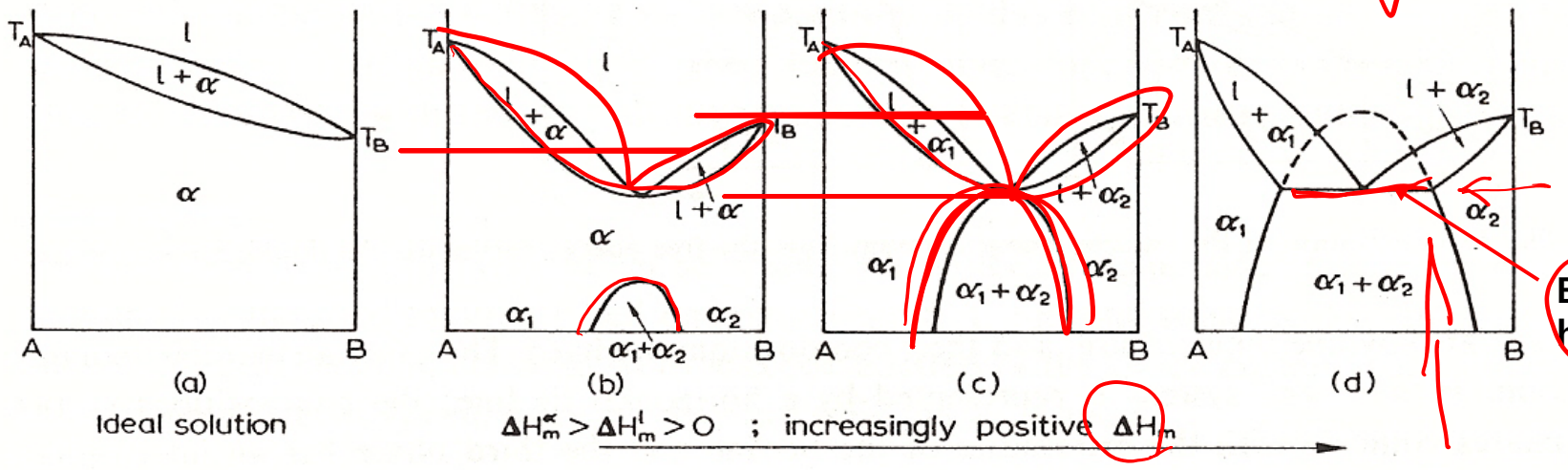

Fig. 43. Effect of increasingly positive departure from ideality in changing the phase diagram for a continuous series of solutions to a eutectic-type.

* Simple Eutectic Systems

- $\Delta H_m >> 0$ and the miscibility gap extends to the melting temperature. (when both solids have the same structure.)

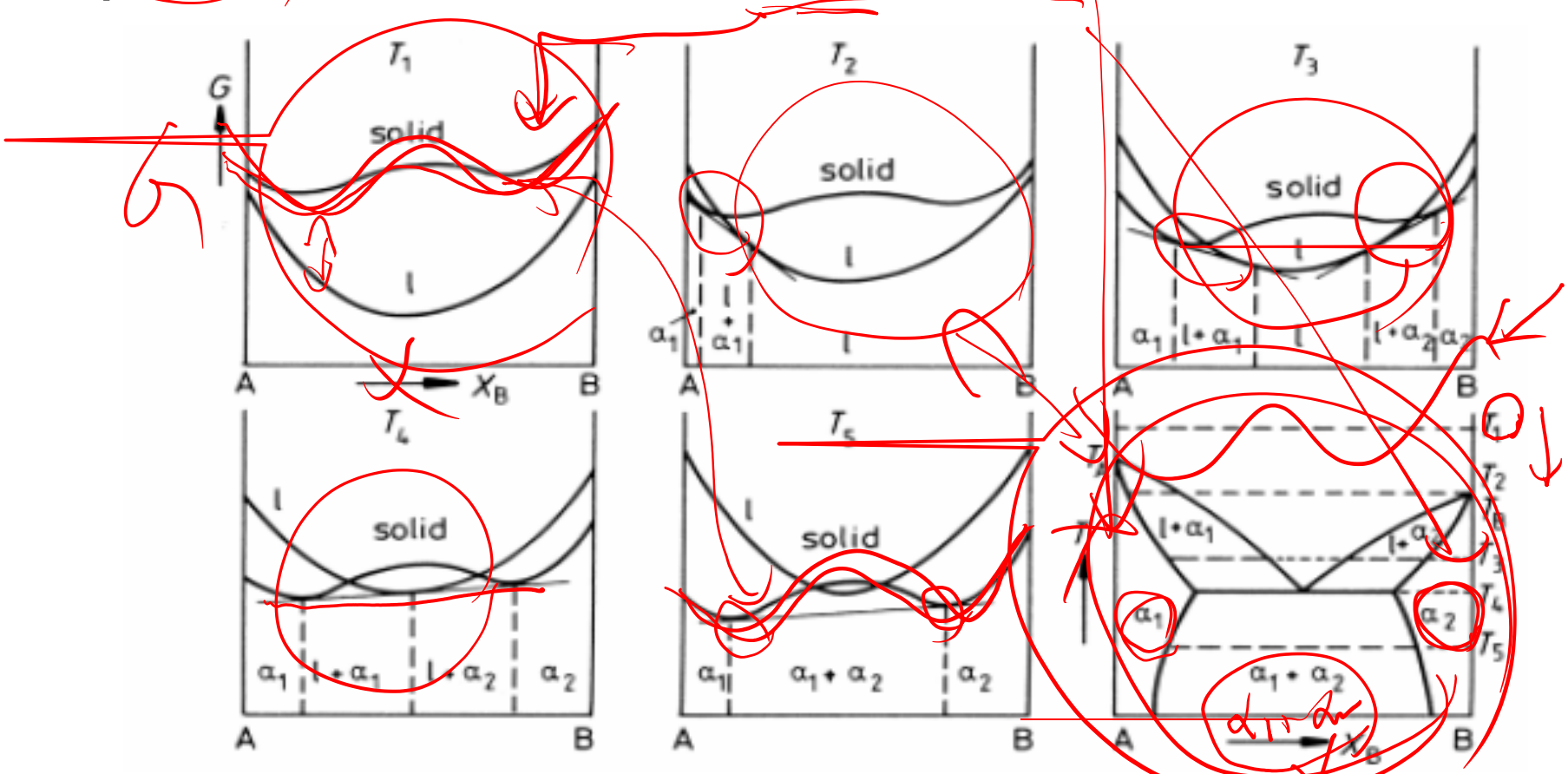

Fig 1.32 The derivation of a eutectic phase diagram where both solid phases have the same crystal structure. (After A.H. Cottrell, *Theoretical Structural Metallurgy*, Edward Arnold, London, 1955,©Sir Alan Cottrell.)

(when each solid has the different crystal structure.)

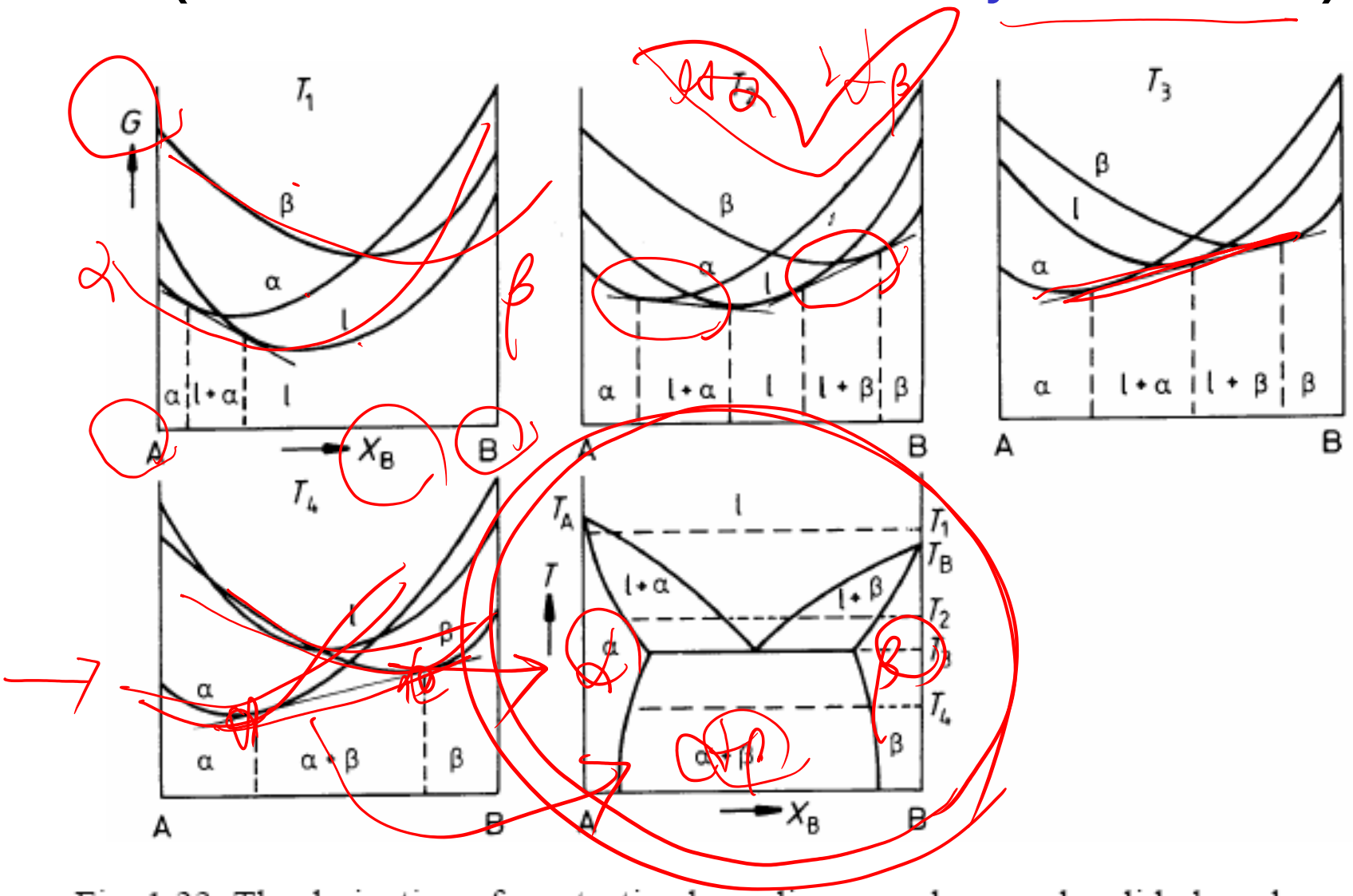

Fig. 1.33 The derivation of a eutectic phase diagram where each solid phase has a different crystal structure. (After A. Prince, *Alloy Phase Equilibria*, Elsevier, Amsterdam, 1966.)

Measurement of R_c in Mg BMG (D_{max}=14 mm)

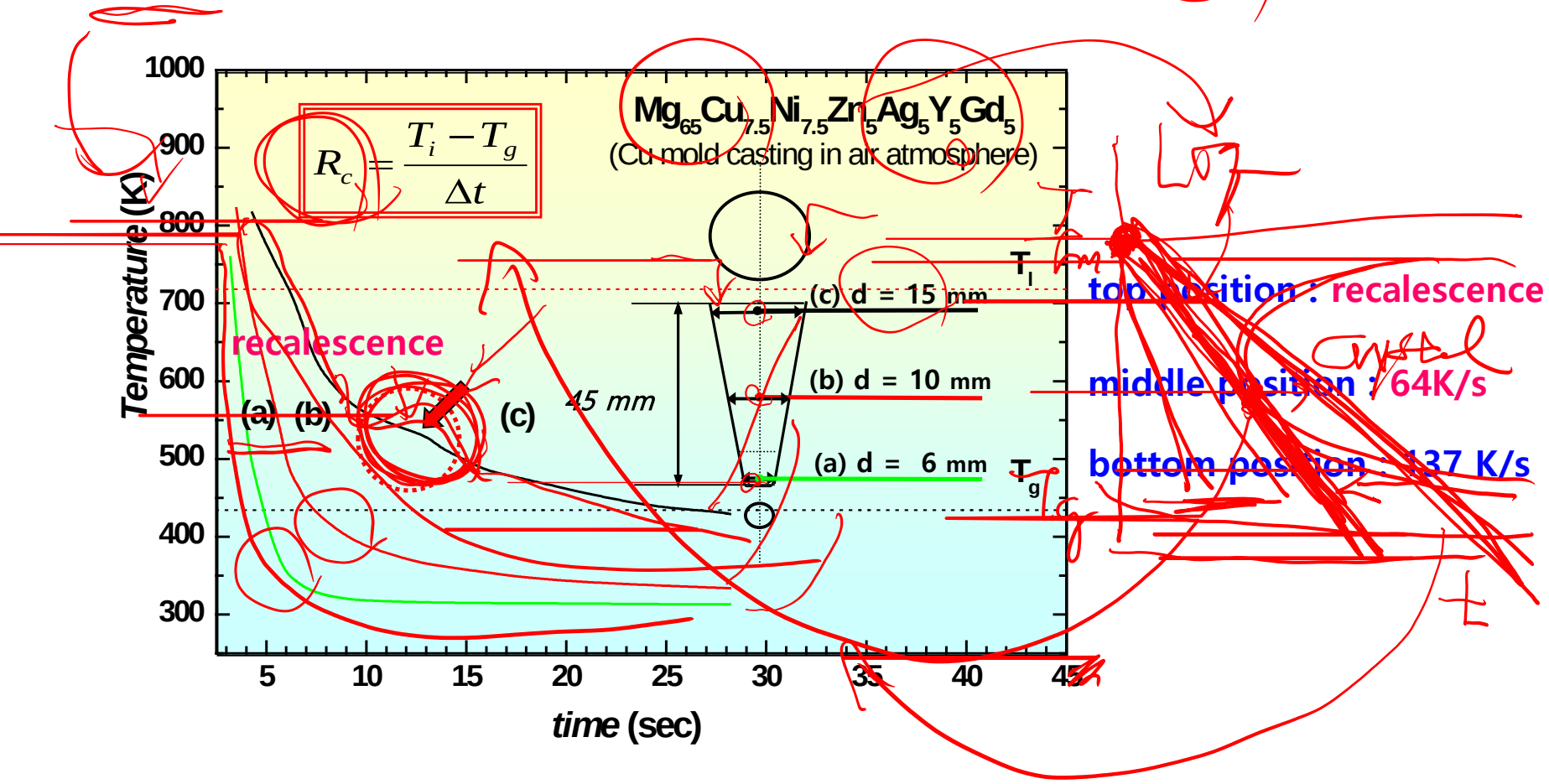

*** Cooling curves** measured at the center of the three transverse cross sections

* JAP 104, 023520 (2008)

Nucleation Theory as Applied to solidification

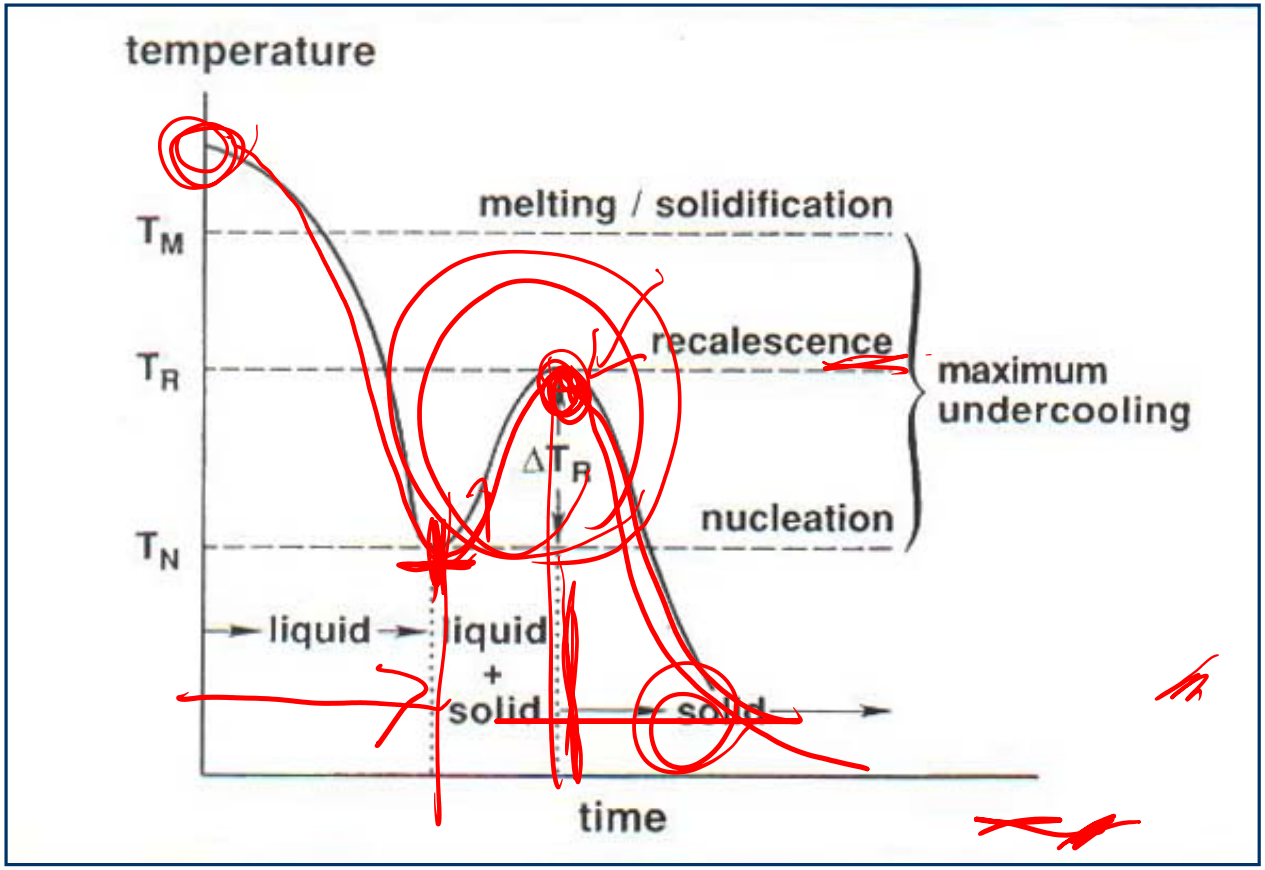

- The recalescence process is illustrated by a temperature versus time plot, showing the temperature rise on nucleation due to release of the heat of fusion.
- A sudden glowing in a undercooled liquid of metal caused by liberation of the latent heat of transformation
- The higher the recalescence temperature, the larger the microstructural scale in the solid.

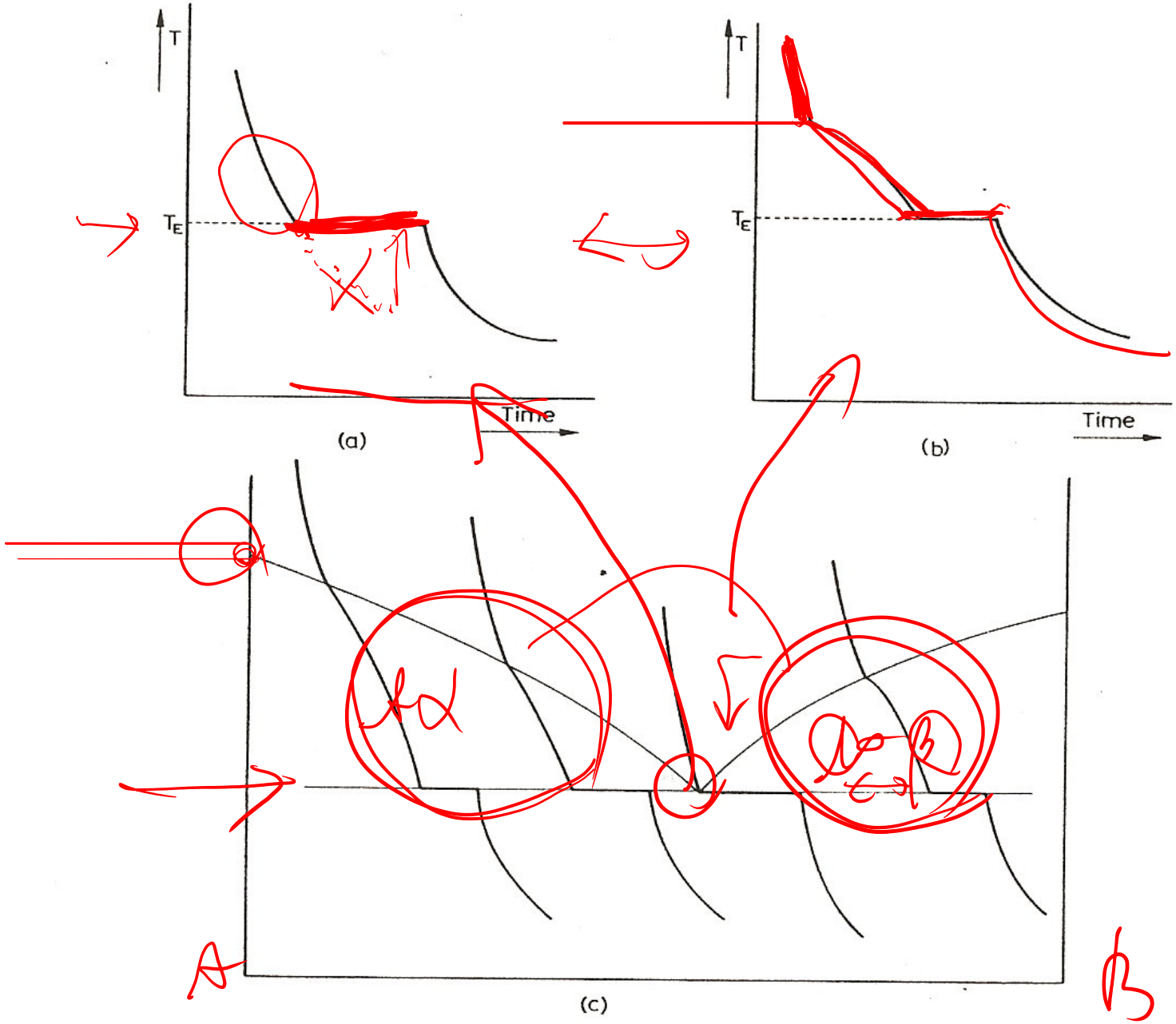

Fig. 48. Cooling curve for (a) the eutectic alloy, (b) hypo-eutectic alloy *N*, and (c) a series of alloys, allowing the determination of the liquidus and eutectic horizontal.

Eutectic Systems

$$\Delta H_{mix}^{L} = 0 \quad \Delta H_{mix}^{S} >> 0$$

The Pb-Sn system is characteristic of a valley in the middle. Such system is known as the **Eutectic** system. The central point is the Eutectic point and the transformation though this point is called Eutectic reaction: **L**✦α+β

Pb has a fcc structure and Sn has a tetragonal structure. The system has three phases: L, α and β.

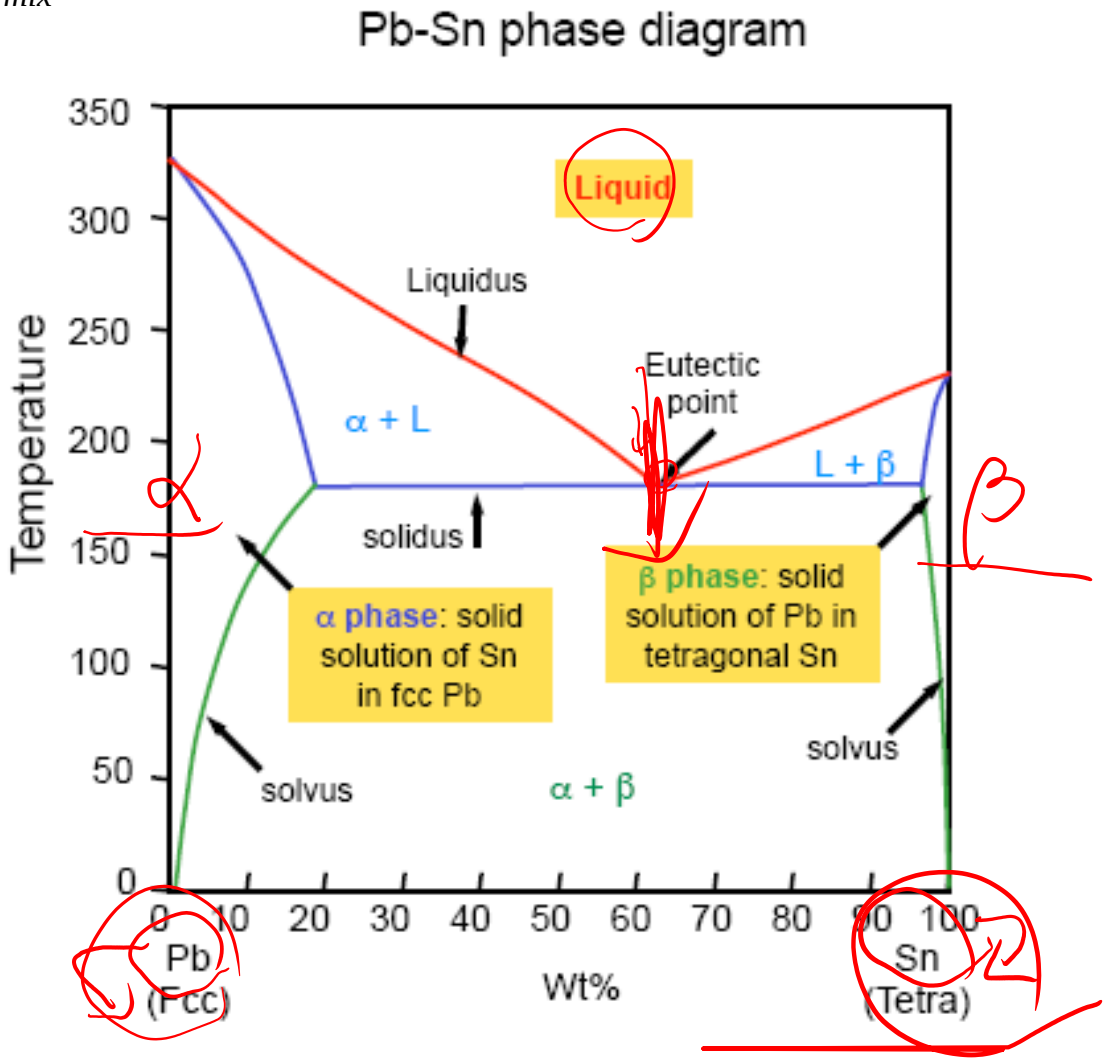

Solidification of Eutectic Systems

Alloy II

At point 1: Liquid

Solidification starts at eutectic point (where liquidus and solidus join)

At point 2: L✦(α+β) (eutectic reaction)

The amounts of α and β increase in proportion with time.

Solidification finishes at the same temperature.

At point 3: α+β

Further cooling leads to the depletion of Sn in α and the depletion of Pb in β.

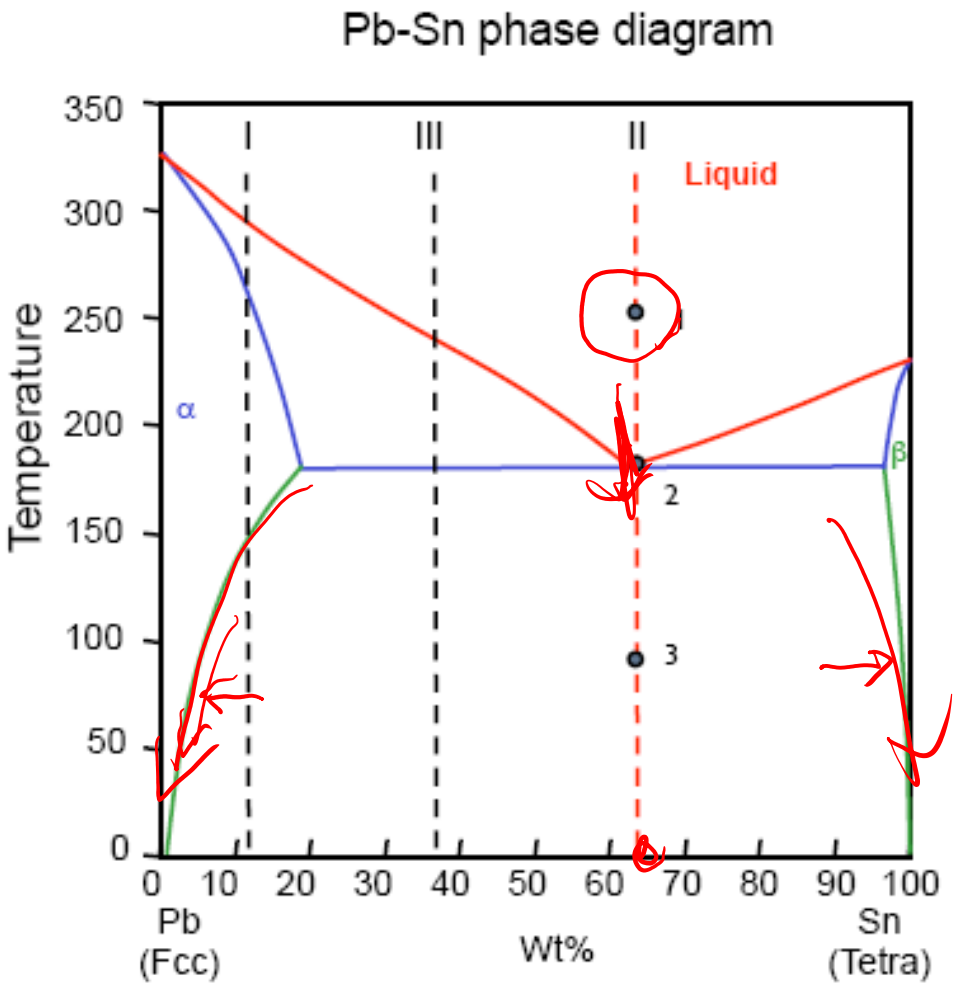

1.5 Binary phase diagrams

Alloy II

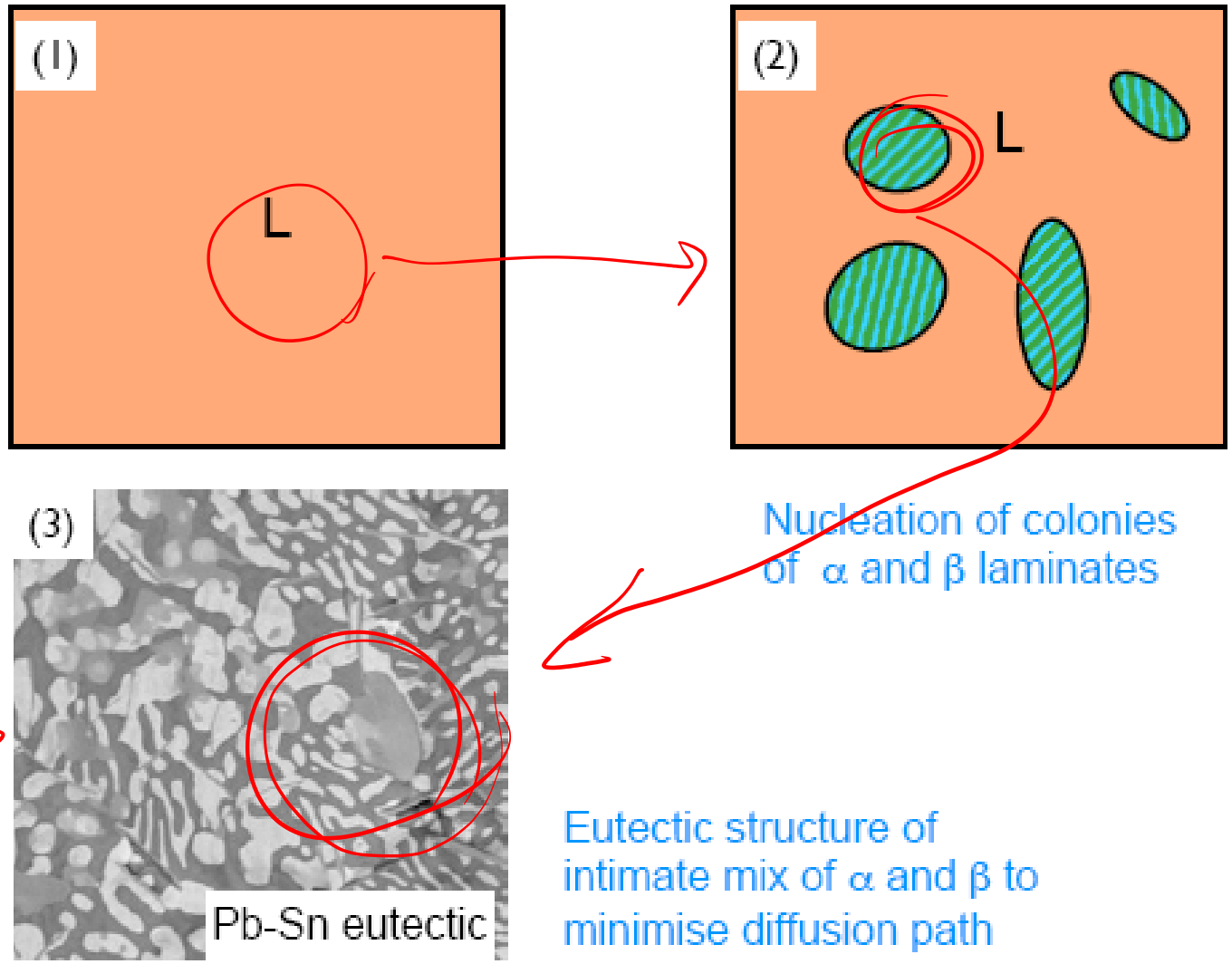

Nucleation of colonies of α and β laminates

Eutectic structure of intimate mix of α and β to minimise diffusion path

4.3.2 Eutectic Solidification: L→α + β

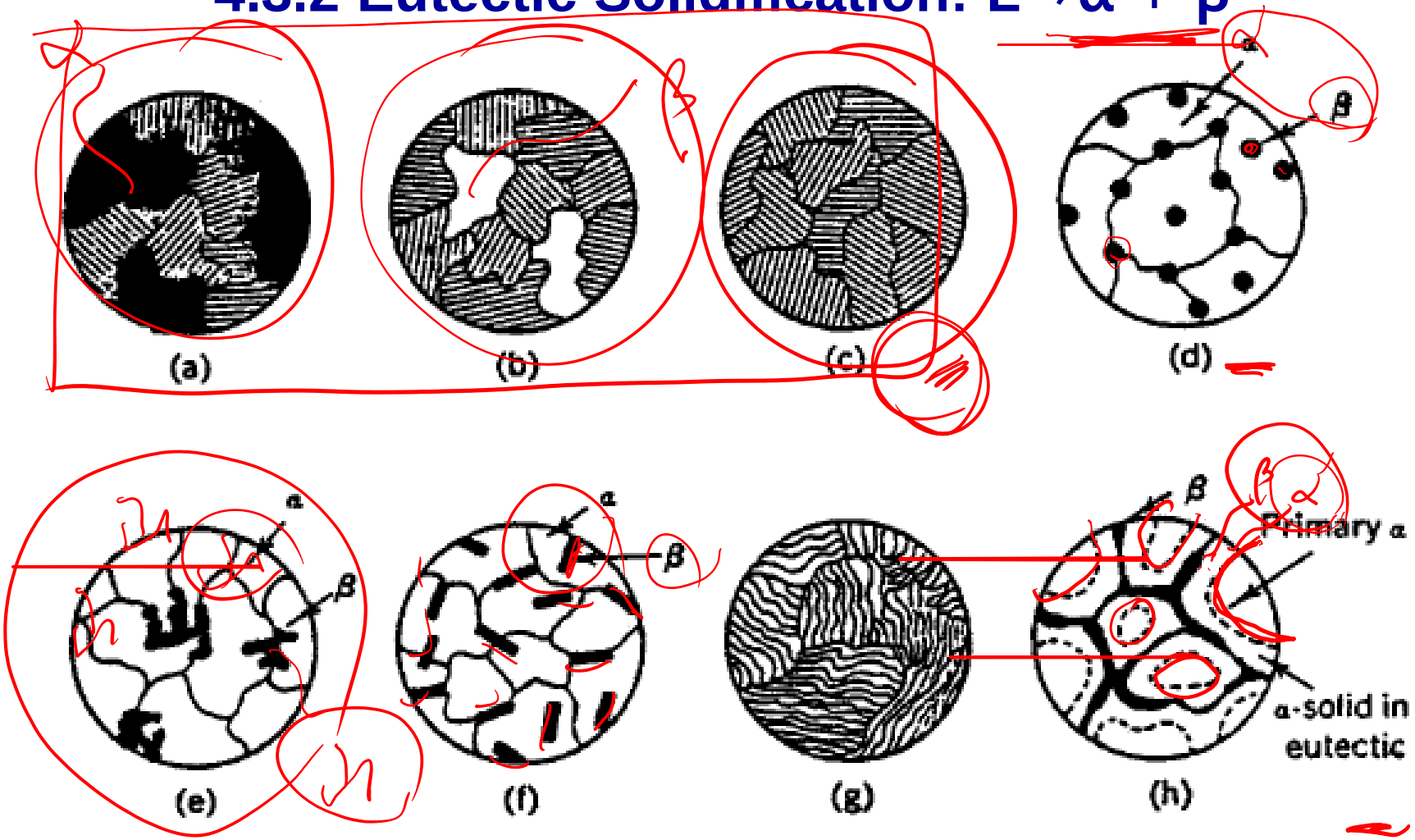

Fig. 14 Schematic representation possible in eutectic structures. (a), (b) and (c) are alloys shown in fig. 13; (d) nodular; (e) Chinese script; (f) acicular; (g) lamellar; and (h) divorced.

4.3.2 Eutectic Solidification

During solidification both phases grow simultaneously behind an essentially planar solid/liquid interface.

Normal eutectic

both phases have low entropies of fusion.

Fig. 4.30 Rod-like eutectic. Al_6Fe rods in Al matrix. Transverse section. Transmission electron micrograph (x 70000).

Anomalous eutectic

One of the solid phases is capable of faceting, i.e., has a high entropy or melting.

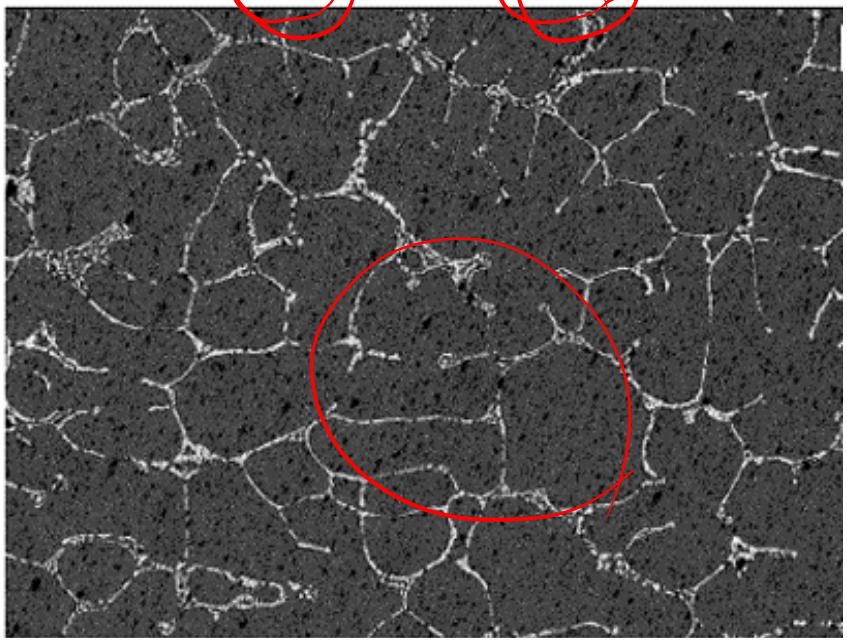

The microstructure of the Pb-61.9%Sn (eutectic) alloy presented a coupled growth of the (Pb)/βSn eutectic. There is a remarkable change in morphology increasing the degree of undercooling with transition from regular lamellar to anomalous eutectic.

http://www.matter.org.uk/solidification/eutectic/anomalous_eutectics.htm

D.A. Porter and K.E. Eastering, "Phase Transformations in Metals and Alloys"

Eutectic

Divorced Eutectic

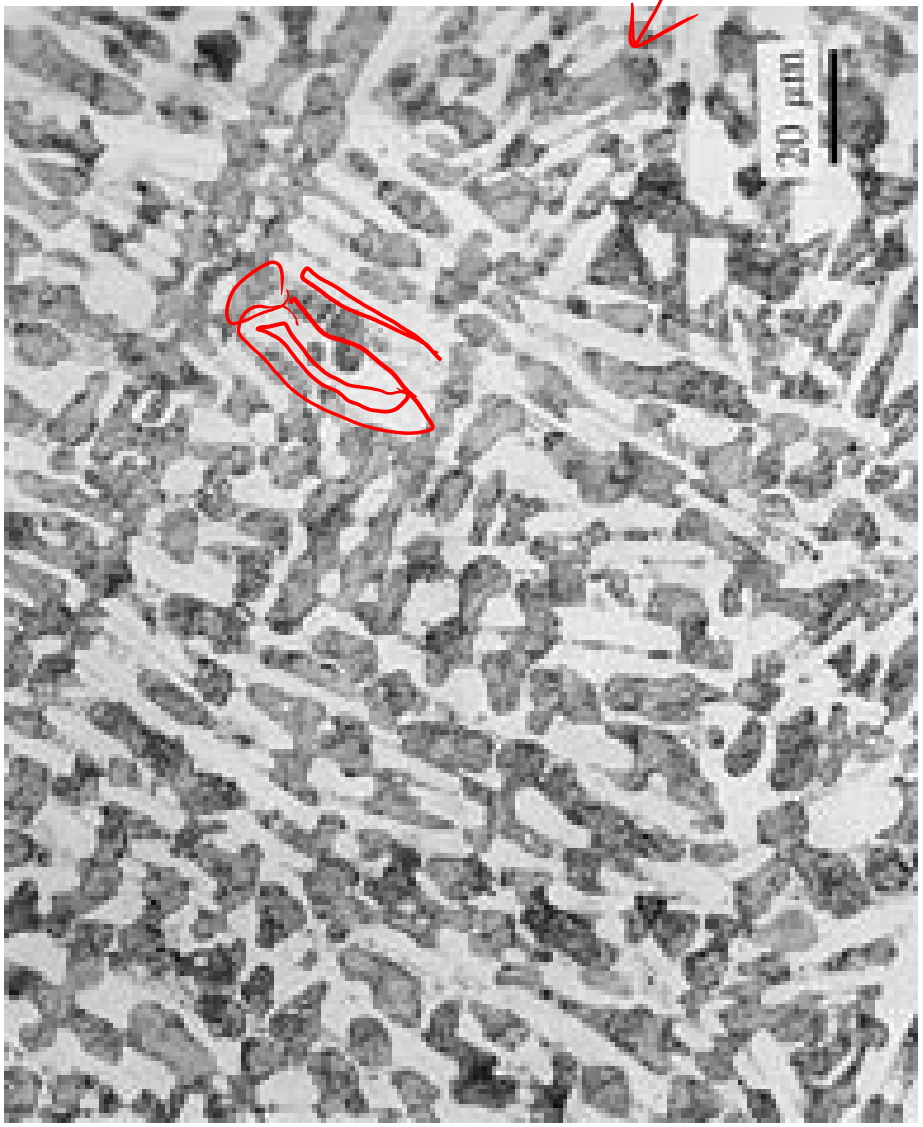

Solidification of Eutectic Systems

Alloy I :

At point 1: Liquid
Solidification starts at liquidus
At point 2: L+α
The amount α ↑ with ↓ T
Solidification finishes at solidus
At point 3: α
Precipitation starts at solvus
At point 4: α+β
Further cooling leads to formation and growth of more β precipitates whereas Sn% in α decreases following the solvus.

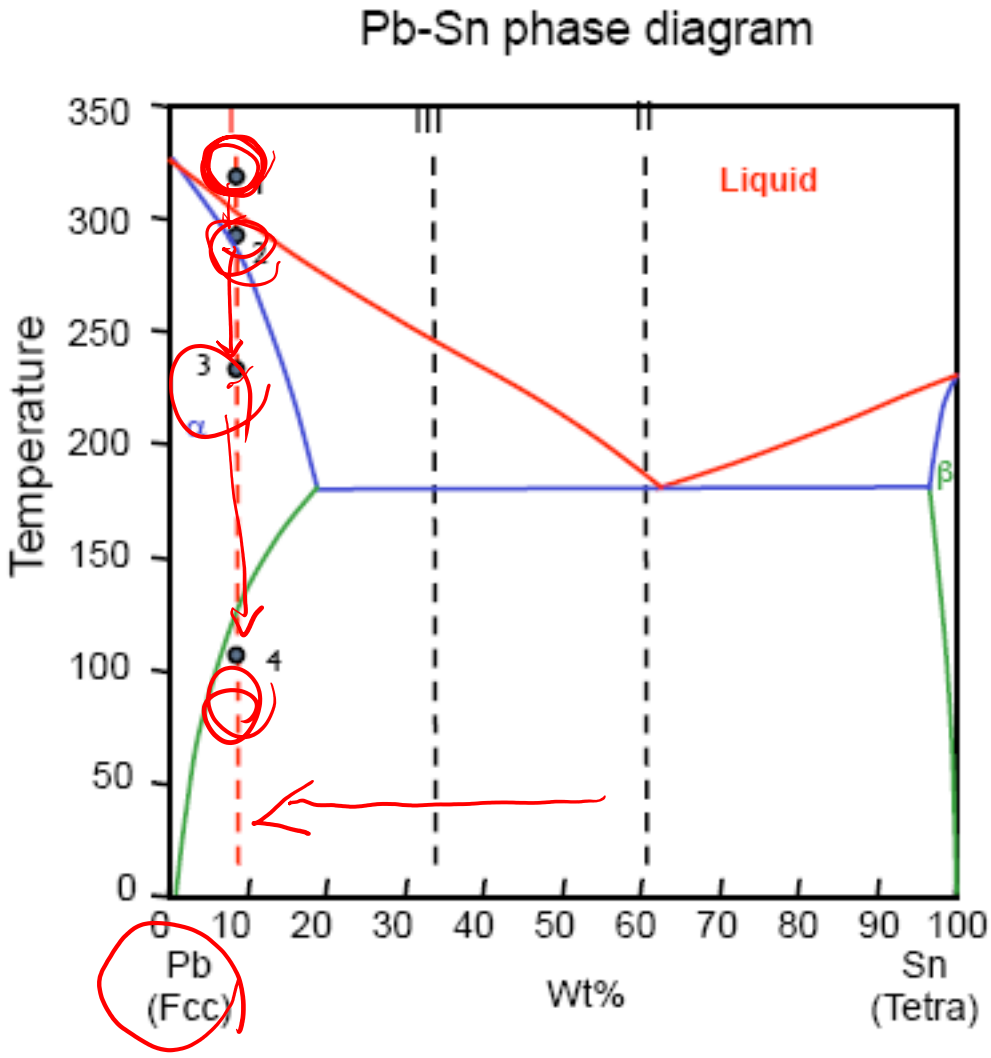

1.5 Binary phase diagrams

Alloy I

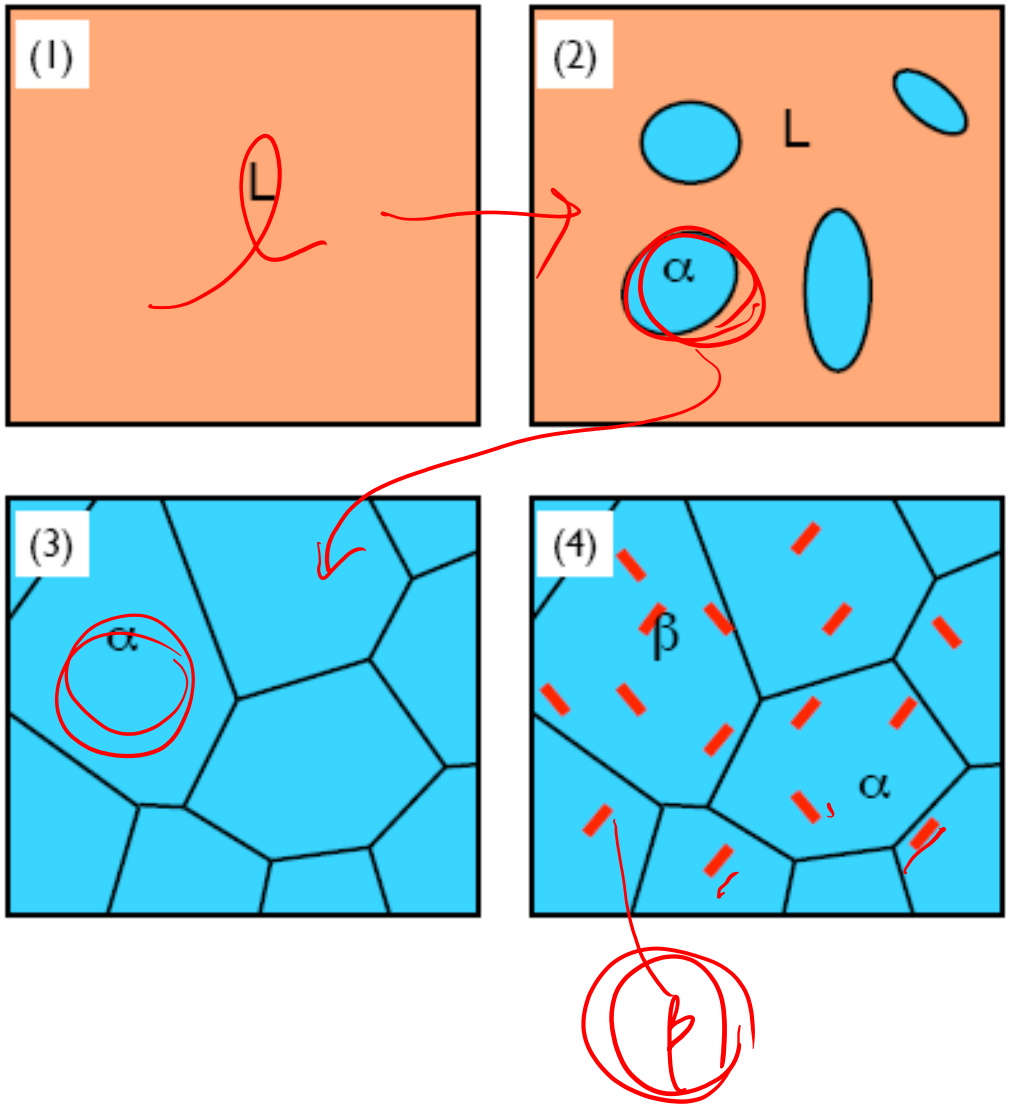

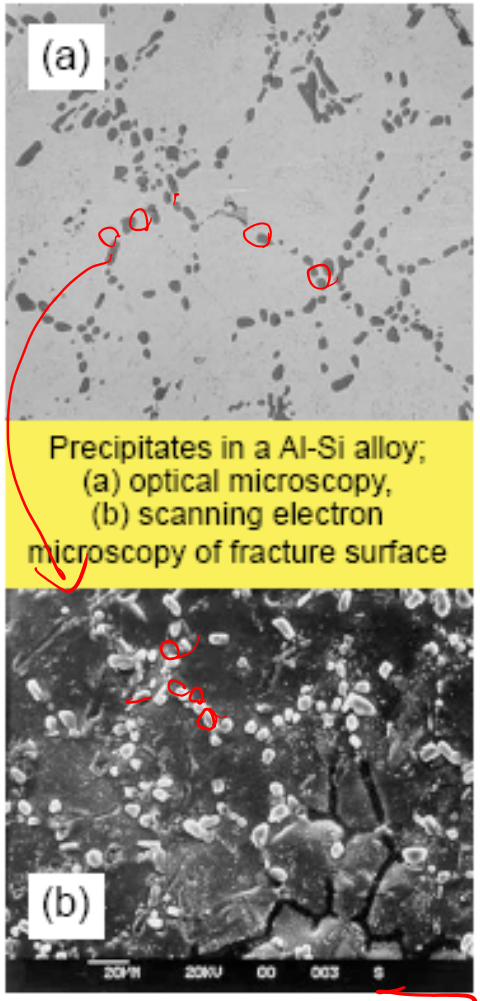

Precipitates in a Al-Si alloy;
(a) optical microscopy,
(b) scanning electron
microscopy of fracture surface

Solidification of Eutectic Systems

Alloy III

At point 1: Liquid
Solidification starts at liquidus
At point 2: L✦L+α (pre-eutectic α)
The amount α ↑ with ↓T
At point 3: L✦ (α+β) (eutectic reaction)
Solidification finishes at the eutectic temperature
At point 4: α+β (pre-eutectic α + (α+β) eutectic mixture)
Further cooling leads to the depletion of Sn in α and the depletion of Pb in β.

The cooling curve of this alloy is a combination of the two cooling curves shown in slide 9.

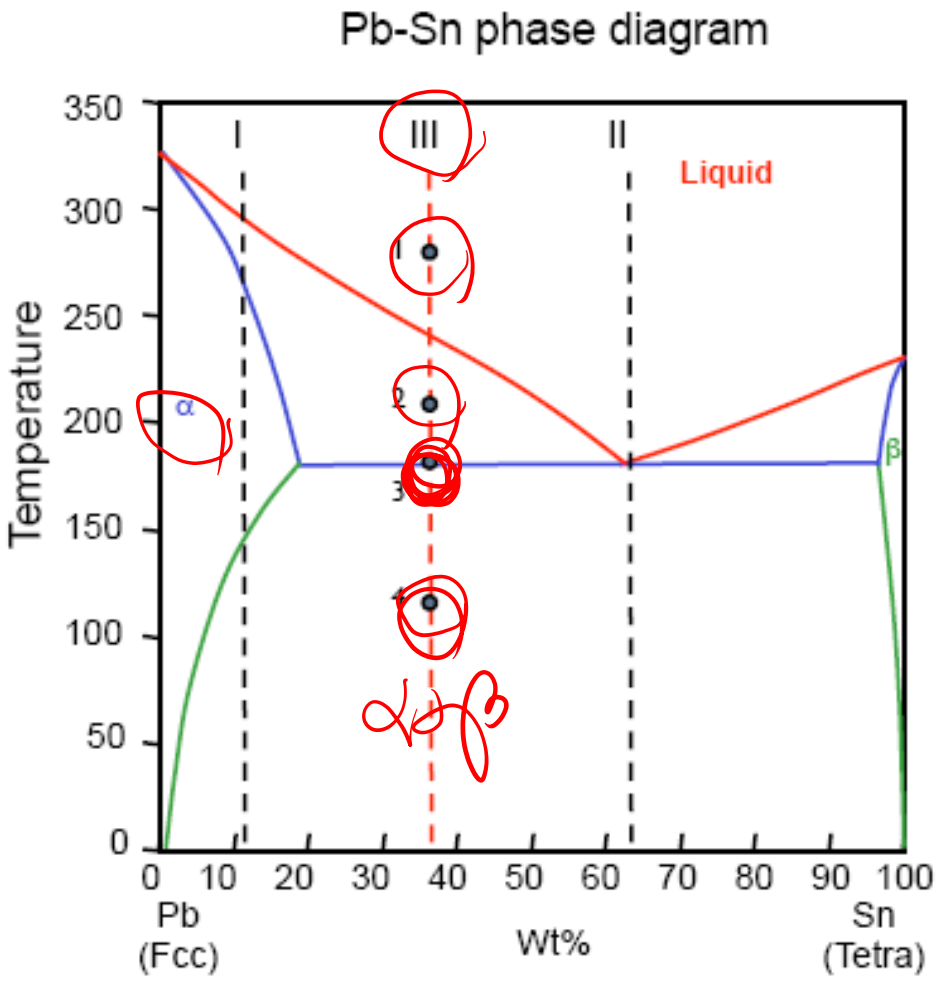

1.5 Binary phase diagrams: Hypoeutectic

Alloy III

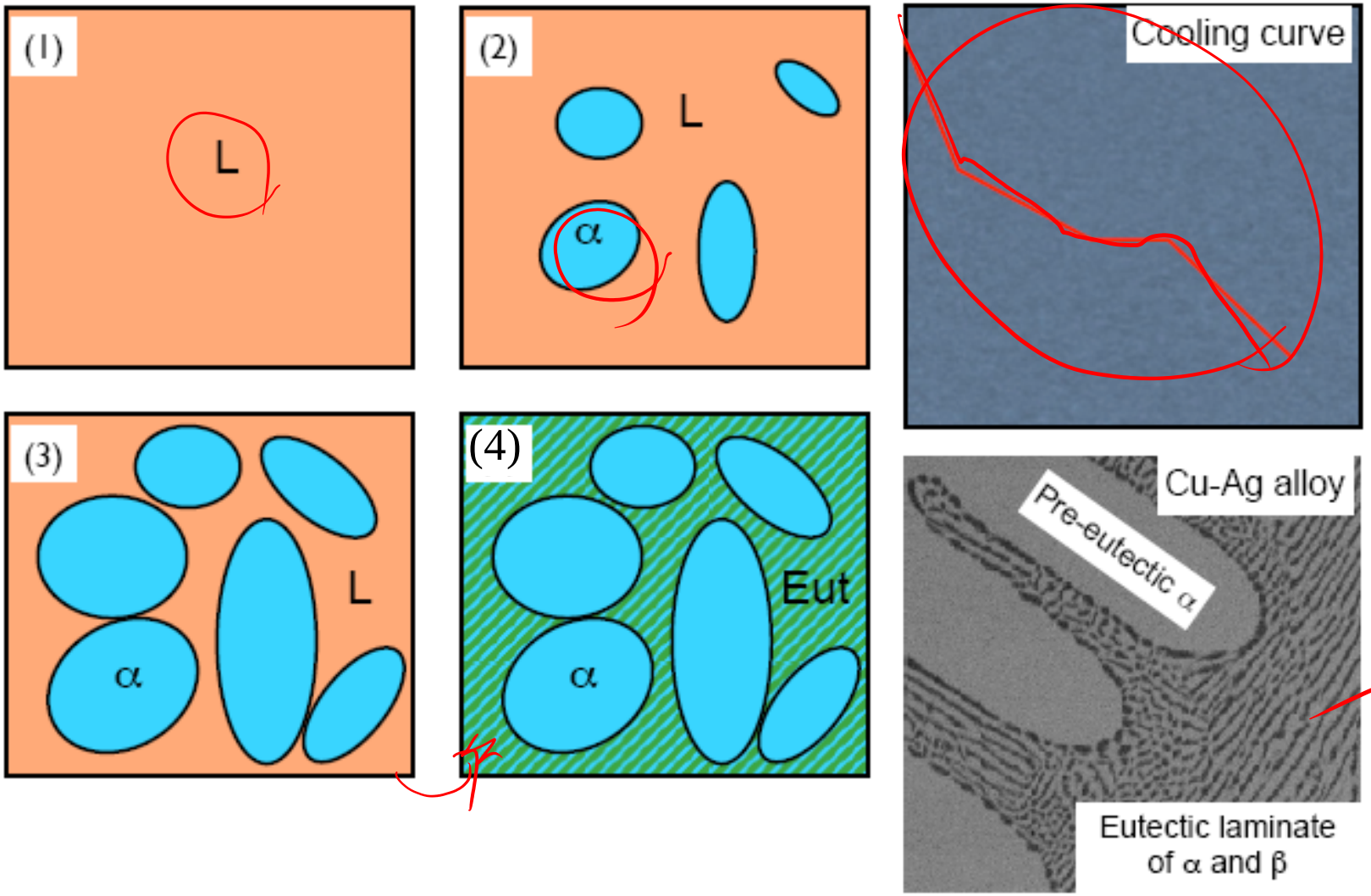

Solidification of Eutectic Systems

Alloy IV

Can you describe the solidification process of alloy IV, including microstructure evolution, morphology of phases and cooling curve?

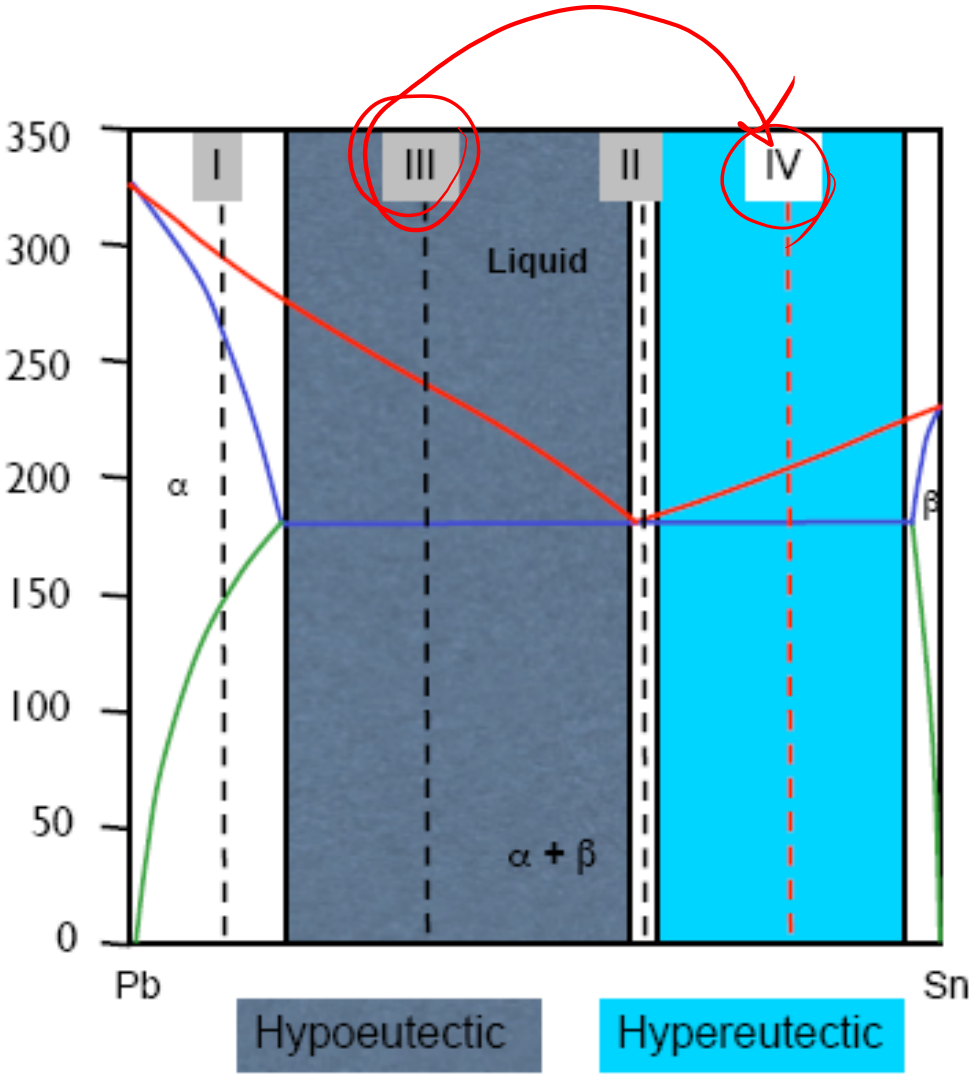

1.5 Binary phase diagrams : Hypereutectic

Alloy IV

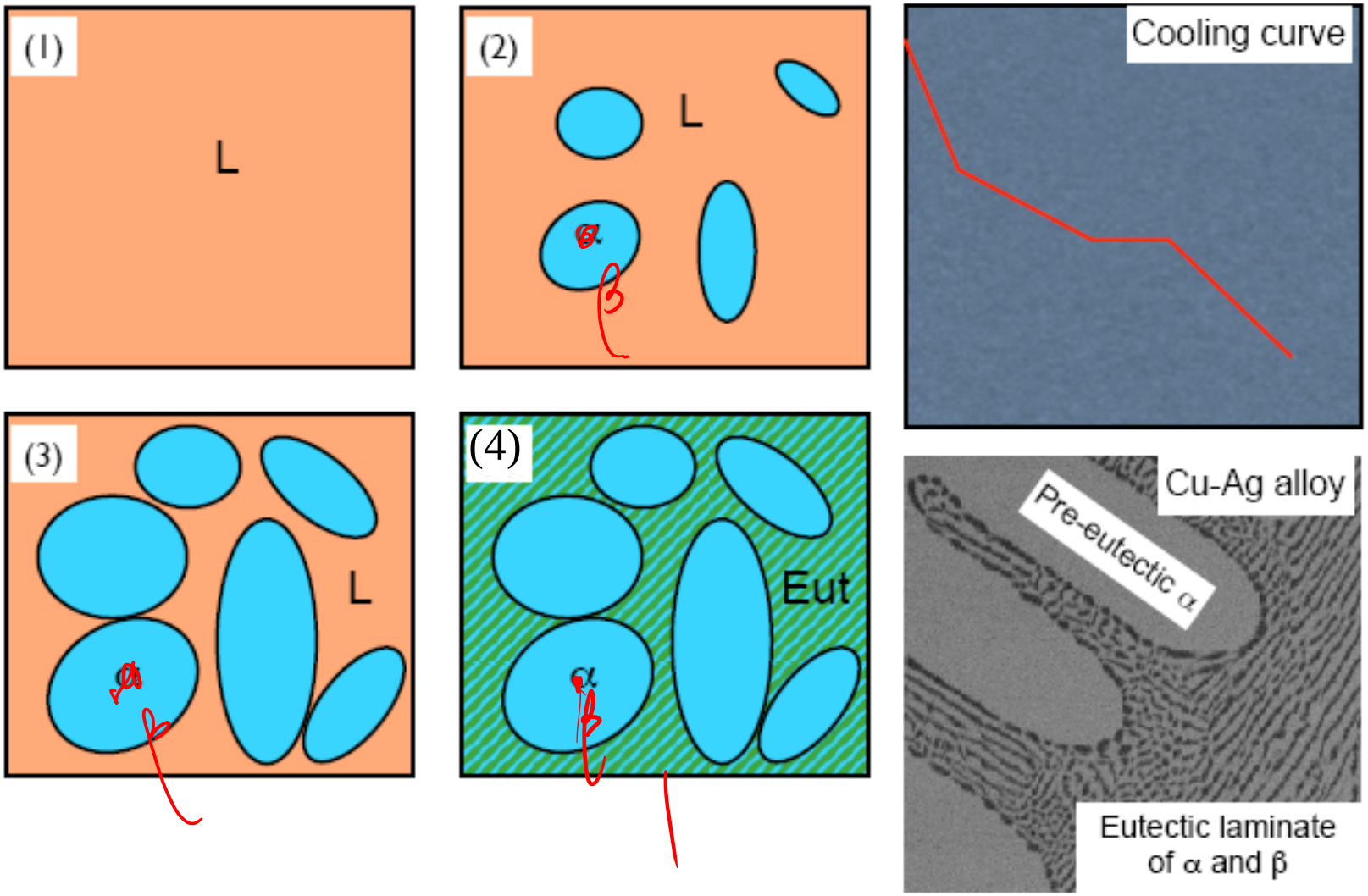

4.2.3. Limiting forms of eutectic phase diagram

1) Complete immiscibility of two metals does not exist.

: The solubility of one metal in another may be so low (e.g. Cu in Ge $<10^{-7}$ at%.)
that it is difficult to detect experimentally, but there will always be a measure of solubility.

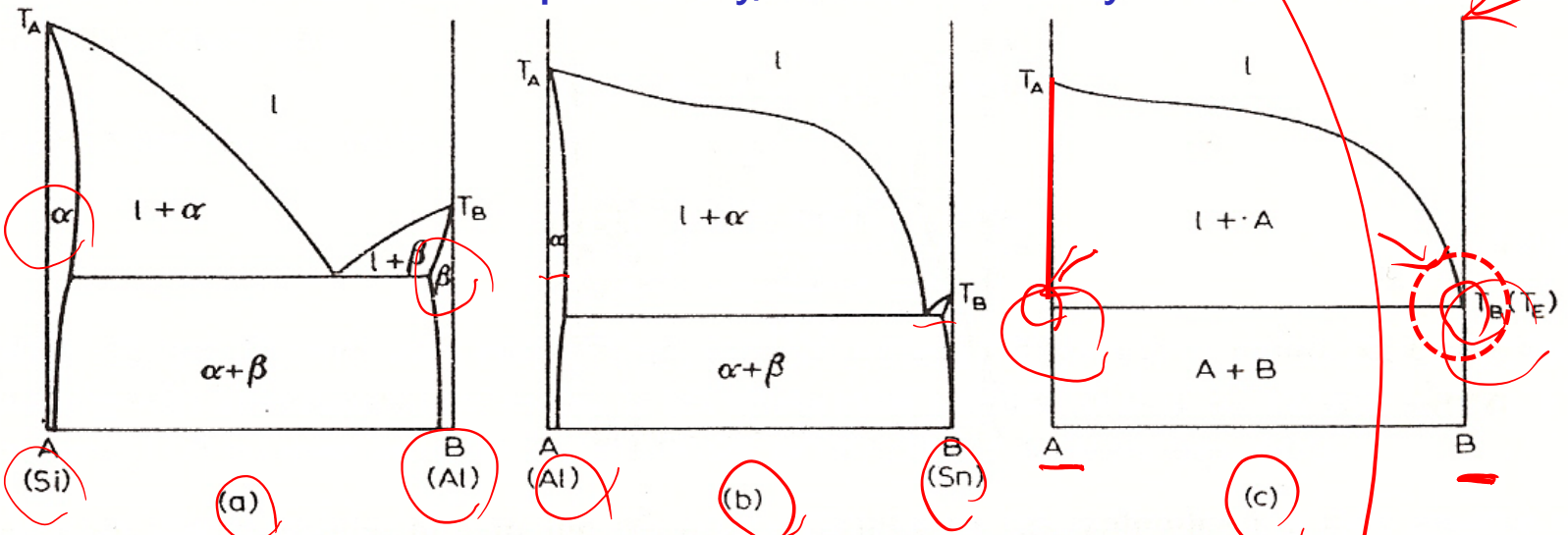

Fig. 53. Evolution of the limiting form of a binary eutectic phase diagram.

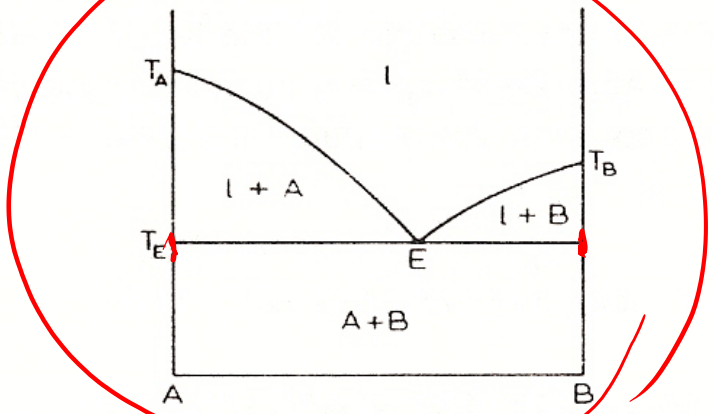

Fig. 54. Impossible form of a binary eutectic phase diagram.

* Effect of T on solid solubility

$T \uparrow \Rightarrow X_B^e \uparrow$

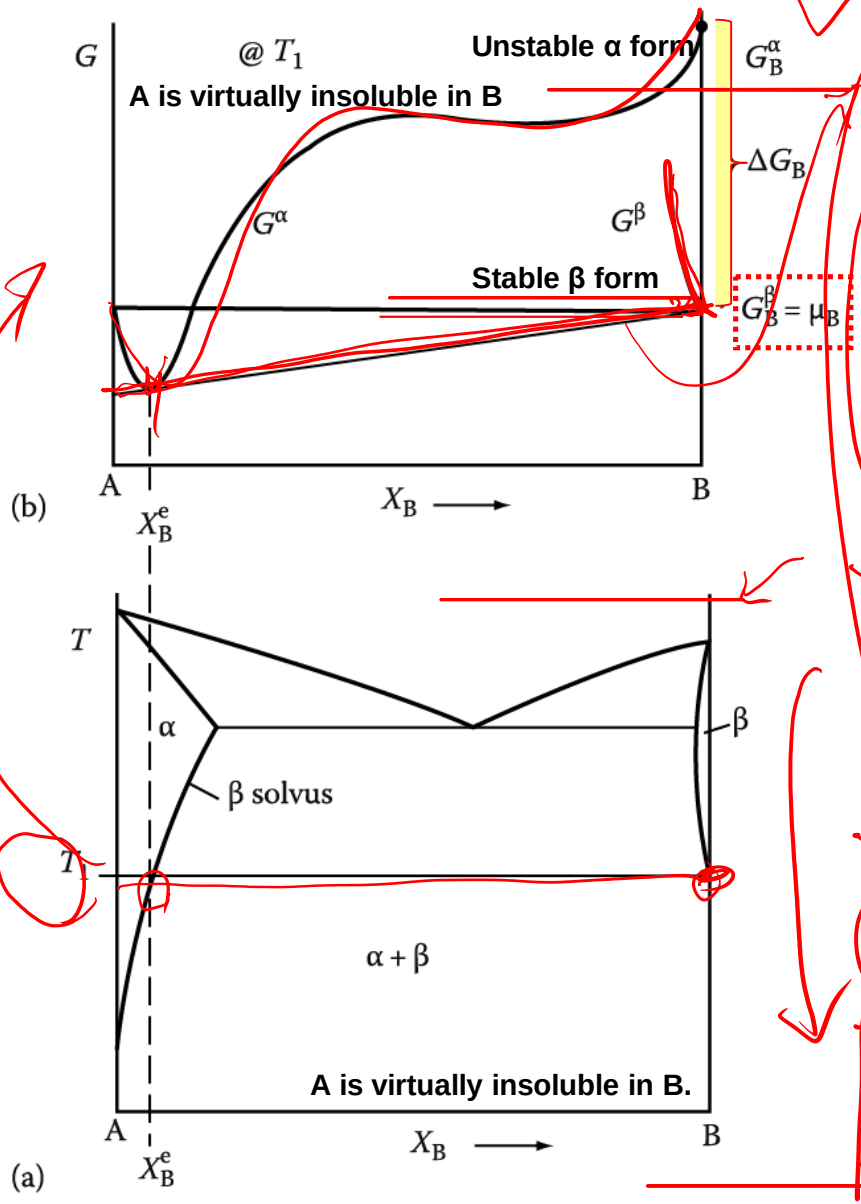

$$\mu_B^\alpha = {}^oG_B^\alpha + \Omega(1-X_B)^2 + RT\ln X_B = \mu_B^\beta \simeq {}^oG_B^\beta$$

$$\Delta G_B^{\beta\to\alpha} = {}^0G_B^\alpha - {}^oG_B^\beta = {}^oG_B^\alpha - \mu_B^\beta = {}^oG_B^\alpha - \mu_B^\alpha$$

$${}^oG_B^\alpha - \mu_B^\alpha = -\Omega(1-X_B)^2 - RT\ln X_B$$

$$\Delta G_B^{\beta\to\alpha} = -\Omega(1-X_B)^2 - RT\ln X_B$$

$$RT\ln X_B = -\Delta G_B^{\beta\to\alpha} - \Omega(1-X_B)^2$$

$$(here,\ X_B^e << 1)$$

$$RT\ln X_B^e = -\Delta G_B^{\beta\to\alpha} - \Omega$$

$$>> \quad X_B^e = \exp\left(-\frac{\Delta G_B^{\beta\to\alpha} + \Omega}{RT}\right)$$

$\Delta G_B^{\beta\to\alpha} = \Delta H_B^{\beta\to\alpha} - T\Delta S_B^{\beta\to\alpha}$ 이므로

$$X_B^e = \exp\left(\frac{\Delta S_B^{\beta\to\alpha}}{R}\right)\exp\left(-\frac{\Delta H_B^{\beta\to\alpha} + \Omega}{RT}\right)$$

$$X_B^e = A\exp\left\{-\frac{Q}{RT}\right\}$$

$T \uparrow \Rightarrow X_B^e \uparrow$

Q : heat absorbed (enthalpy) when 1 mole of β dissolves in A rich α as a dilute solution.

* Limiting forms of eutectic phase diagram

The solubility of one metal in another may be so low.

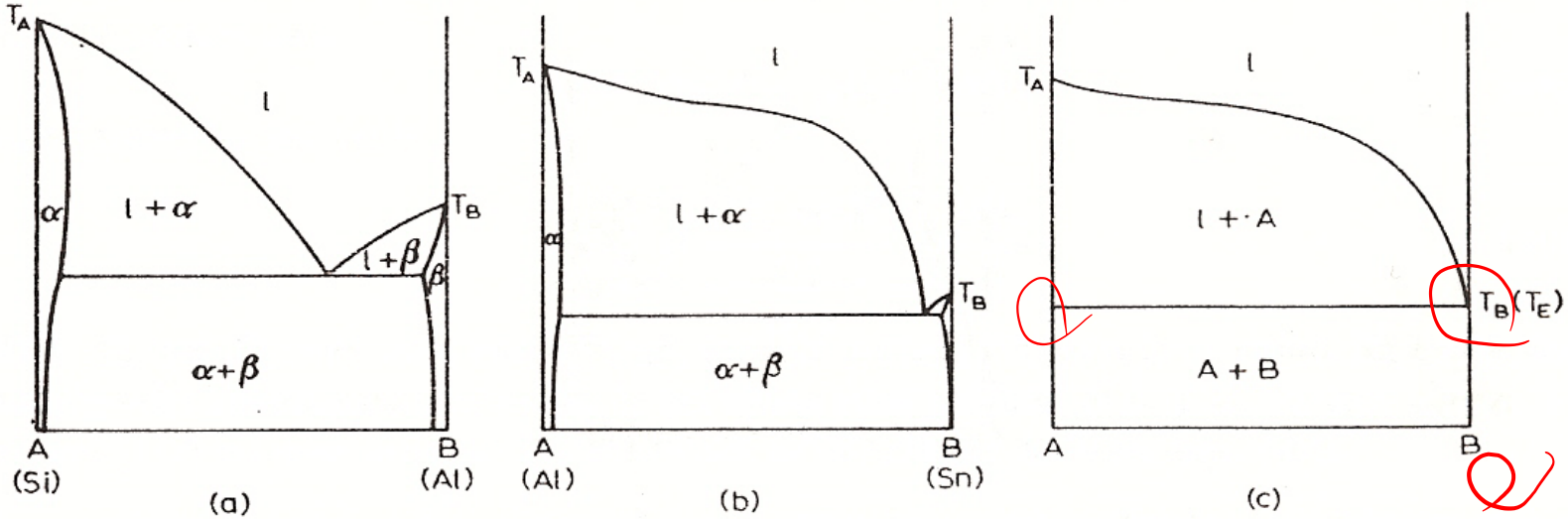

Fig. 53. Evolution of the limiting form of a binary eutectic phase diagram.

$$X_B^e = A\exp\left\{-\frac{Q}{RT}\right\}$$

a) $T \uparrow \Rightarrow X_B^e \uparrow$

b) It is interesting to note that, except at absolute zero, X_B^e can never be equal to zero, that is, no two compo -nents are ever completely insoluble in each other.

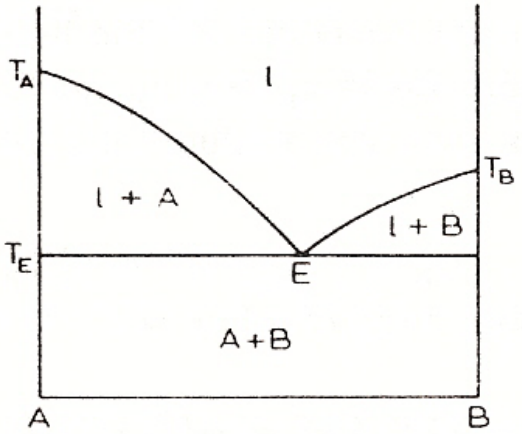

Fig. 54. Impossible form of a binary eutectic phase diagram.

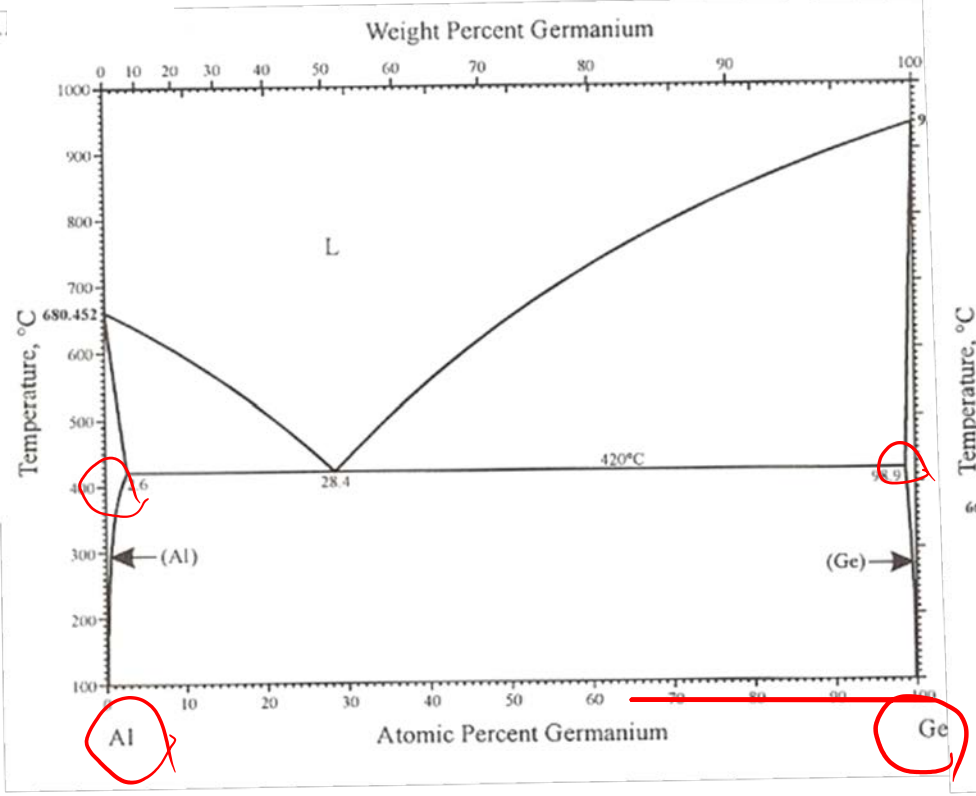
Weight Percent Germanium
Temperature, °C
Atomic Percent Germanium
L
680.452
420°C
28.4
(Al)
(Ge)
Al
Ge

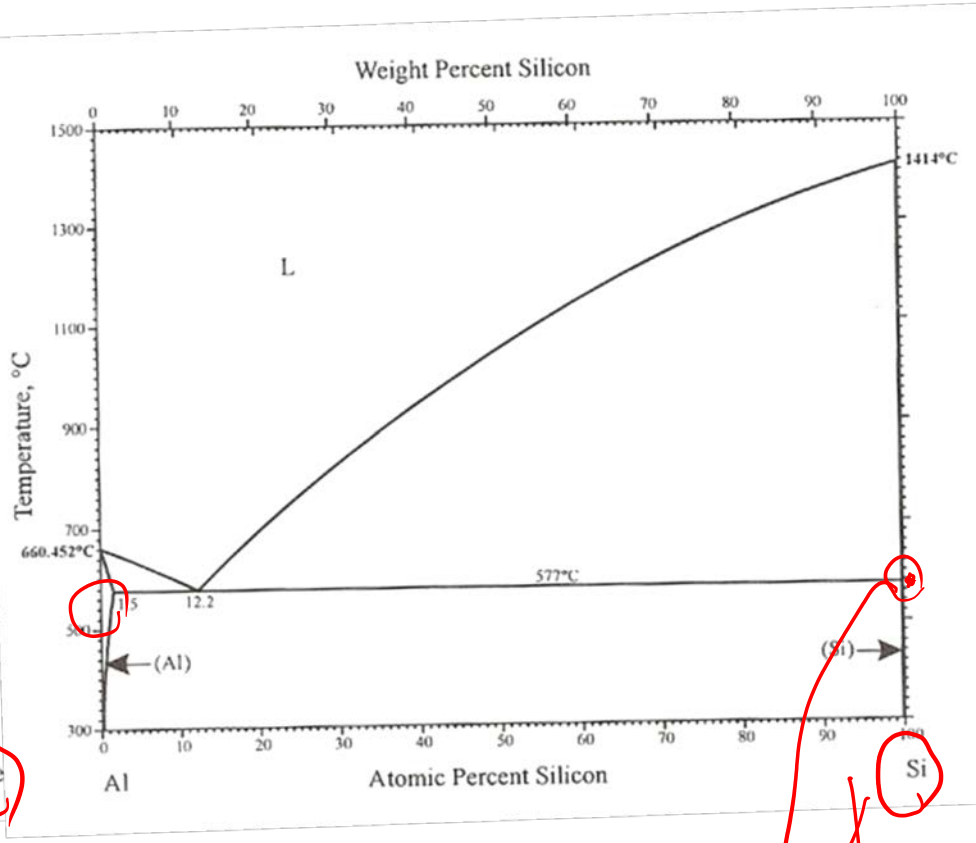
Weight Percent Silicon
Temperature, °C
Atomic Percent Silicon
L
1414°C
660.452°C
577°C
12.2
(Al)
(Si)
Al
Si

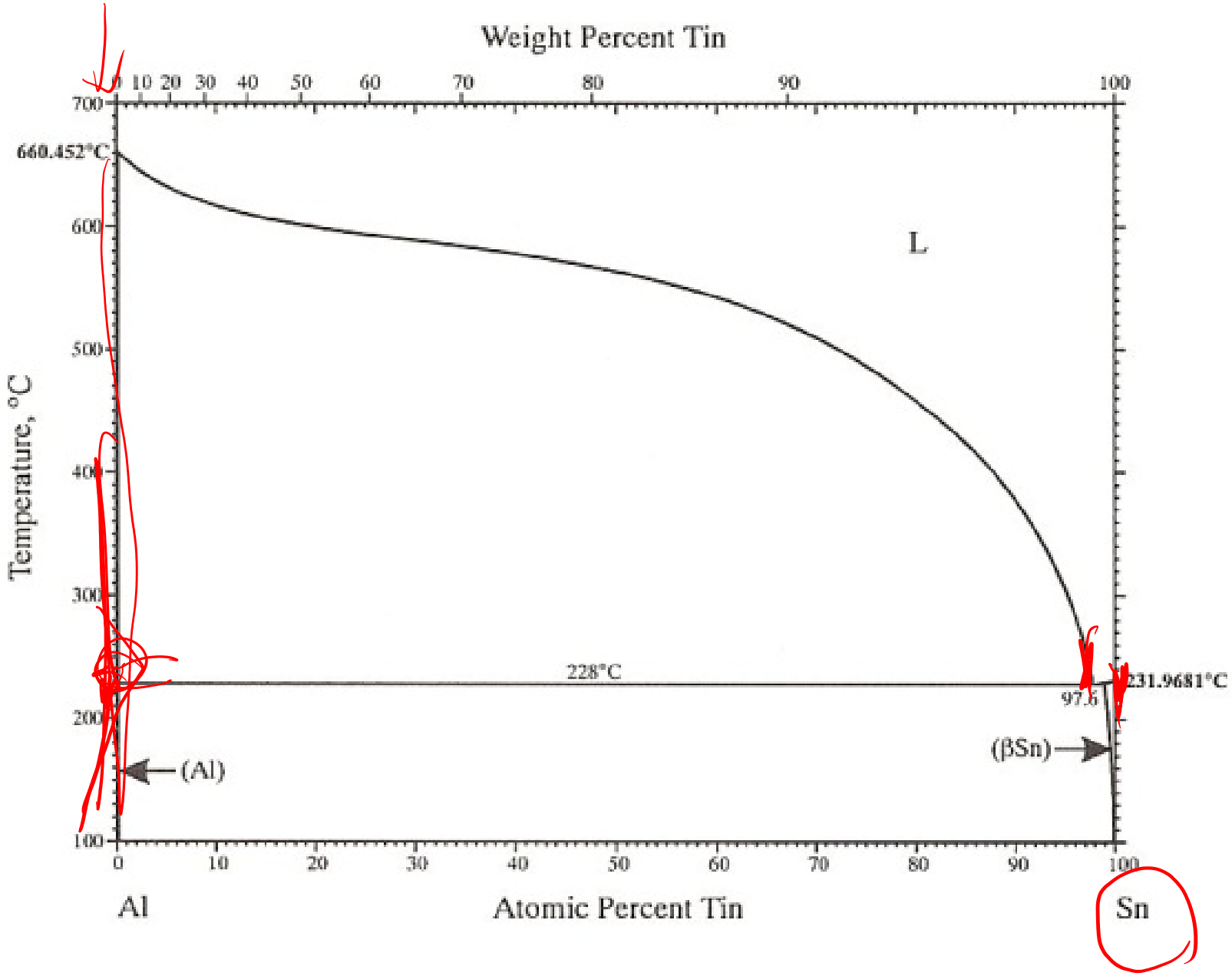
Weight Percent Tin
0 10 20 30 40 50 60 70 80 90 100
700
660.452°C
600
500
400
300
228°C
200
100
L
97.6
231.9681°C
(βSn)
(Al)
Temperature, °C
0 10 20 30 40 50 60 70 80 90 100
Al
Atomic Percent Tin
Sn

4.2.5. 2) Retrograde solidus curves

: A maximum solubility of the solute at a temperature between the melting point of the solvent and an invariant reaction isothermal

Solidus curve in the systems with low solubility
Ex) semiconductor research using Ge and Si as solvent metals

A high value of ΔH_B^S (or a large difference in the melting points of the components) is associate with a significant difference in atomic radii for A and B, which can lead to a large strain energy contribution to the heat of solutions.

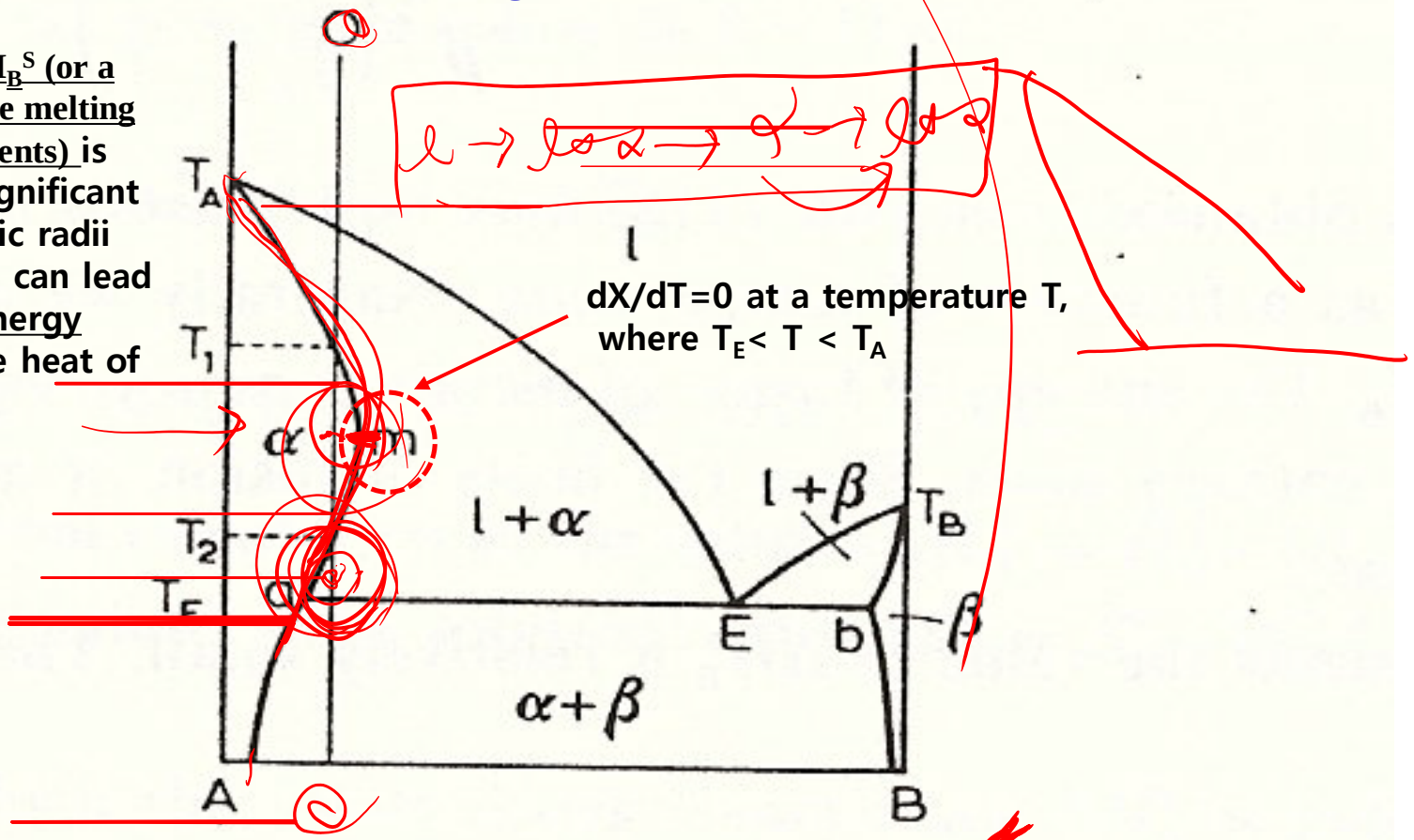

Fig. 57. Partial re-melting associated with retrograde solubility.

Intensive Homework 5: Understanding of retrograde solidus curves from a thermodynamic standpoint

4.2.5. Disposition of phase boundaries at the eutectic horizontal

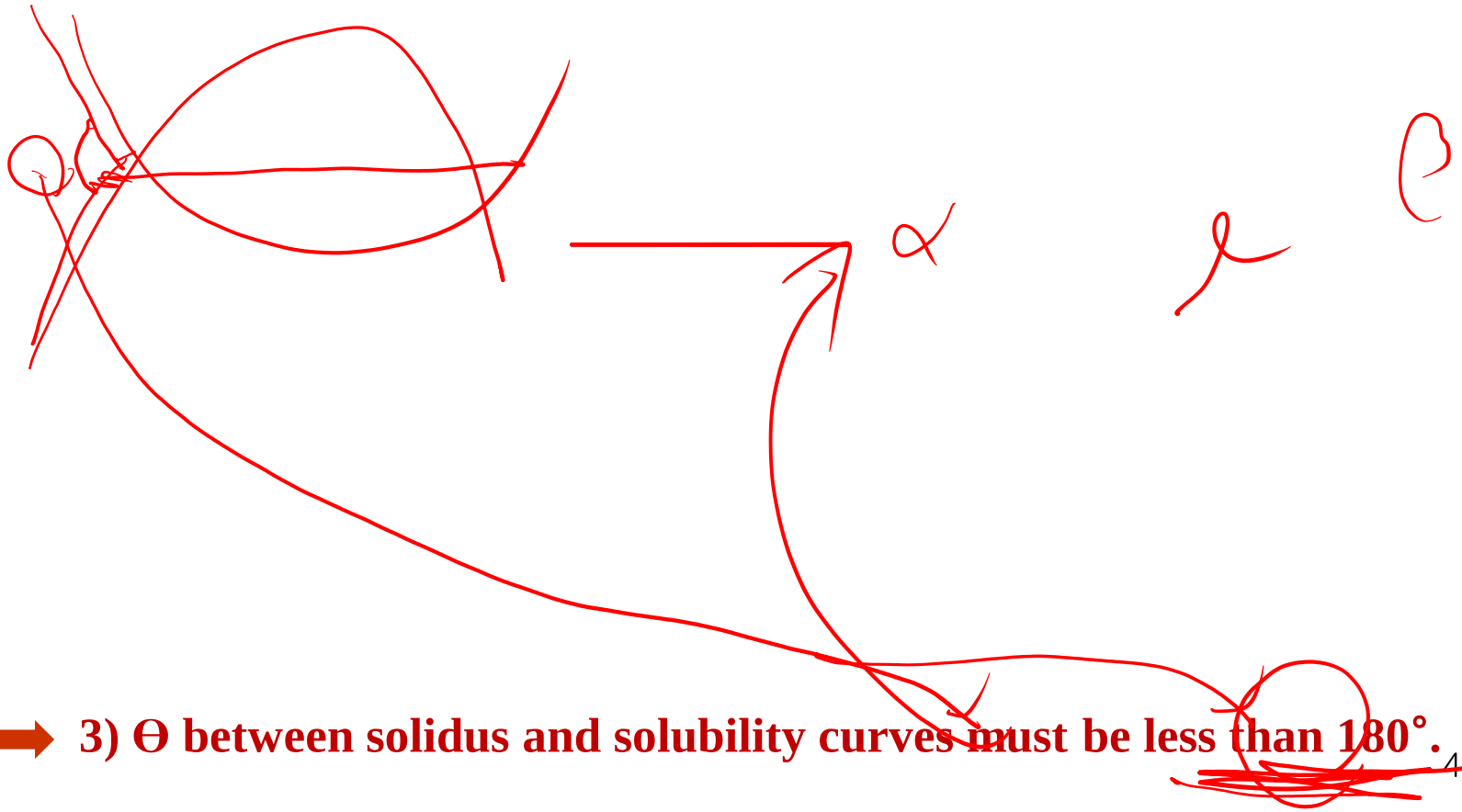

➡ **3) Θ between solidus and solubility curves must be less than 180°.**

4.2.5. Disposition of phase boundaries at the eutectic horizontal

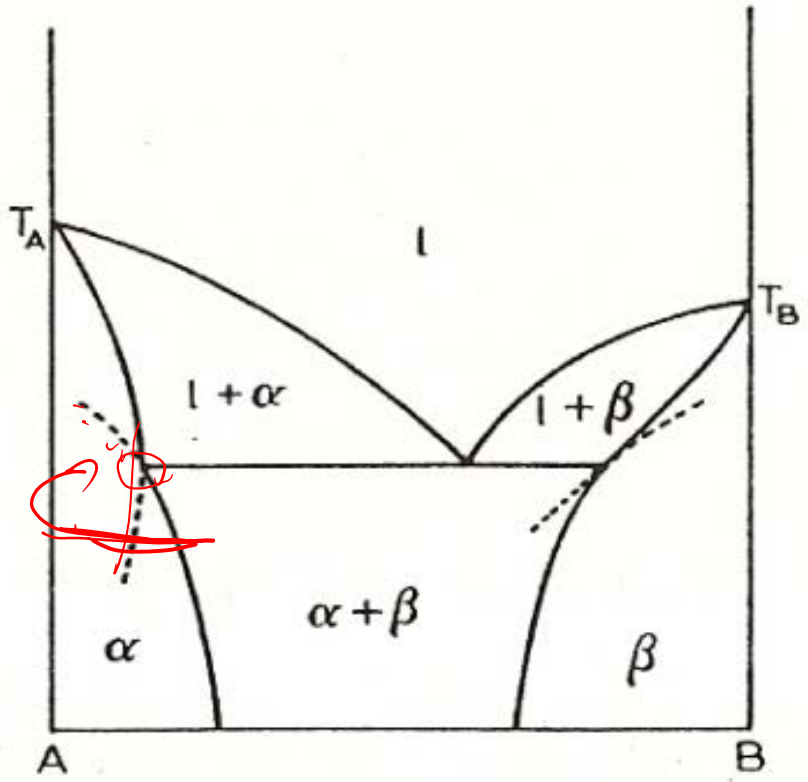

Fig. 60. Impossible dispositions of phase boundaries at a eutectic horizontal.

Θ between solidus and solubility curves must be less than 180°.

This is a general rule applicable to all curves which meet at an invariant reaction horizontal in a binary diagram, whether they be eutectic, peritectics, eutectoid, etc., horizontals.

Contents for today's class

- Binary phase diagrams

1) Simple Phase Diagrams

* **Pressure-Temperature-Composition phase diagram for a system with continuous series of solutions**

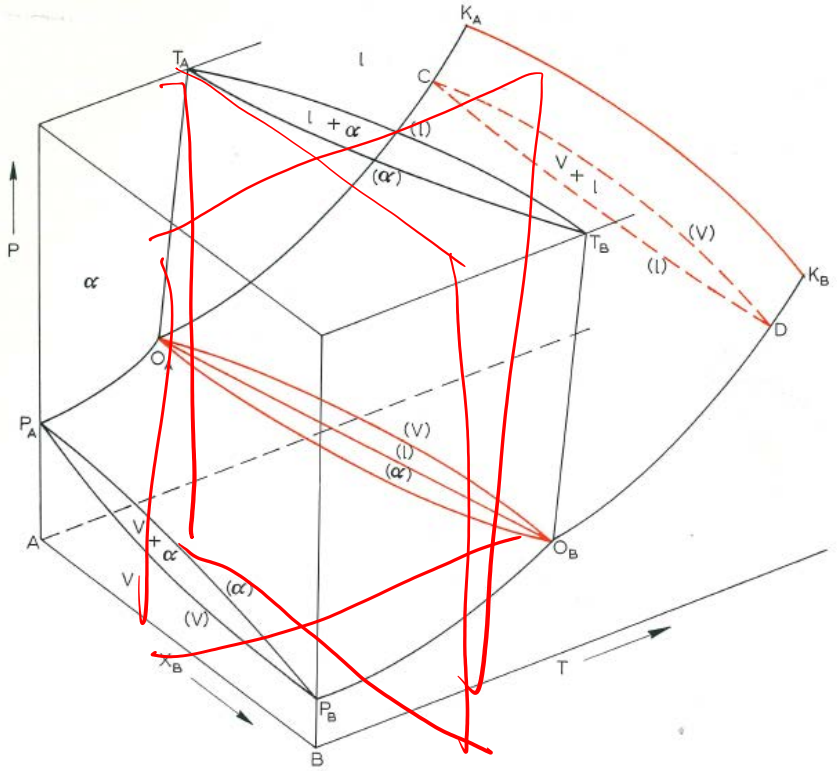

Fig. 35. Pressure–temperature–composition phase diagram for a system with continuous series of solutions

3) Simple Eutectic Systems

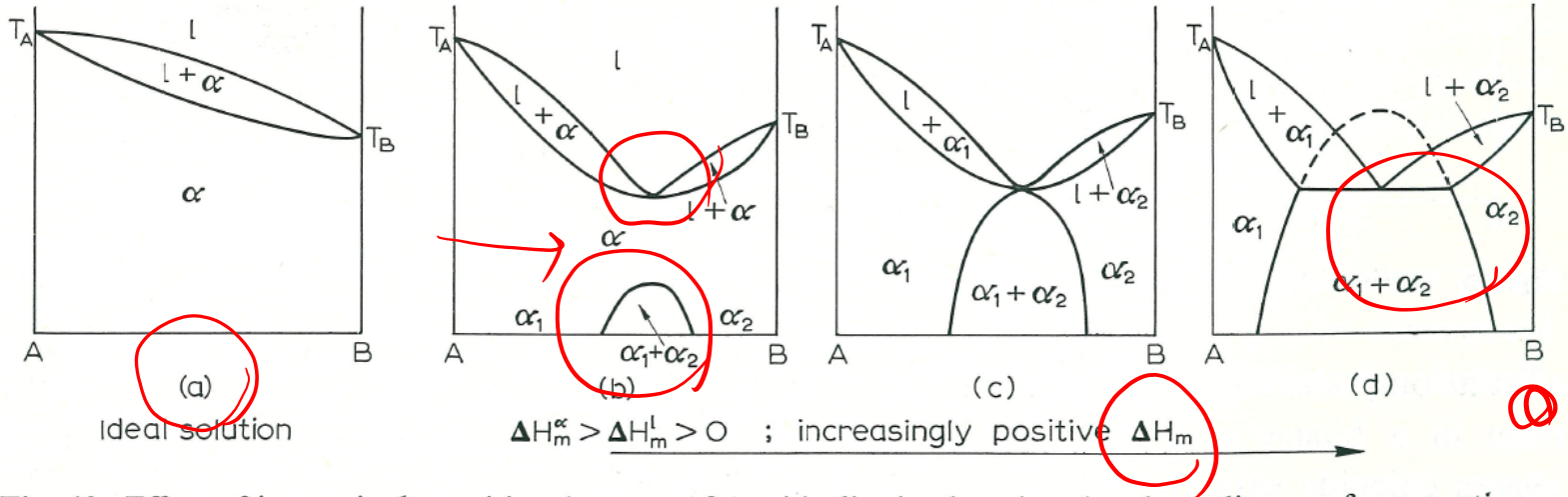

Fig. 43. Effect of increasingly positive departure from ideality in changing the phase diagram for a continuous series of solutions to a eutectic-type.

By plotting a series of the free energy-composition curves at different temperatures we established the manner in which the phase compositions changes with temperature. In other words, we determined the phase limits or phase boundaries as a function of temperature. A phase diagram is nothing more than a presentation of data on the position of phase boundaries as a function of temperature.

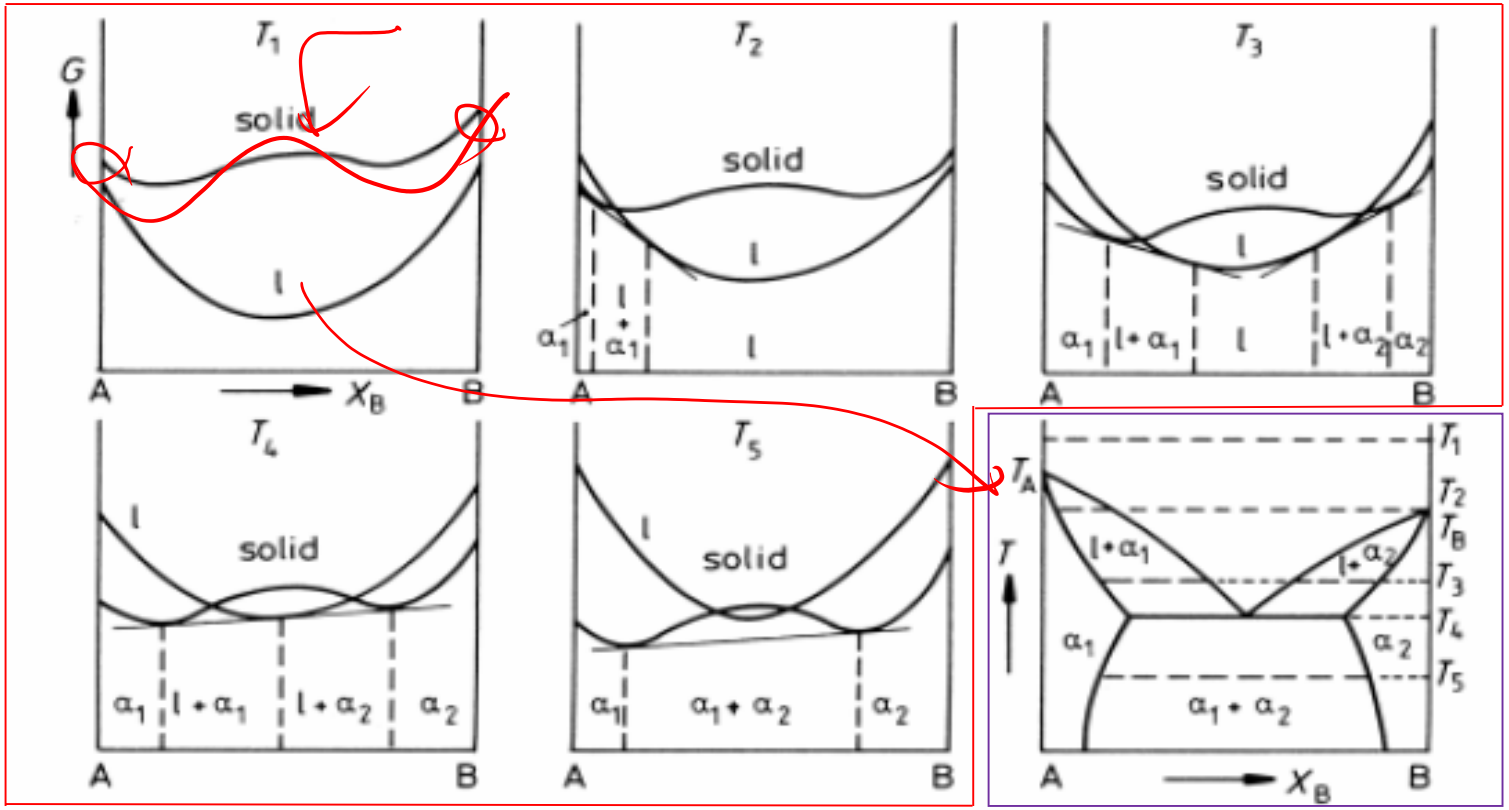

Fig 1.32 The derivation of a eutectic phase diagram where both solid phases have the same crystal structure. (After A.H. Cottrell, *Theoretical Structural Metallurgy*, Edward Arnold, London, 1955,©Sir Alan Cottrell.)

same crystal structure

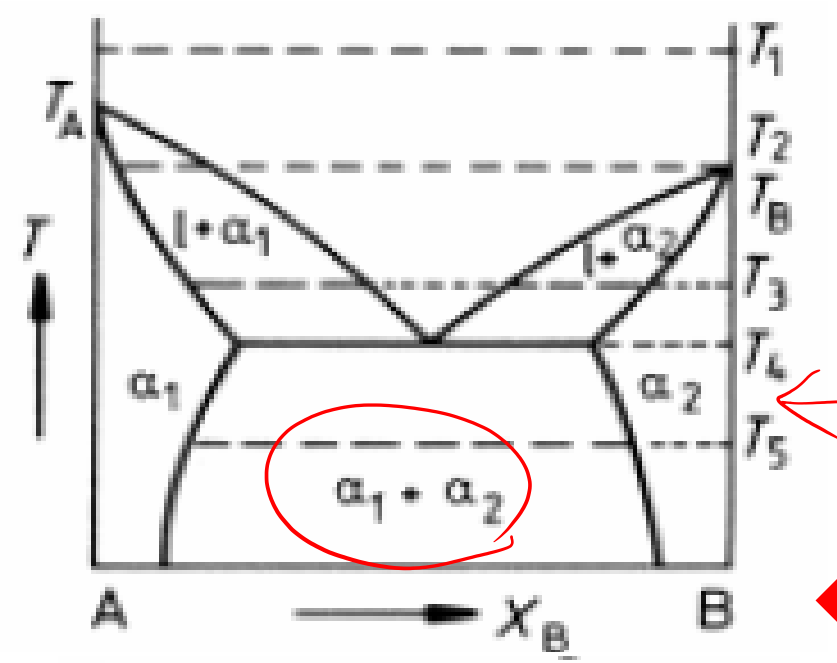

different crystal structure

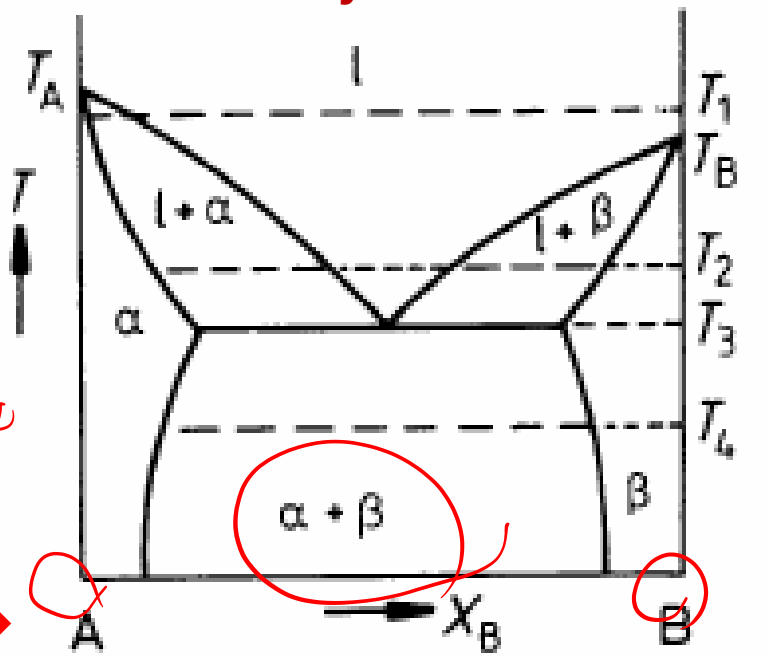

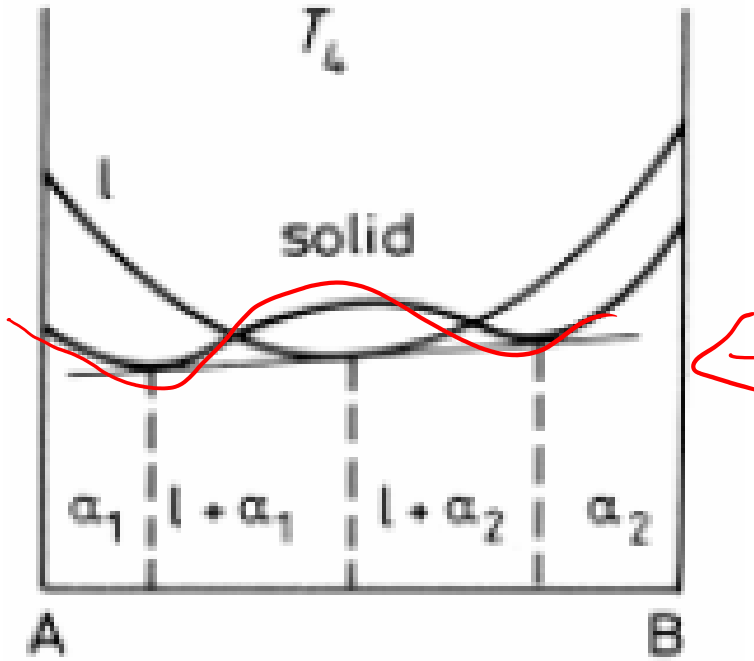

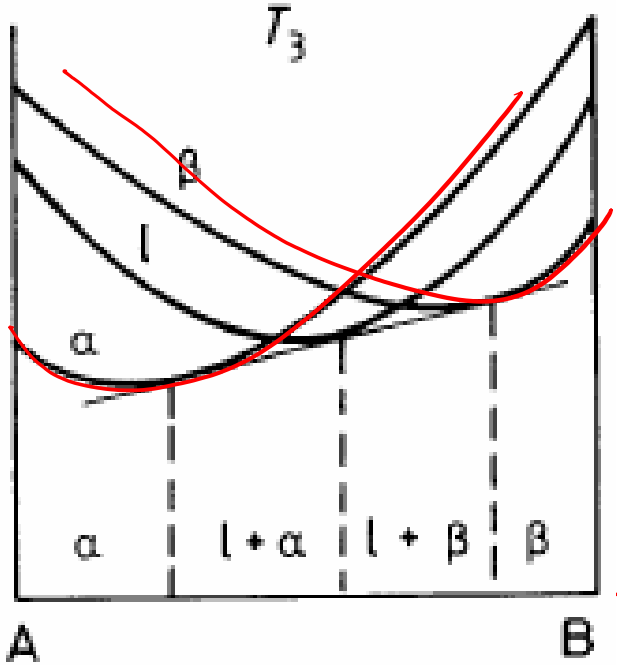

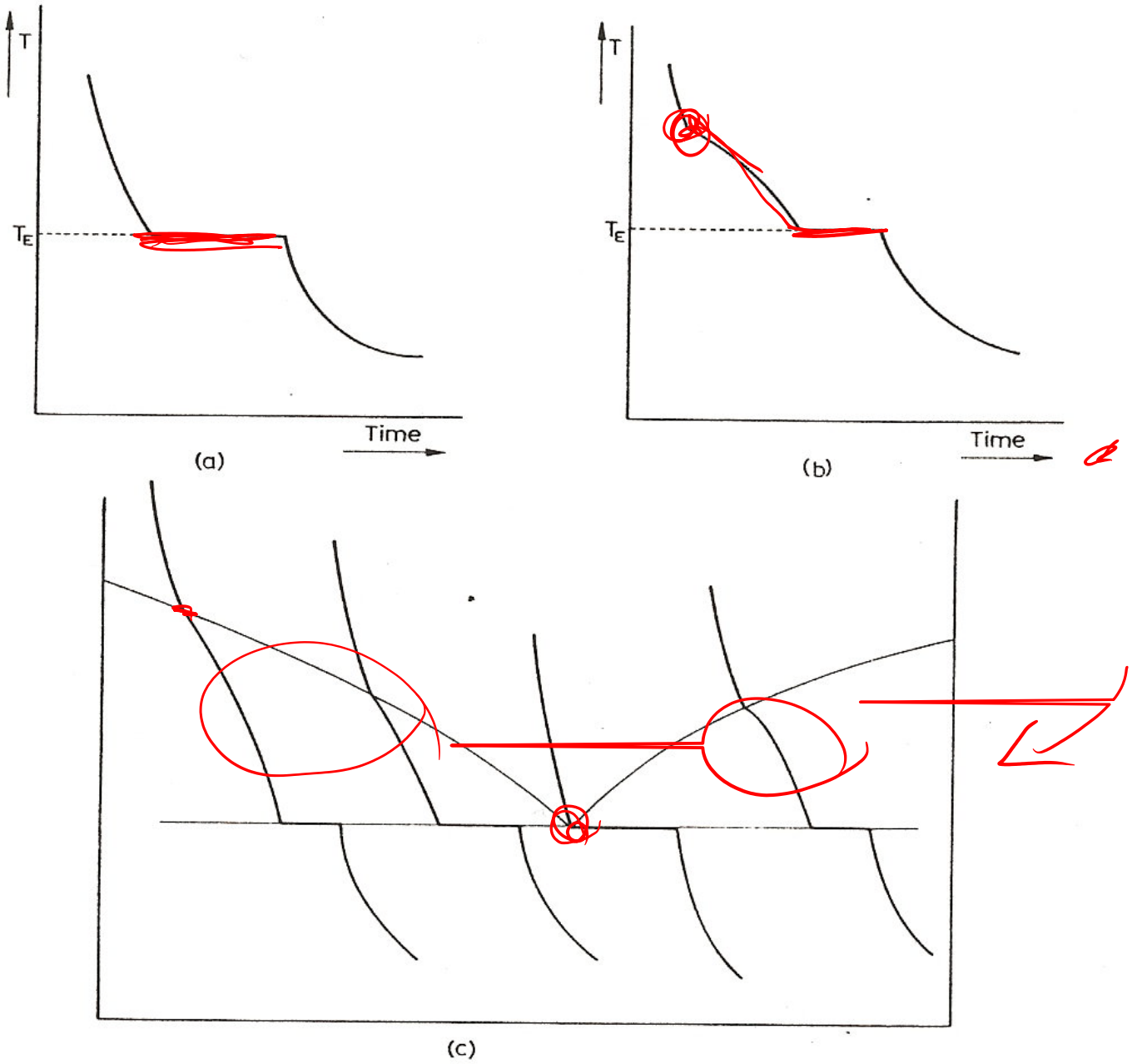

Fig. 48. Cooling curve for (a) the eutectic alloy, (b) hypo-eutectic alloy *N*, and (c) a series of alloys, allowing the determination of the liquidus and eutectic horizontal.

4.2.3. Limiting forms of eutectic phase diagram

1) Complete immiscibility of two metals does not exist.

: The solubility of one metal in another may be so low (e.g. Cu in Ge $<10^{-7}$ at%.)
that it is difficult to detect experimentally, but there will always be a measure of solubility.

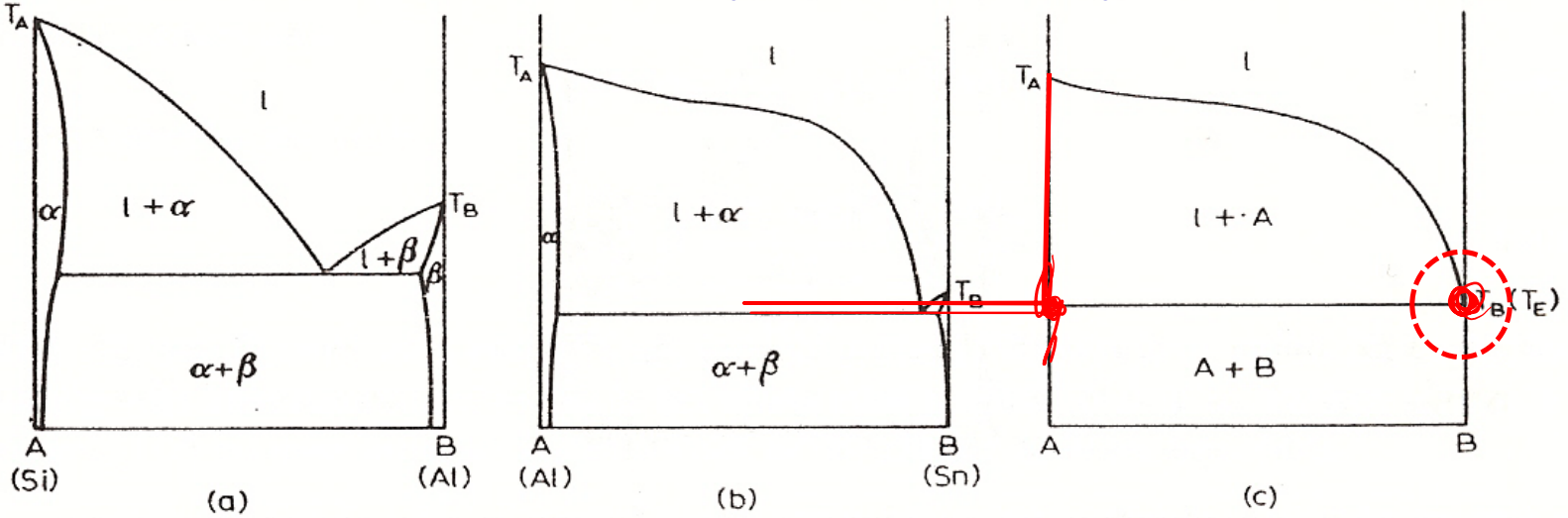

Fig. 53. Evolution of the limiting form of a binary eutectic phase diagram.

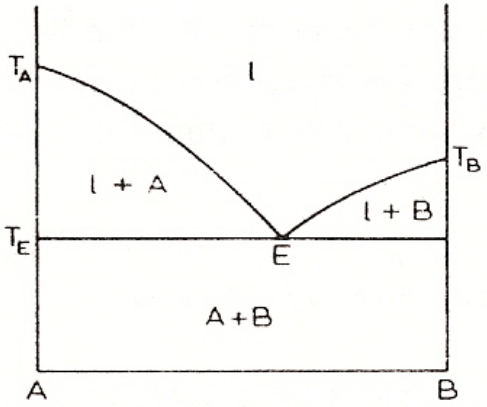

Fig. 54. Impossible form of a binary eutectic phase diagram.

4.2.5. 2) Retrograde solidus curves

: A maximum solubility of the solute at a temperature between the melting point of the solvent and an invariant reaction isothermal

Solidus curve in the systems with low solubility
Ex) semiconductor research using Ge and Si as solvent metals

A high value of ΔH_B^S (or a large difference in the melting points of the components) is associate with a significant difference in atomic radii for A and B, which can lead to a large strain energy contribution to the heat of solutions.

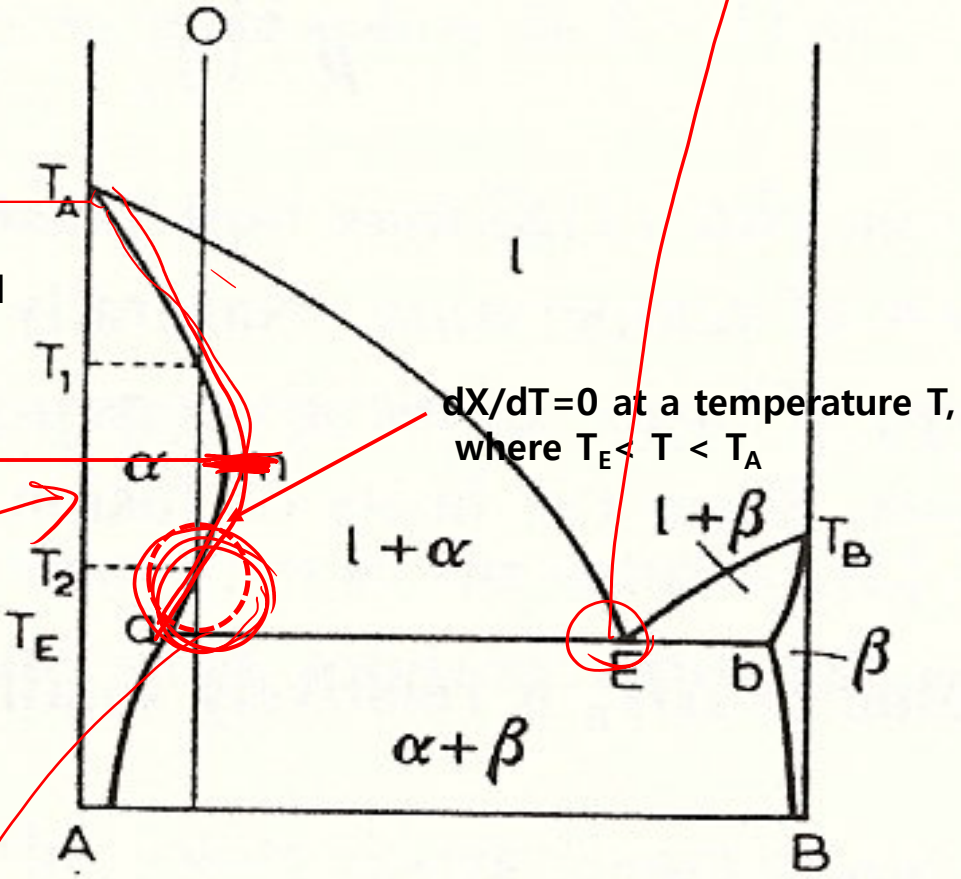

dX/dT=0 at a temperature T, where $T_E < T < T_A$

Fig. 57. Partial re-melting associated with retrograde solubility.

Intensive Homework 5: Understanding of retrograde solidus curves from a thermodynamic standpoint

4.2.5. Disposition of phase boundaries at the eutectic horizontal

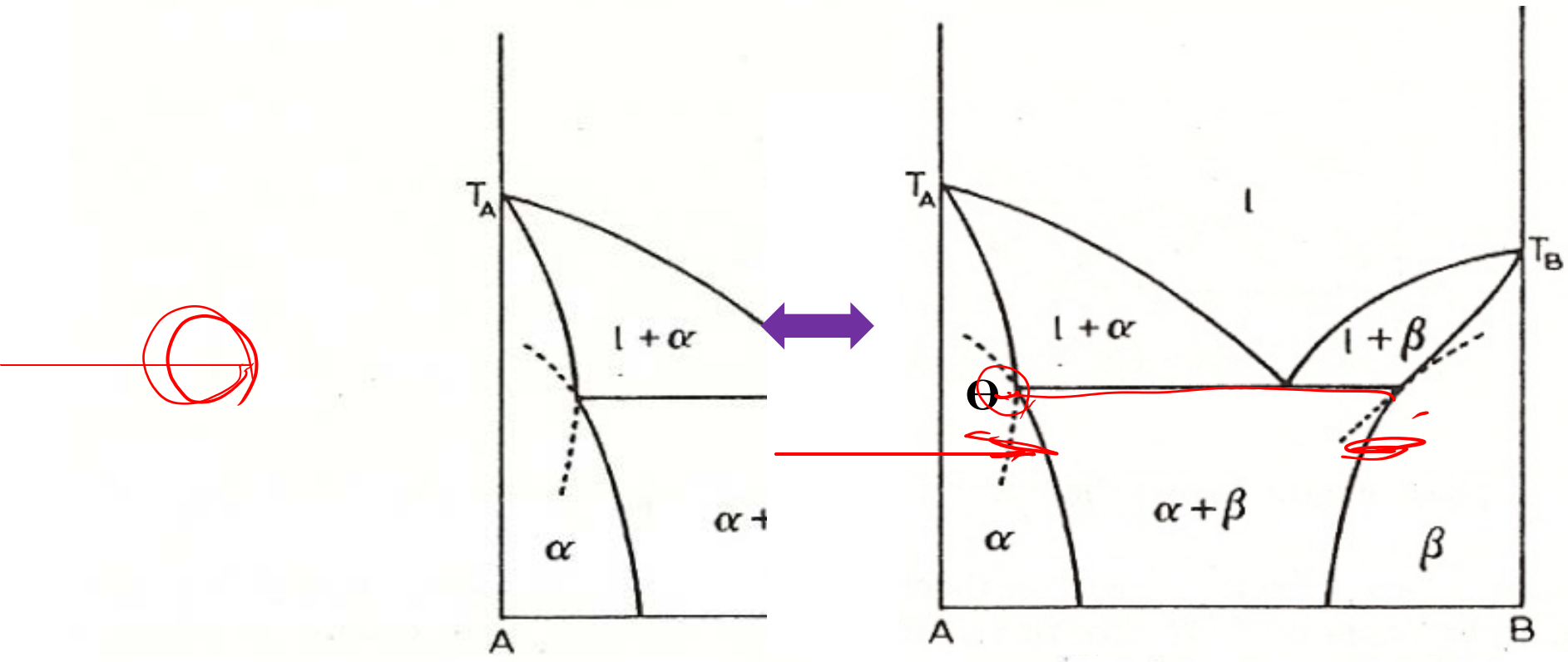

Fig. 60. Impossible dispositions of phase boundaries at a eutectic horizontal.

3) Θ between solidus and solubility curves must be less than 180°.

This is a general rule applicable to all curves which meet at an invariant reaction horizontal in a binary diagram, whether they be eutectic, peritectics, eutectoid, etc., horizontals.

2021 Spring

"Phase Equilibria *in* Materials"

03.25.2021

Eun Soo Park

Office: 33-313
Telephone: 880-7221
Email: espark@snu.ac.kr
Office hours: by an appointment

Contents for previous class

CHAPTER 4
Binary Phase Diagrams

Three-Phase Equilibrium Involving Limited Solubility of the Components in the Solid State but Complete Solubility in the Liquid State

* Three-Phase Equilibrium : Eutectic Reactions

a) Structural Factor: Hume-Rothery Rules

Empirical rules for substitutional solid-solution

complete solid solution ⟷ **limited solid solution**

Similar atomic radii, the same valency and crystal structure

b) The eutectic reaction

c) Limiting forms of eutectic phase diagrams

d) Retrogade solidus curves

Contents for previous class

- Binary phase diagrams

1) Simple Phase Diagrams

* **Pressure-Temperature-Composition phase diagram for a system with continuous series of solutions**

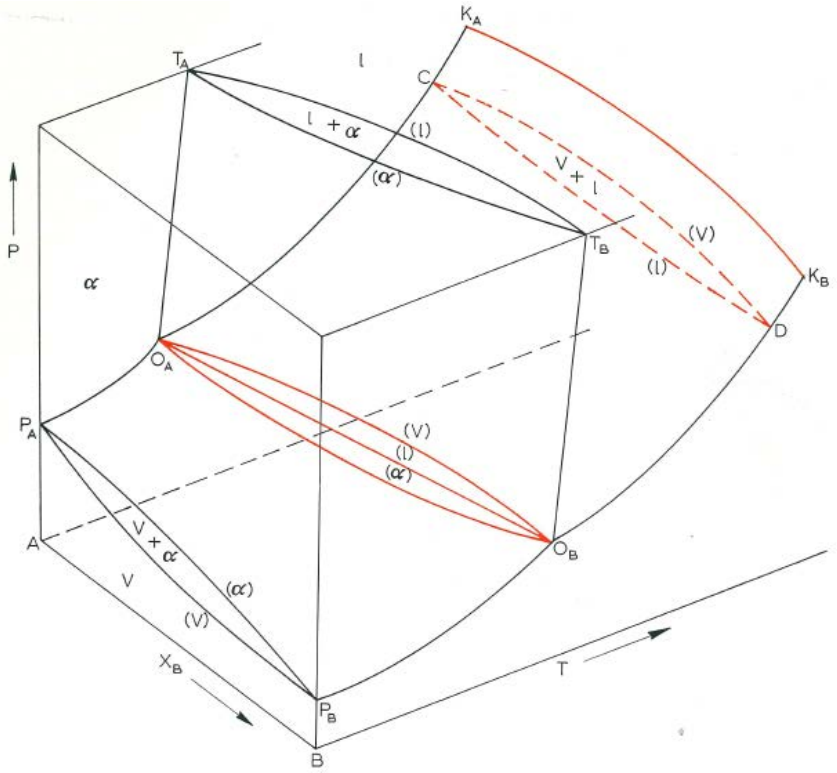

Fig. 35. Pressure–temperature–composition phase diagram for a system with continuous series of solutions

3) Simple Eutectic Systems

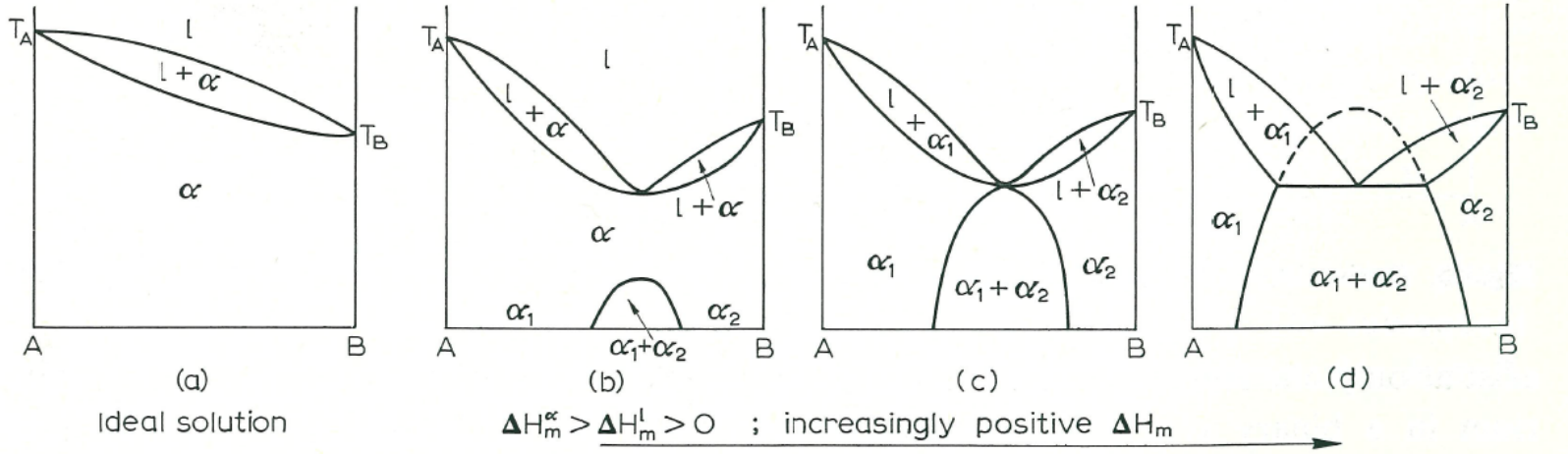

Fig. 43. Effect of increasingly positive departure from ideality in changing the phase diagram for a continuous series of solutions to a eutectic-type.

By plotting a series of the free energy-composition curves at different temperatures we established the manner in which the phase compositions changes with temperature. In other words, we determined the phase limits or phase boundaries as a function of temperature. A phase diagram is nothing more than a presentation of data on the position of phase boundaries as a function of temperature.

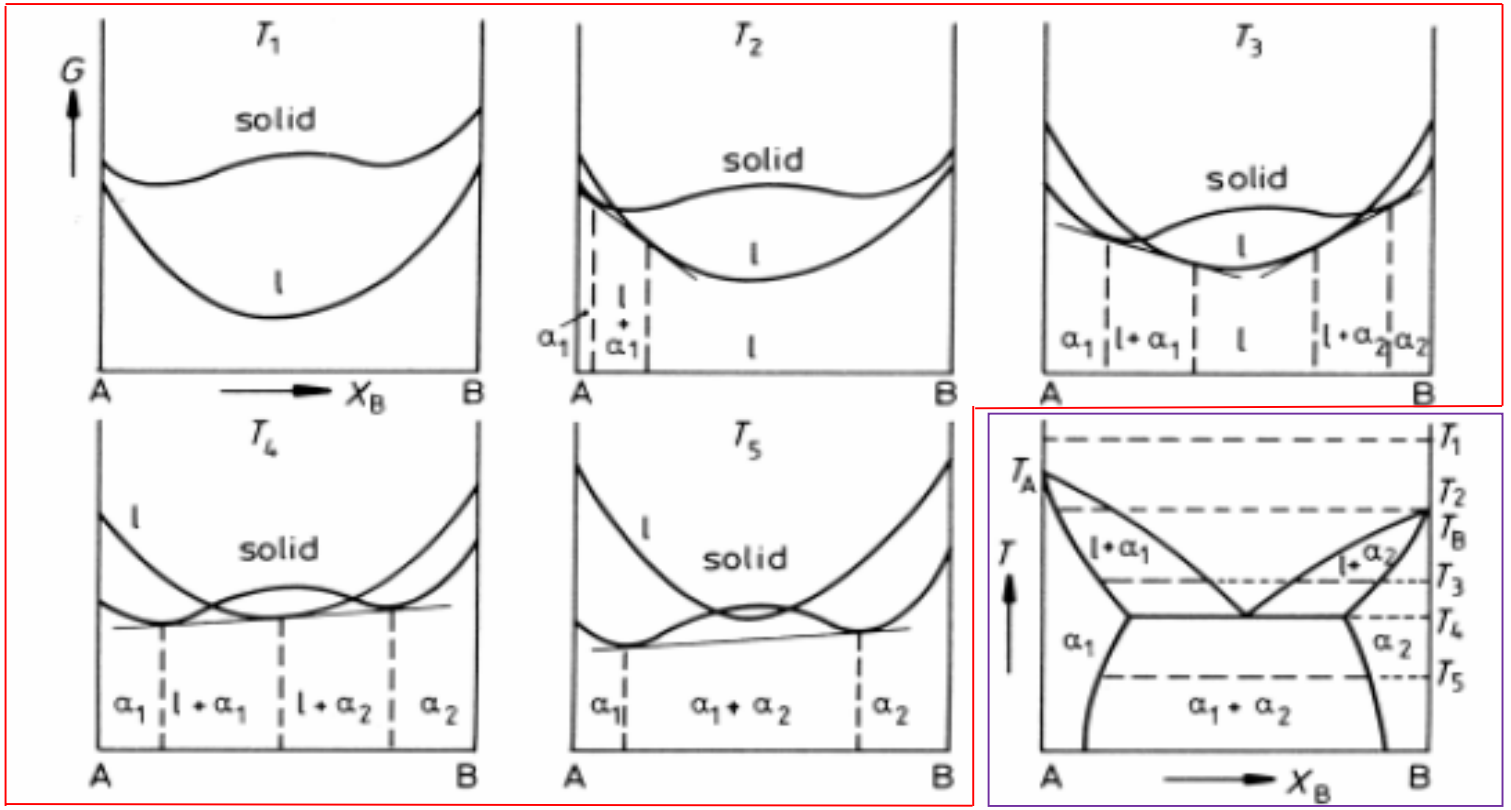

Fig 1.32 The derivation of a eutectic phase diagram where both solid phases have the same crystal structure. (After A.H. Cottrell, *Theoretical Structural Metallurgy*, Edward Arnold, London, 1955,©Sir Alan Cottrell.)

same crystal structure

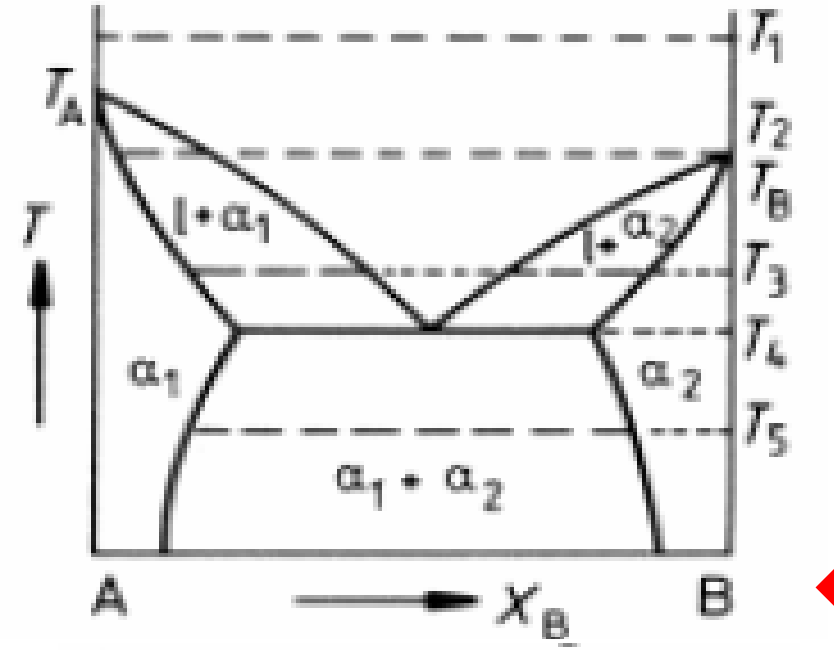

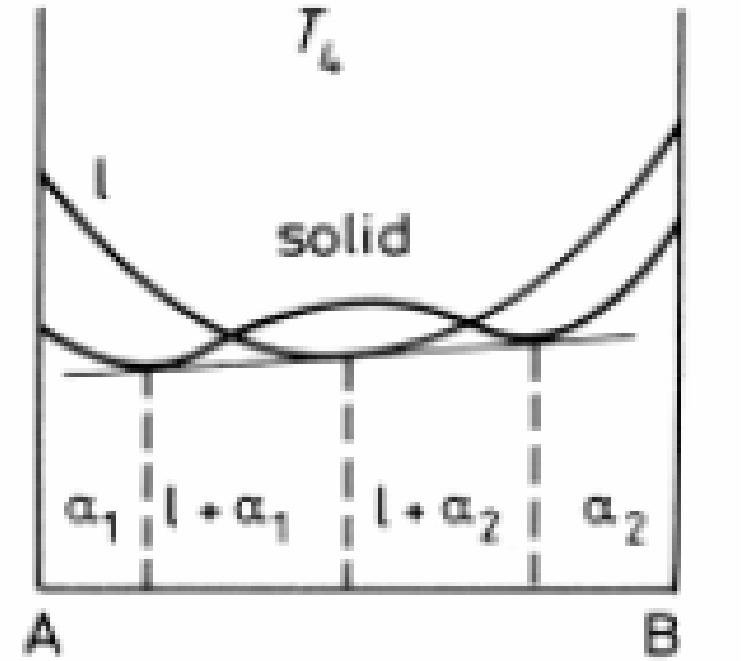

different crystal structure

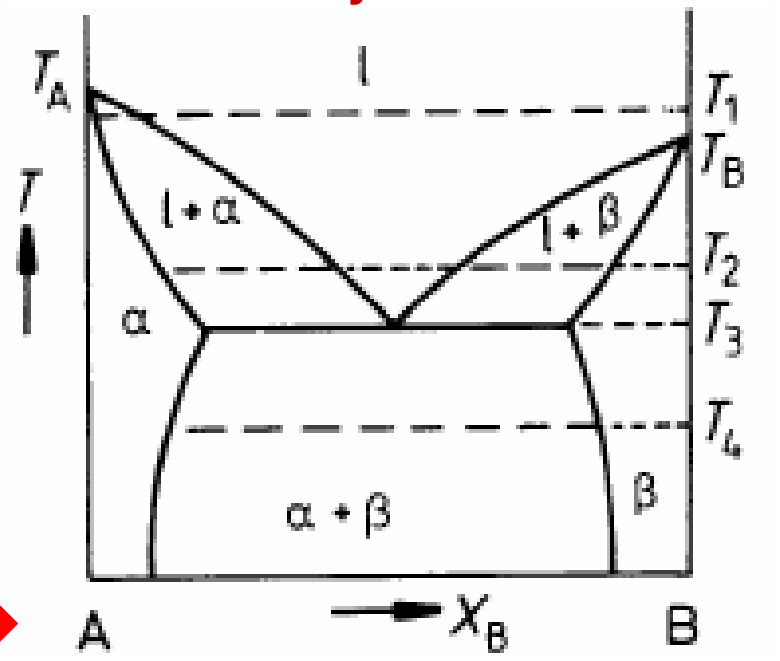

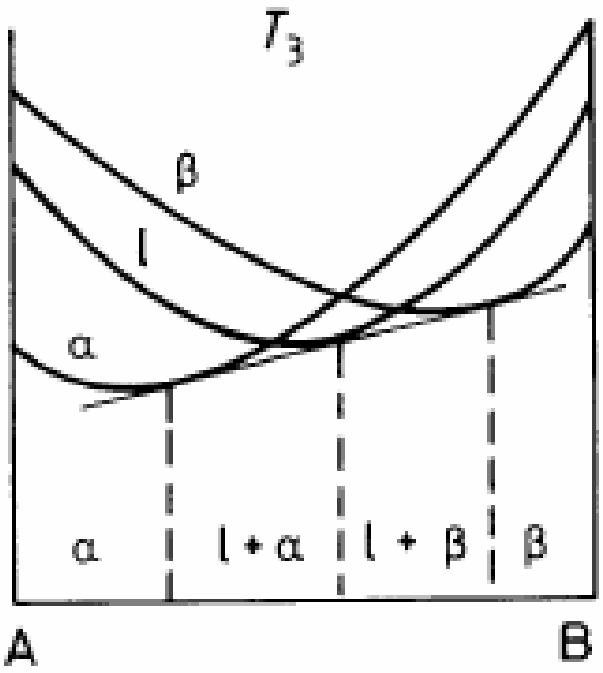

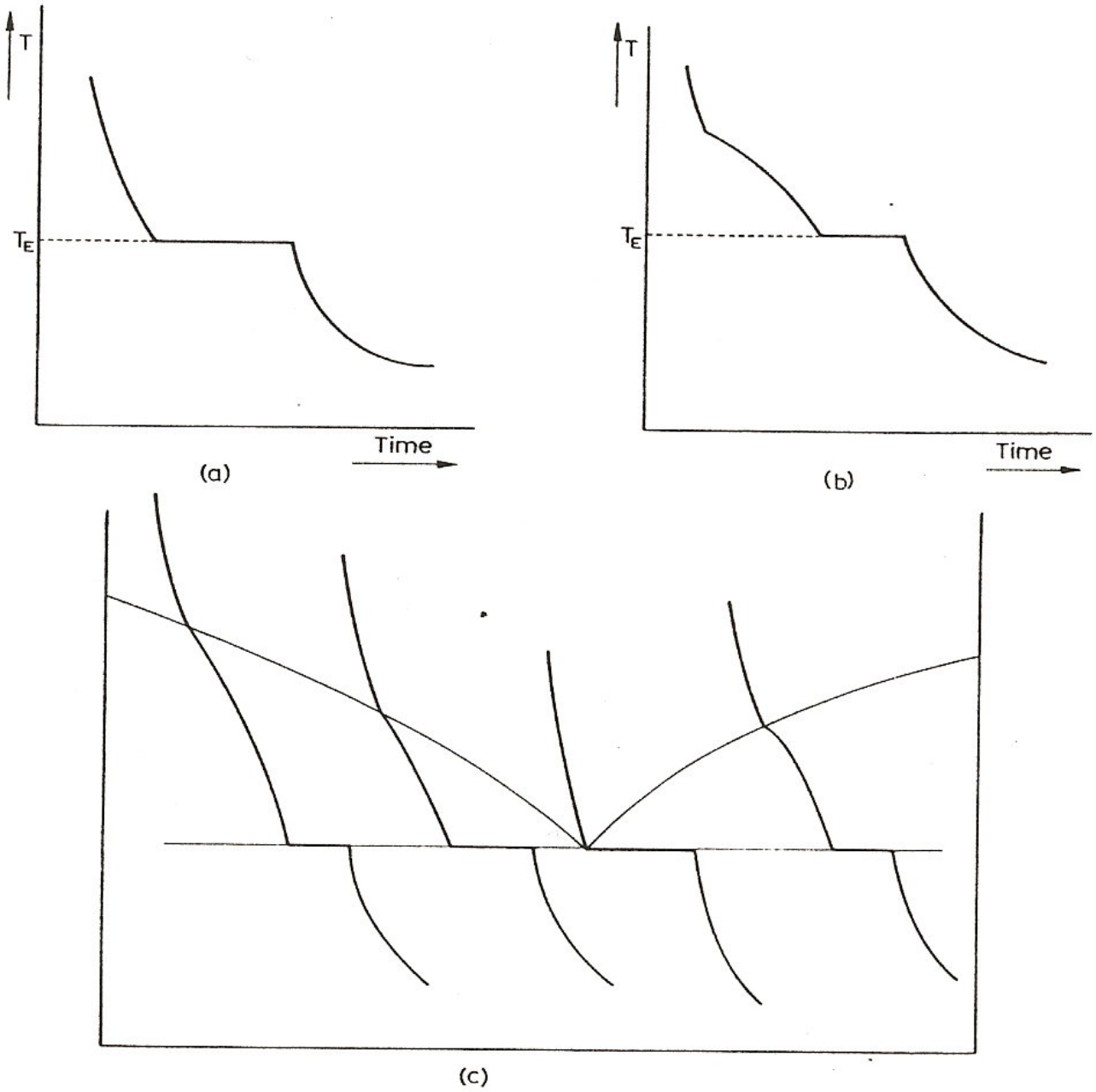

Fig. 48. Cooling curve for (a) the eutectic alloy, (b) hypo-eutectic alloy *N*, and (c) a series of alloys, allowing the determination of the liquidus and eutectic horizontal.

4.2.3. Limiting forms of eutectic phase diagram

1) Complete immiscibility of two metals does not exist.

: The solubility of one metal in another may be so low (e.g. Cu in Ge $<10^{-7}$ at%.)
that it is difficult to detect experimentally, but there will always be a measure of solubility.

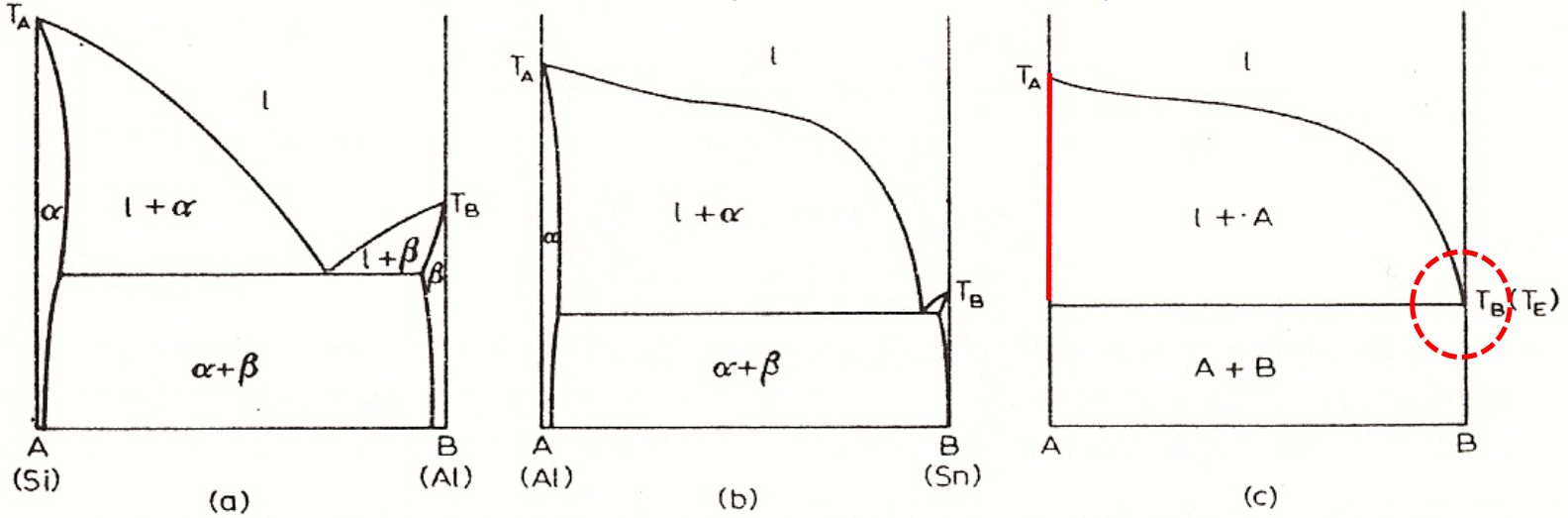

Fig. 53. Evolution of the limiting form of a binary eutectic phase diagram.

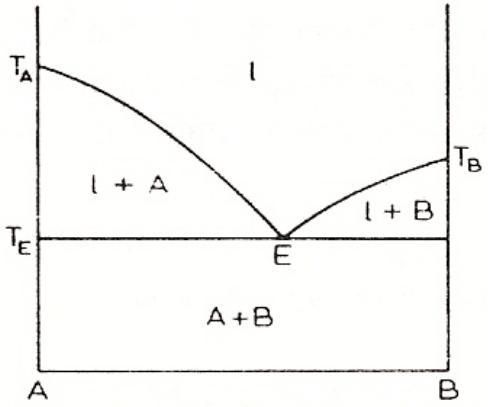

Fig. 54. Impossible form of a binary eutectic phase diagram.

4.2.5. 2) Retrograde solidus curves

: A maximum solubility of the solute at a temperature between the melting point of the solvent and an invariant reaction isothermal

Solidus curve in the systems with low solubility

Ex) semiconductor research using Ge and Si as solvent metals

A high value of ΔH_B^S (or a large difference in the melting points of the components) is associate with a significant difference in atomic radii for A and B, which can lead to a large strain energy contribution to the heat of solutions.

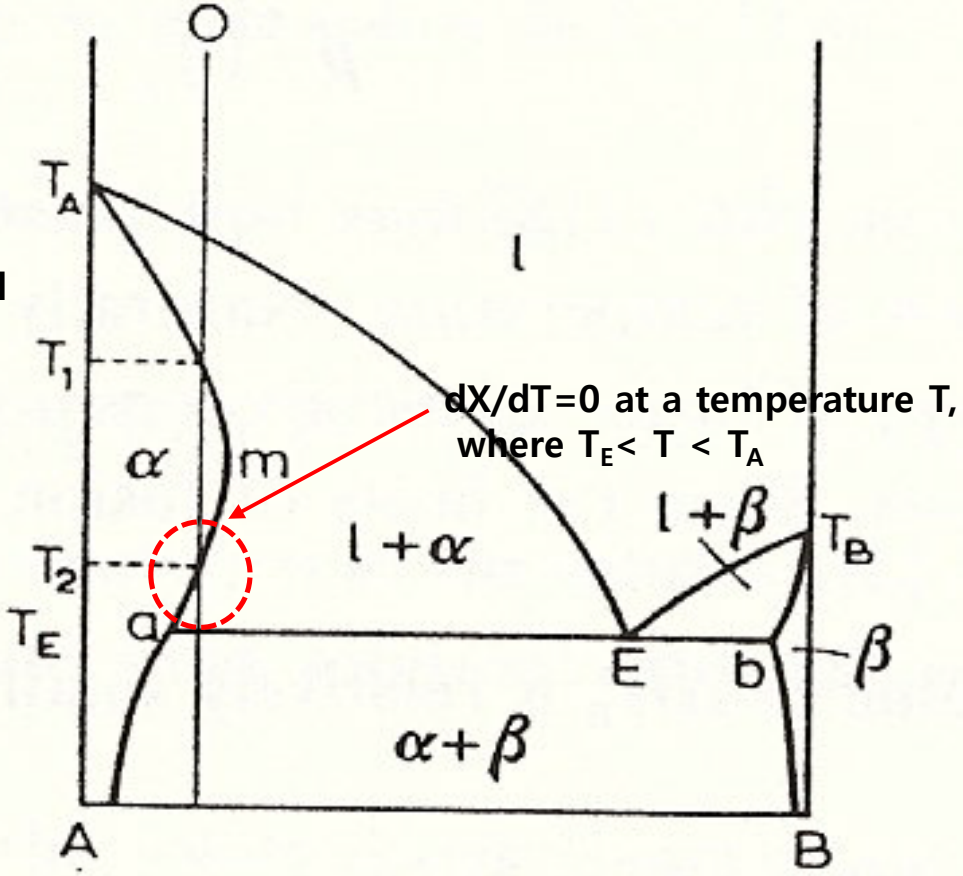

Fig. 57. Partial re-melting associated with retrograde solubility.

Intensive Homework 5: Understanding of retrograde solidus curves from a thermodynamic standpoint

4.2.5. Disposition of phase boundaries at the eutectic horizontal

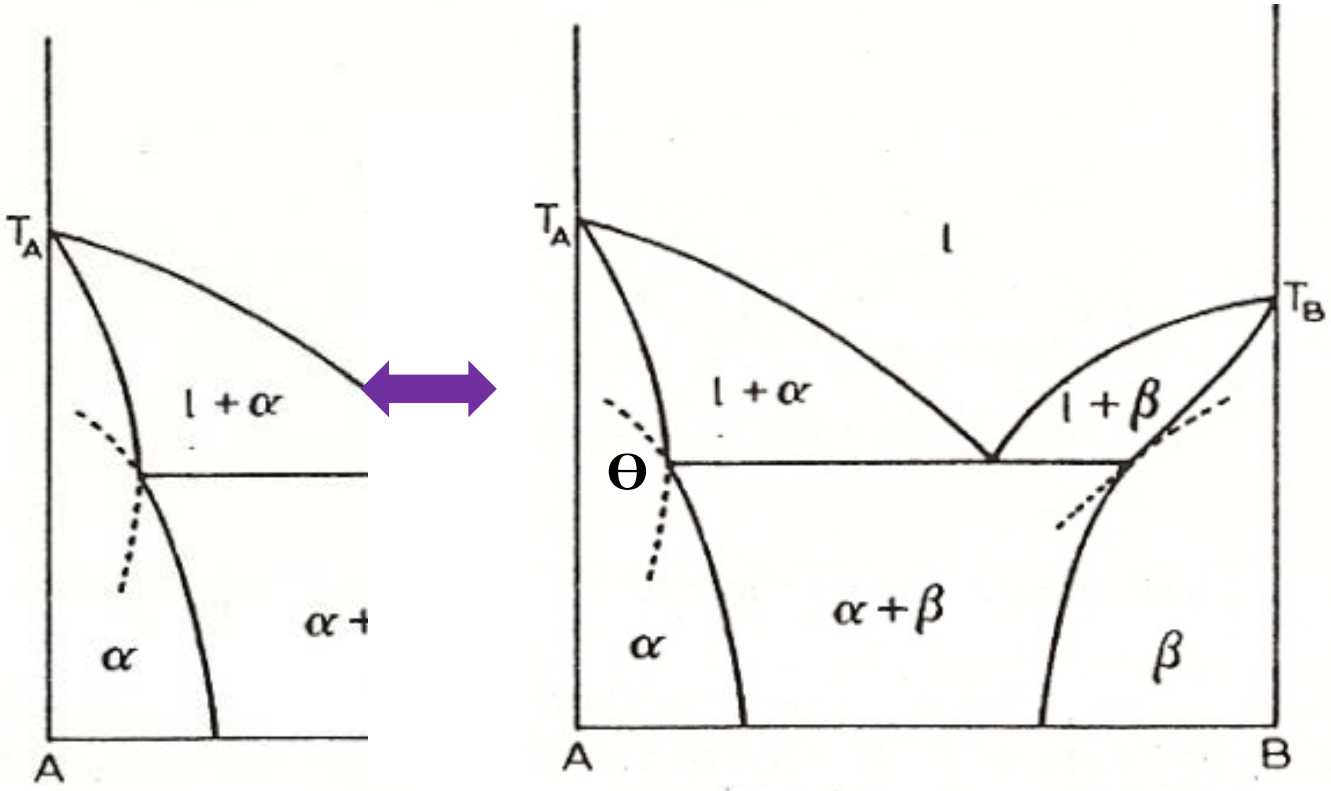

Fig. 60. Impossible dispositions of phase boundaries at a eutectic horizontal.

3) Θ between solidus and solubility curves must be less than 180°.

This is a general rule applicable to all curves which meet at an invariant reaction horizontal in a binary diagram, whether they be eutectic, peritectics, eutectoid, etc., horizontals.

Contents for today's class

CHAPTER 4
Binary Phase Diagrams

Three-Phase Equilibrium Involving Limited Solubility of the Components in the Solid State but Complete Solubility in the Liquid State

4.3. Three-Phase Equilibrium : Peritectic Reactions

- Eutectoid reaction

- Peritectic reaction

  Formation of intermediate phases by peritectic reaction

  Non-stoichiometeric compounds

- Congruent transformations

The Gibbs Phase Rule: quantitative data

In chemistry, Gibbs' phase rule describes the possible number of degrees of freedom (F) in a closed system at equilibrium, in terms of the number of separate phases (P) and the number of chemical components (C) in the system. It was deduced from thermodynamic principles by Josiah Willard Gibbs in the 1870s.

Gibbs phase rule **F =C+N-P**

F: degree of freedom
C: number of chemical variables
N: number of non-chemical variables
P: number of phases

In general, Gibbs' rule then follows, as:

$$F = C - P + 2$$ (from T, P).

From Wikipedia, the free encyclopedia

According to the condensed Phase Rule, $f = c - p + 1$

For a binary system the equilibria possible are summarized below.

Number of components	*Number of phases*	*Variance*	*Equilibrium*	
$c = 2$	$p = 1$	$f = 2$	bivariant	$p = c - 1$
$c = 2$	$p = 2$	$f = 1$	monovariant	$p = c$
$c = 2$	$p = 3$	$f = 0$	invariant	$p = c + 1$

Invariant reactions which have been observed in binary diagrams are listed below, together with the nomenclature given to such reactions.

$l \rightleftharpoons \alpha + \beta$	eutectic reaction	(*e.g.* Ag–Cu system)
$\gamma \rightleftharpoons \alpha + \beta$	eutectoid reaction	(*e.g.* C–Fe system)
$l_1 \rightleftharpoons \alpha + l_2$	monotectic reaction	(*e.g.* Cu–Pb system)
$\alpha \rightleftharpoons \beta + l$	metatectic reaction	(*e.g.* Ag–Li system)
$l + \alpha \rightleftharpoons \beta$	peritectic reaction	(*e.g.* Cu–Zn system)
$\alpha + \beta \rightleftharpoons \gamma$	peritectoid reaction	(*e.g.* Al–Cu system)
$l_1 + l_2 \rightleftharpoons \alpha$	syntectic reaction	(*e.g.* K–Zn system)

Invariant reactions involving liquid phases have a name ending in *–tectic* whilst those occurring completely in the solid state end in *–tectoid*.

Eutectoid reaction

Eutectoid reaction :

$$\gamma_{eutectoid} \underset{T_{eu.}}{\overset{cooling}{\rightleftharpoons}} \alpha + \beta$$

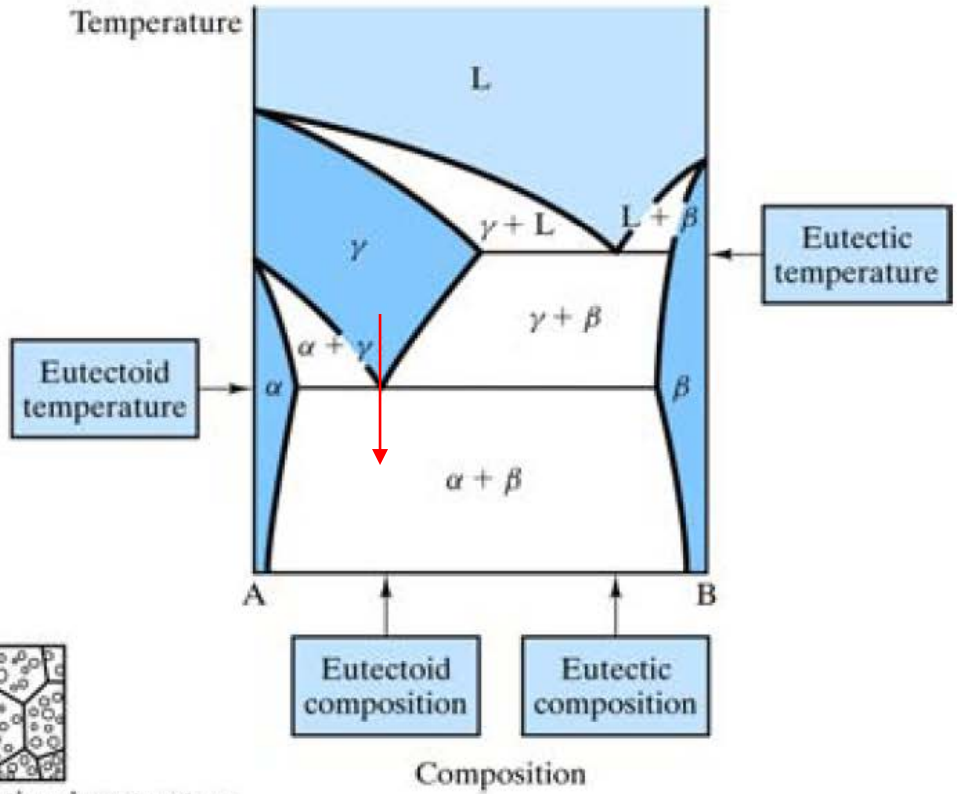

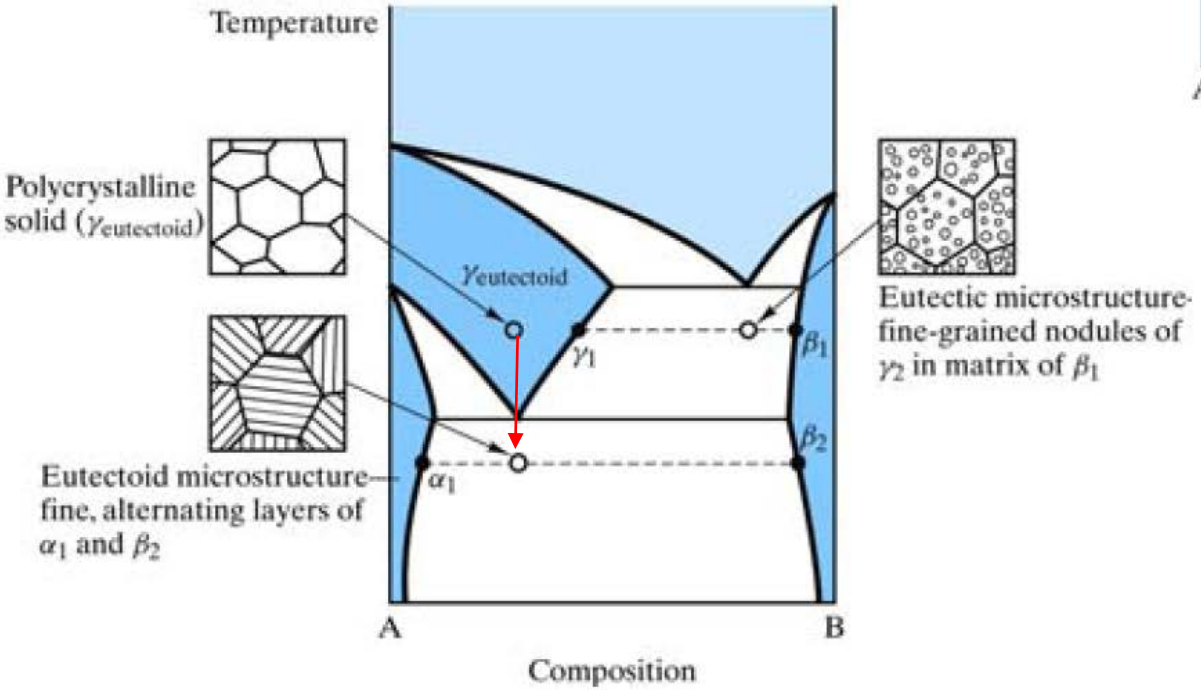

Peritectic reaction

Peritectic reaction : AB $\overset{heating}{\rightleftharpoons}$ **L + B**

Congruent melting : $S_{x1} \xrightarrow{melting} L_{x1}$

Incongruent melting : $S_{x1} \xrightarrow{melting} L_{x2}$

Which one here??

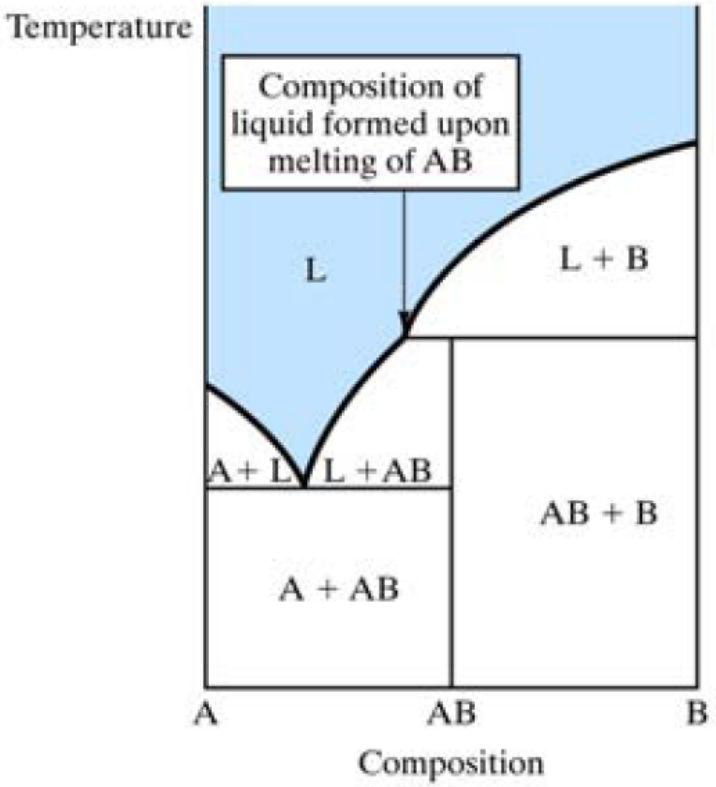

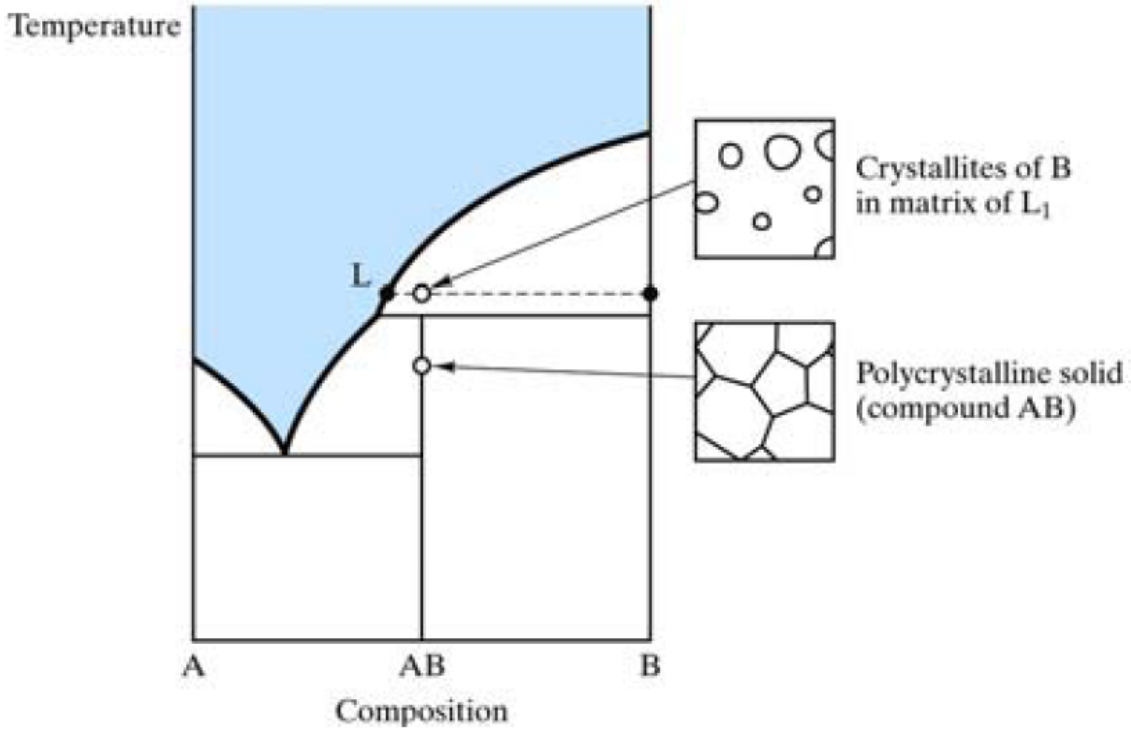

Peritectic reaction

Considerable difference between the melting points

$$\Delta H^{\alpha}_{mix} > \Delta H^{l}_{mix} > 0$$

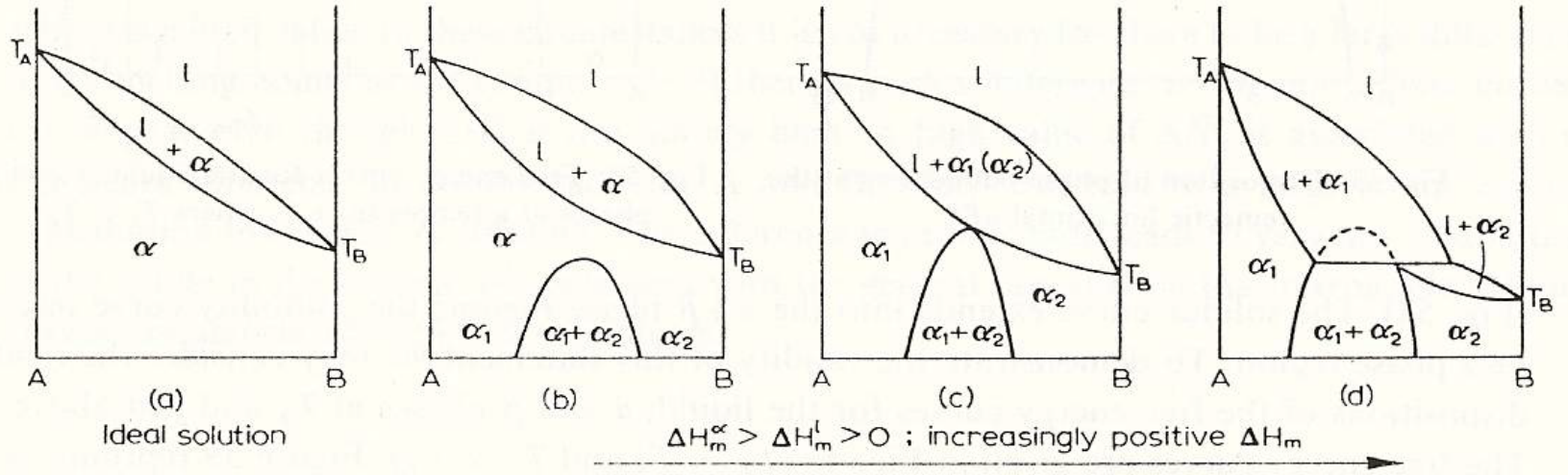

Fig. 61. Effect of increasingly positive departure from ideality in changing the phase diagram from a continuous series of solutions to a peritectic-type.

Eutectic reaction

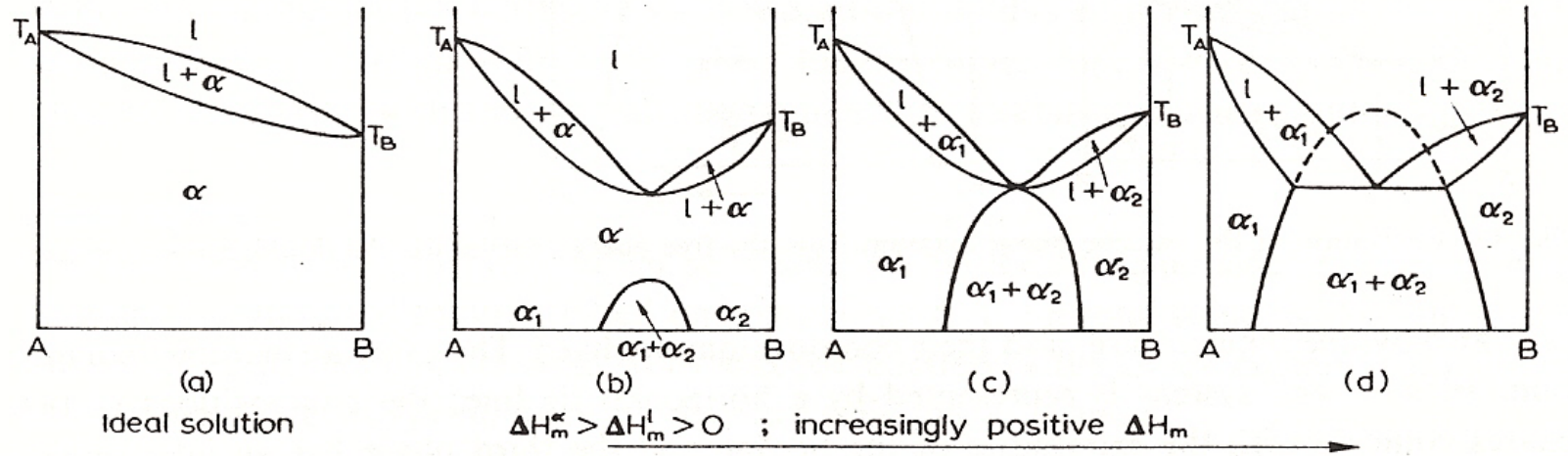

Fig. 43. Effect of increasingly positive departure from ideality in changing the phase diagram for a continuous series of solutions to a eutectic-type.

Eutectic: L→α+β

Peritectic: L+α → β

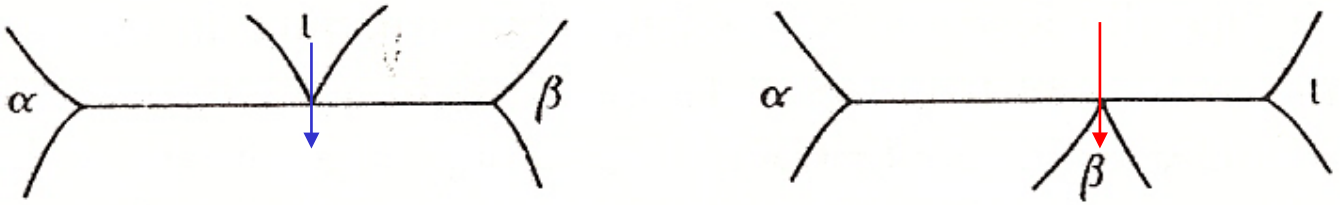

Fig. 63. Relationship between eutectic and peritectic reactions.

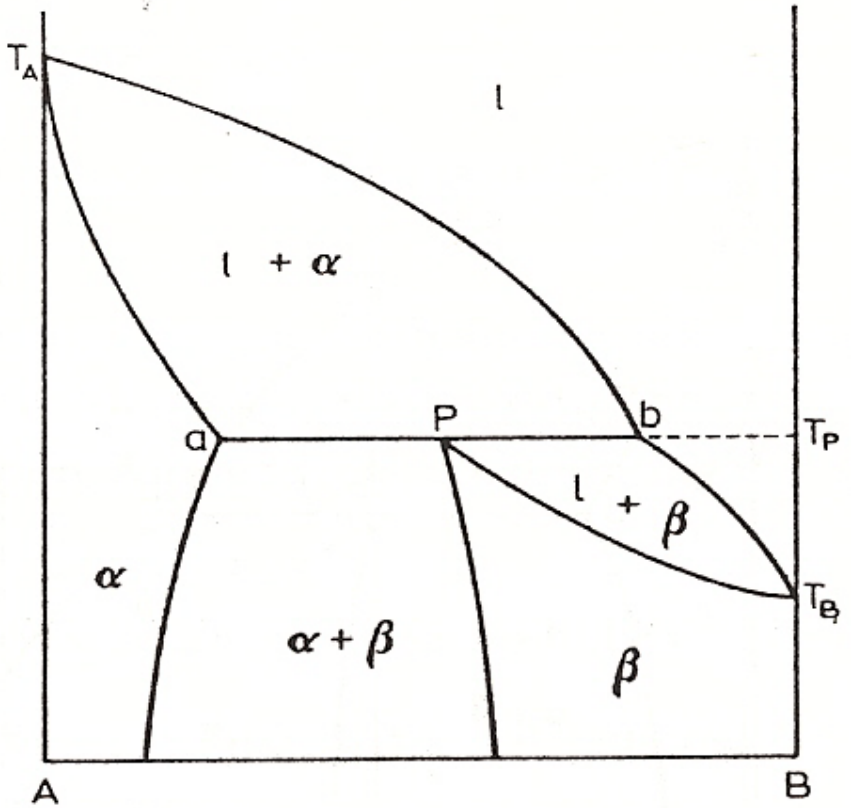

Fig. 64. Binary peritectic phase diagram.

Peritectic reaction

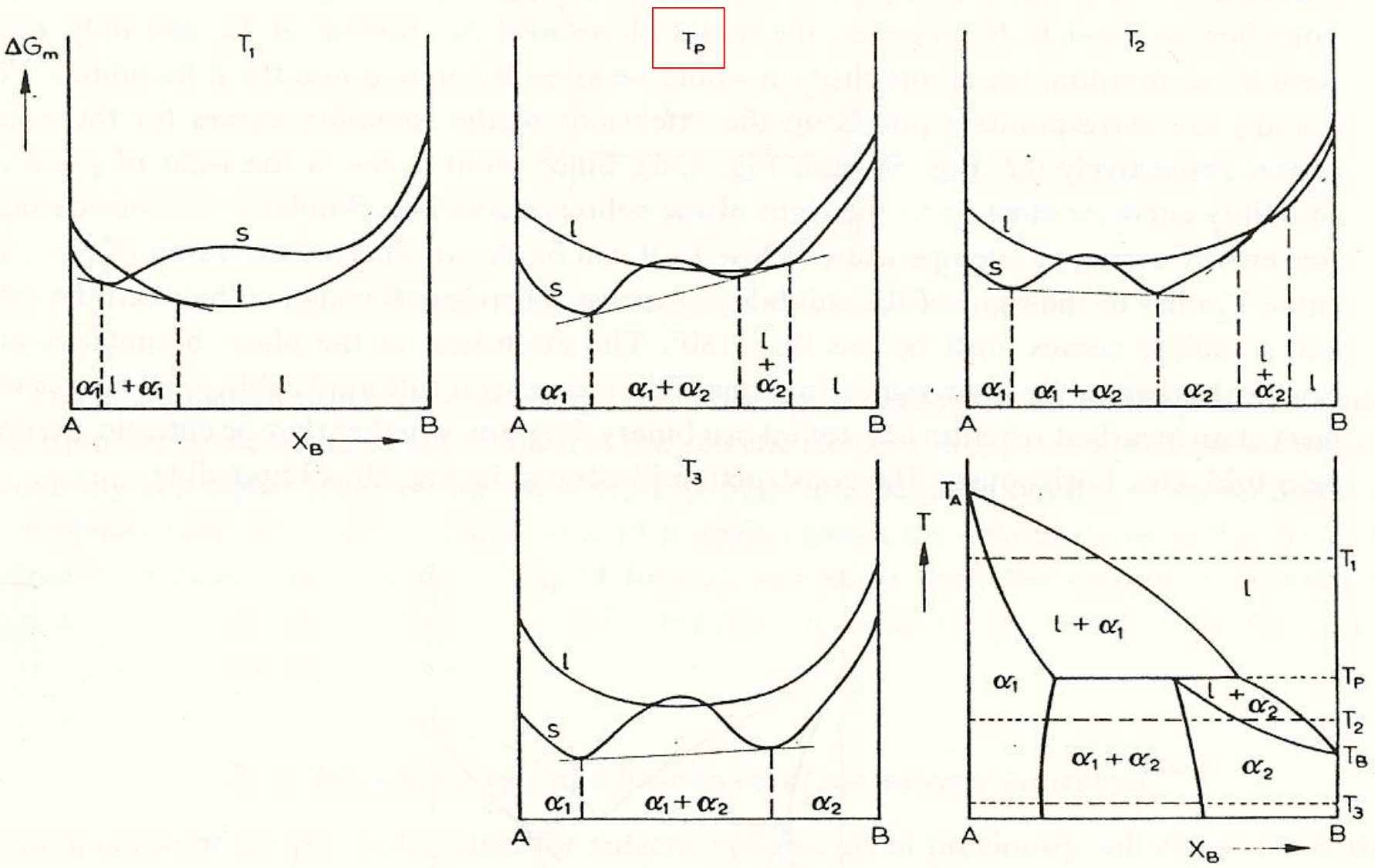

Fig. 62. Derivation of the peritectic phase diagram from the free energy curves for the liquid and solid phases.

Peritectic reaction

- **Surrounding or Encasement: During peritectic reaction, L+ α⟶ β , the beta phase created surrounds primary alpha.**
- **Beta creates diffusion barrier resulting in coring.**

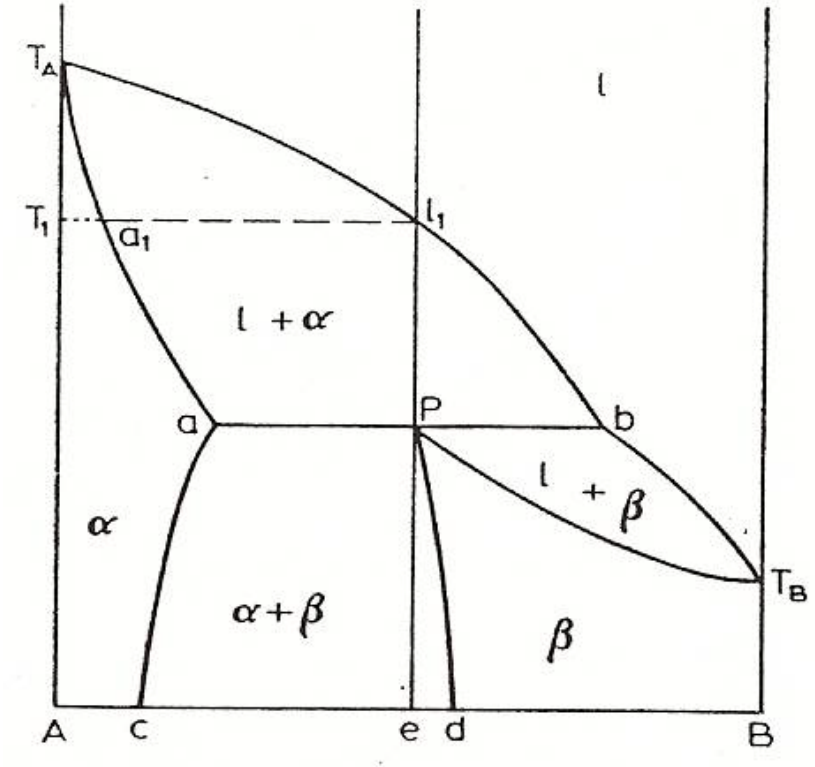

Fig. 65. Freezing of the peritectic alloy *P*.

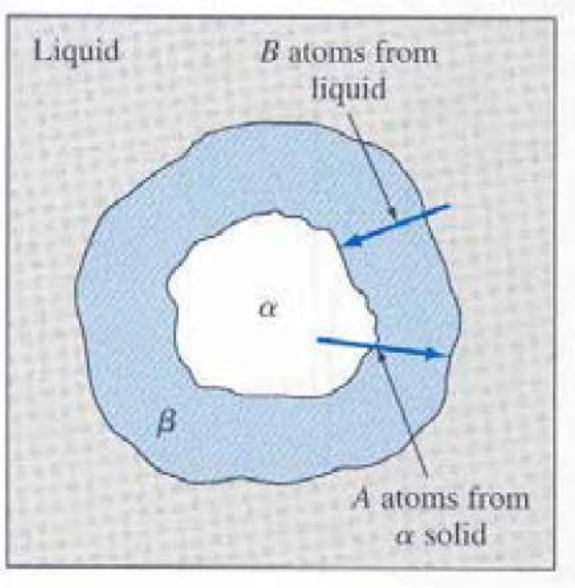

Figure 8.19

Peritectic solidification

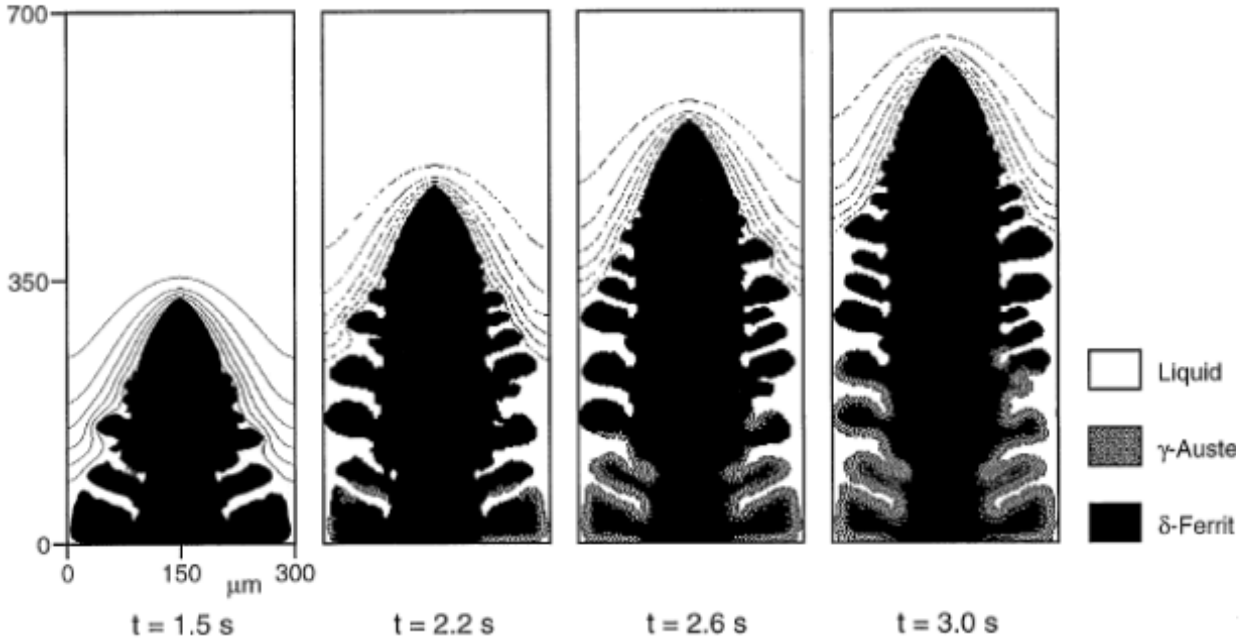

Figure 7. Phase-field simulation of peritectic reaction [3].

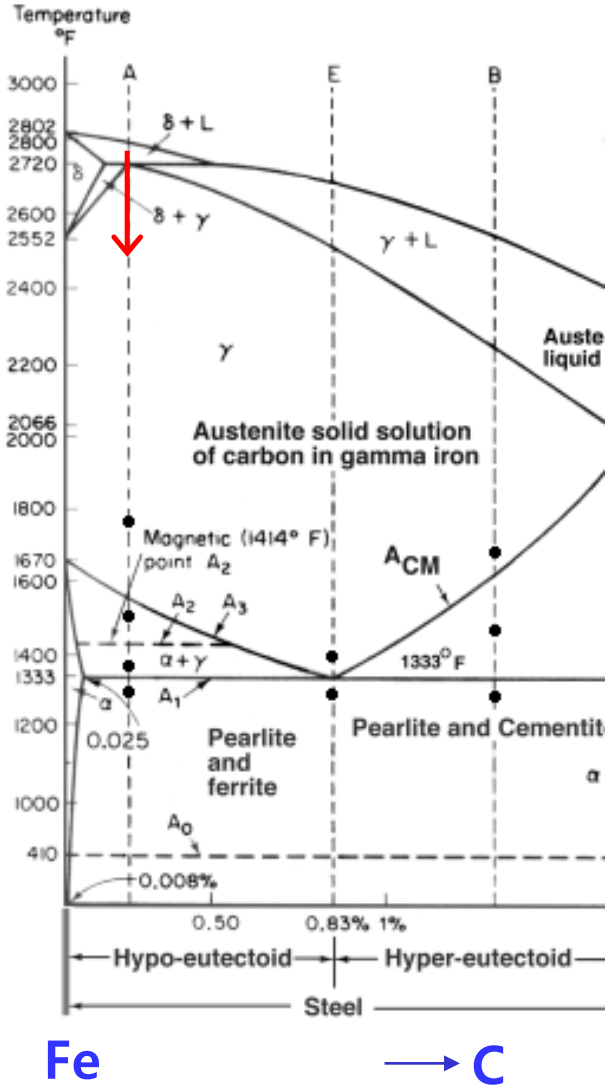

Peritectic solidification

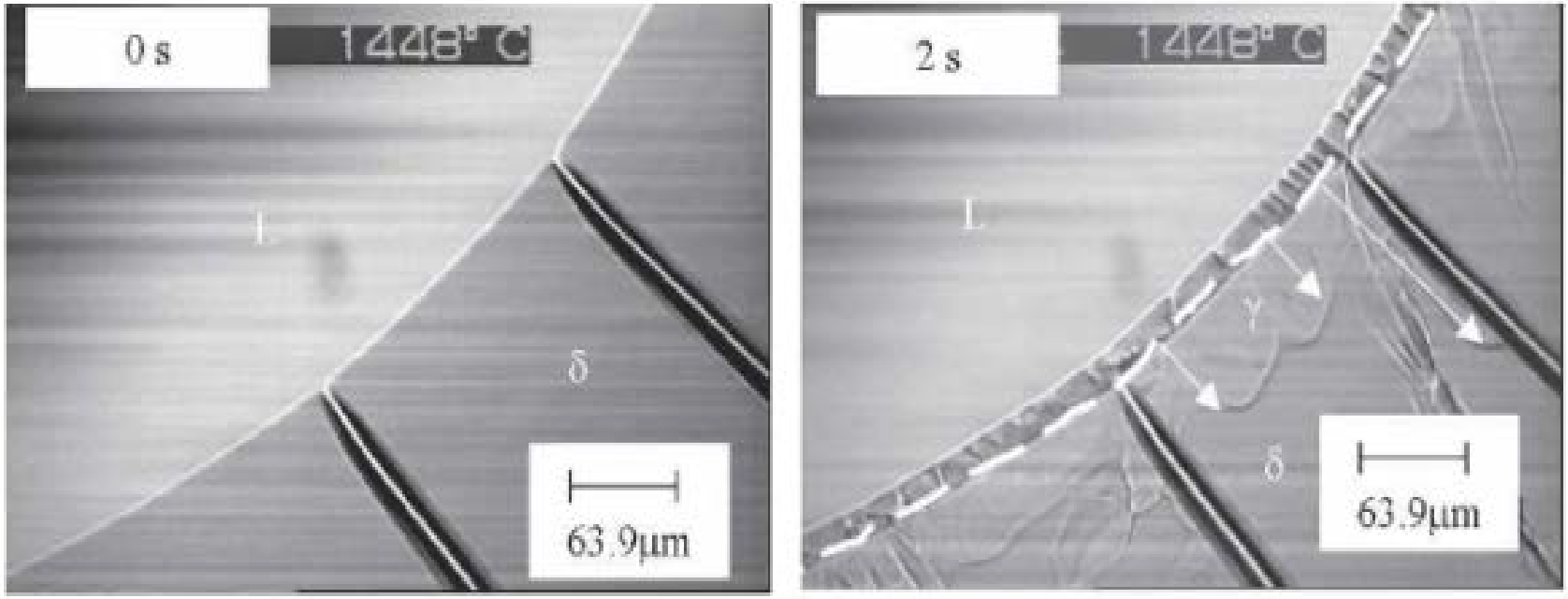

Figure 5. Peritectic reaction in Fe-0.18 pct C alloy: cooling rate =10 K/min [2].

Peritectic solidification (δ+L→γ)

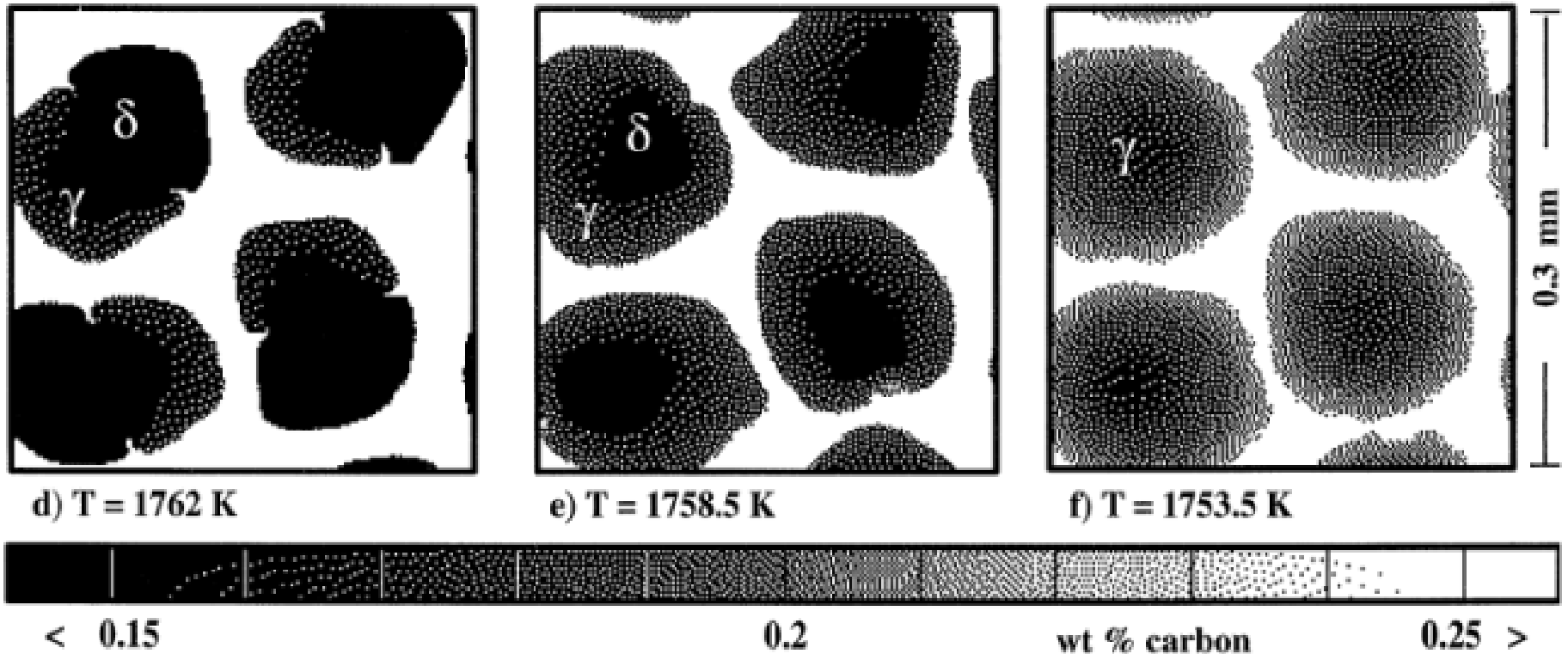

Figure 6. Phase-field simulation of peritectic reaction [3].

Peritectic Alloy System

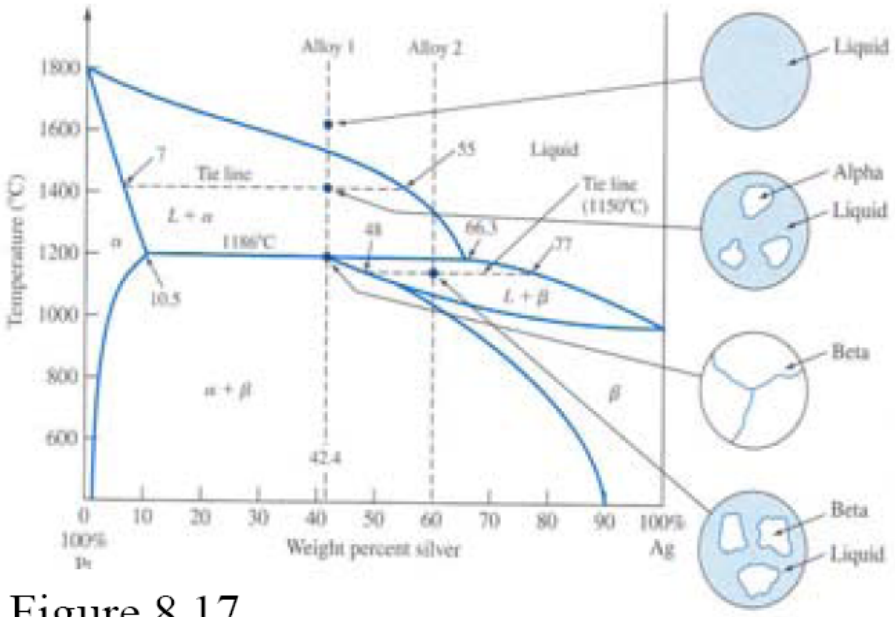

Figure 8.17

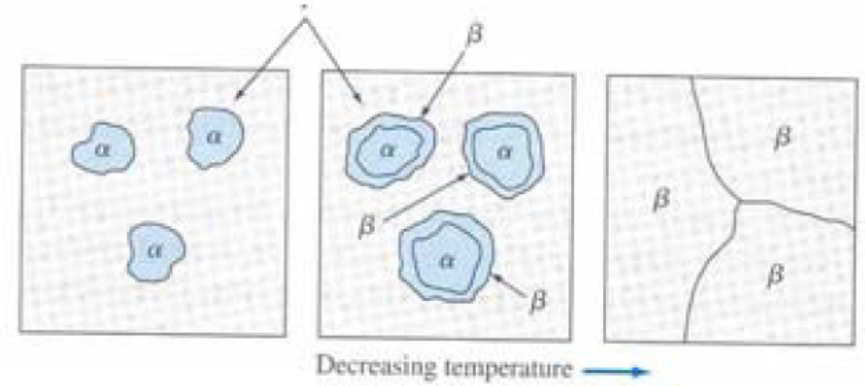

Figure 8.18

- **At 42.4 % Ag & 1400^{0}C**

Phases present	Liquid	Alpha
Composition	55% Ag	7%Ag
Amount of Phases	$\frac{42.4-7}{55-7}$	$\frac{55-42.4}{55-7}$
	= 74%	= 26%

- **At 42.4% Ag and 1186^{0}C + ΔT**

Phases present	Liquid	Alpha
Composition	66.3% Ag	10.5%Ag
Amount of Phases	$\frac{42.4-10.5}{66.3-10.5}$	$\frac{66.3-42.4}{66.3-10.5}$
	= 57%	=43%

Phases present Liquid Alpha

- **At 42.4% Ag and 1186^{0}C – ΔT**

Phase Present Beta only

Composition 42.4% Ag

Amount of Phase 100%

4.3.4. Formation of intermediate phases by peritectic reaction

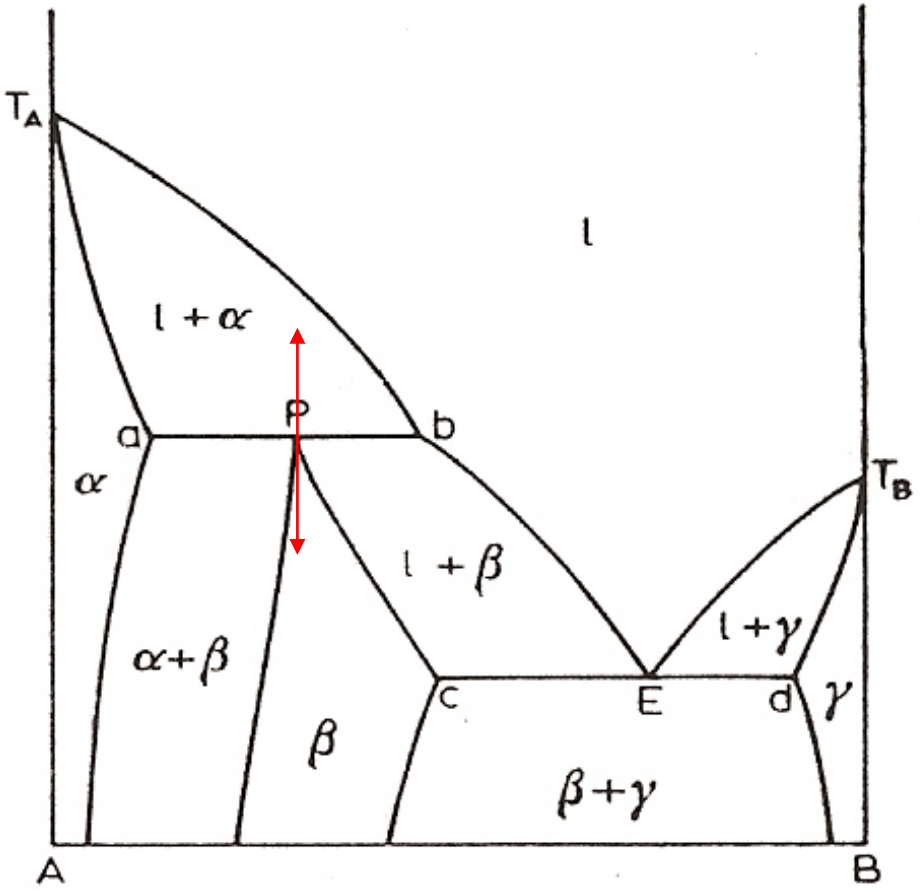

Fig. 68. Formation of an intermediate phase, β, by peritectic reaction.

β: different crystal structure with those of the component

older literature_ intermediate phases ~regarded as a chemical compounds

Thus, called intermetallic compounds but, cannot expect from valency considerations & not fixed composition (different with chemical compounds)

e.g. In the Hf-W system,
the formation of an intermediate phase, HfW_2 by peritectic reaction

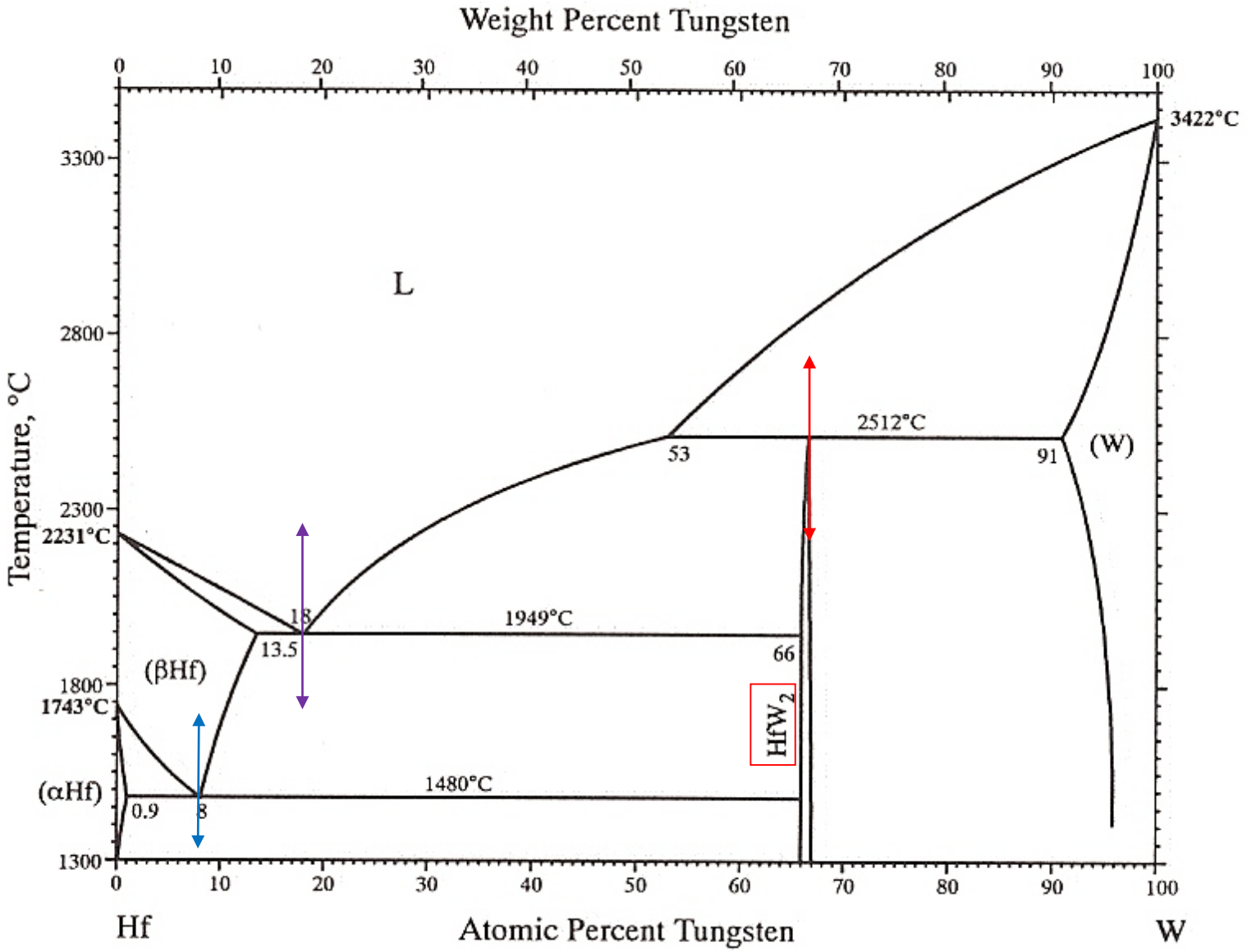

Intermediate Phase_"different crystal structure as either of the pure component"

3 main factors determining the structure of Intermediate phase ?

1) Relative atomic size

- Laves phase (size difference: 1.1~1.6 ex: $MgCu_2$)
  fill space most efficiently ~ stable
- Interstitial compound: MX, M_2X, MX_2, M_6X
  M= Cubic or HCP ex: Zr, Ti, V, Cr, etc, X= H, B, C, and N

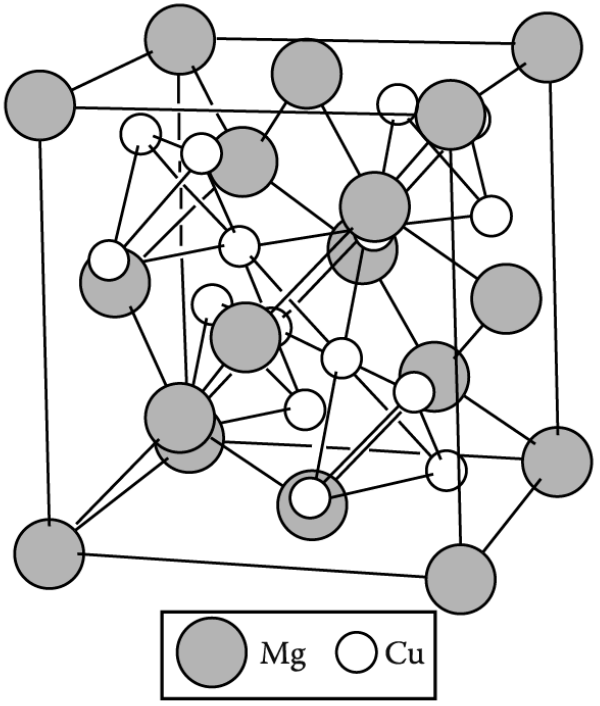

$MgCu_2$ (A Laves phase)

2) Relative valency electron

- electron phases ex_α & β brass
  # of valency electrons per unit cell
  → depending on compositional change

3) Electronegativity

- very different electronegativites → ionic bond_normal valency compounds
  ex Mg_2Sn

* Intermediate phases

(1) Size-factor compounds ~ relatively large size differences of the constituent atoms

e.g. a) Laves phases, which are intermediate phases based on the formula AB_2, where atom A has the larger atomic diameter.

b) Interstitial compounds: metal carbides, nitrides and borides

(2) Electron compounds ~ similar electrochemical properties and a favorable size-factor occurs at one of three valency electron-to–atom ratios.

e.g. a) 3:2 electron compounds CuZn, Cu_3Ga, and Cu_5Sn
different %Cu, same electron concentration and similar crystal structure (BCC)

b) 21:13 electron compounds γ brass (complex cubic lattice with 52 atoms per unit cell)

c) 7:4 electron compounds close-packed hexagonal structure similar to ε brass

(3) Normal valency compounds (partly-ionic compounds) ~ obey the valency rules

e.g. Mg_2Si, Mg_2Sn, Mg_2Pb and Mg_3Sb_2/
much common in ionic compounds such as NaCl and CaF2

4.3.4. Formation of intermediate phases by peritectic reaction

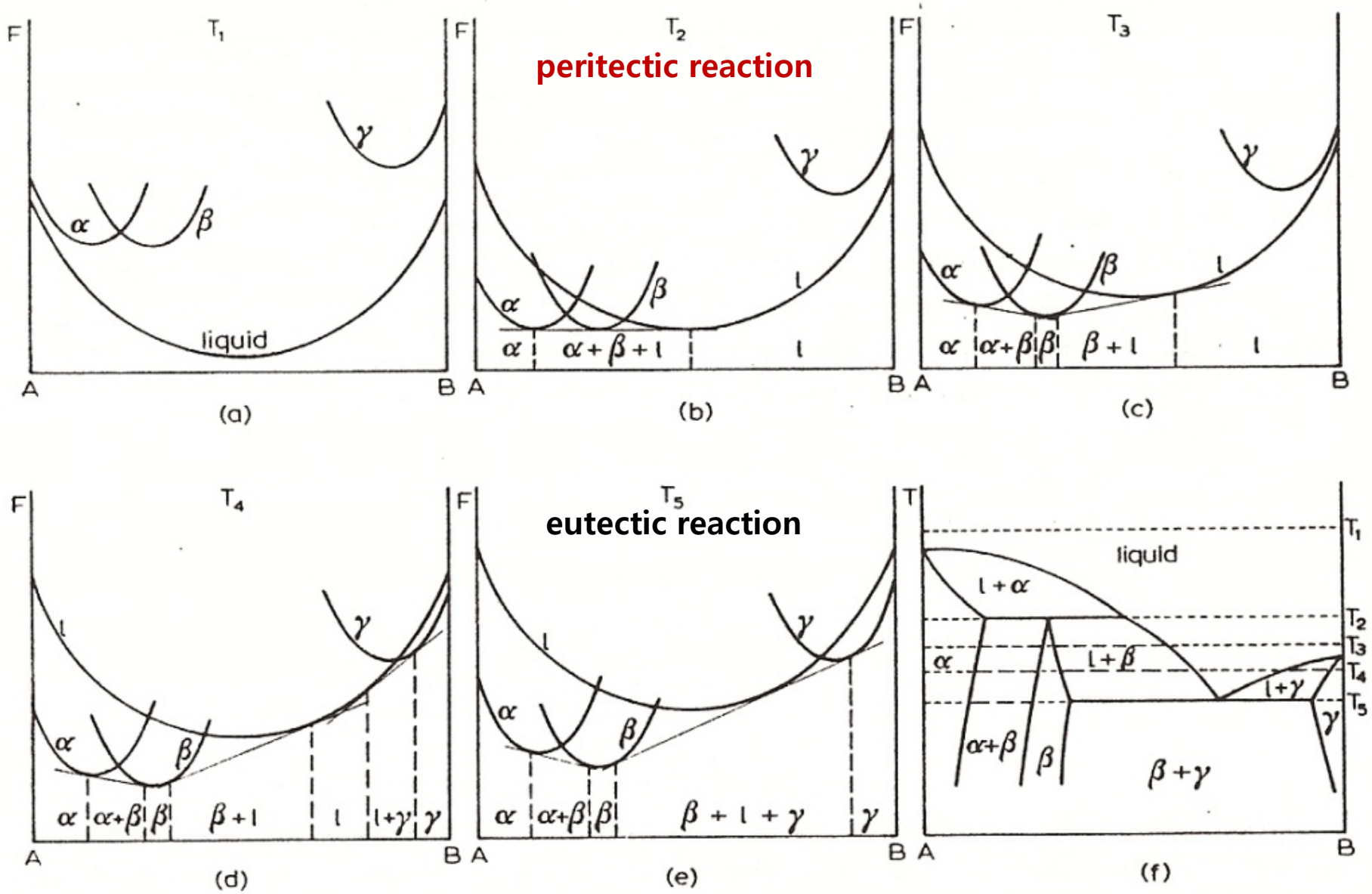

Fig. 69. Derivation of the phase diagram (Fig. 68) from the free energy curves of the liquid, α, β and γ phases. (After A. H. COTTRELL; courtesy Edward Arnold.)

4.3.4. Formation of intermediate phases by peritectic reaction

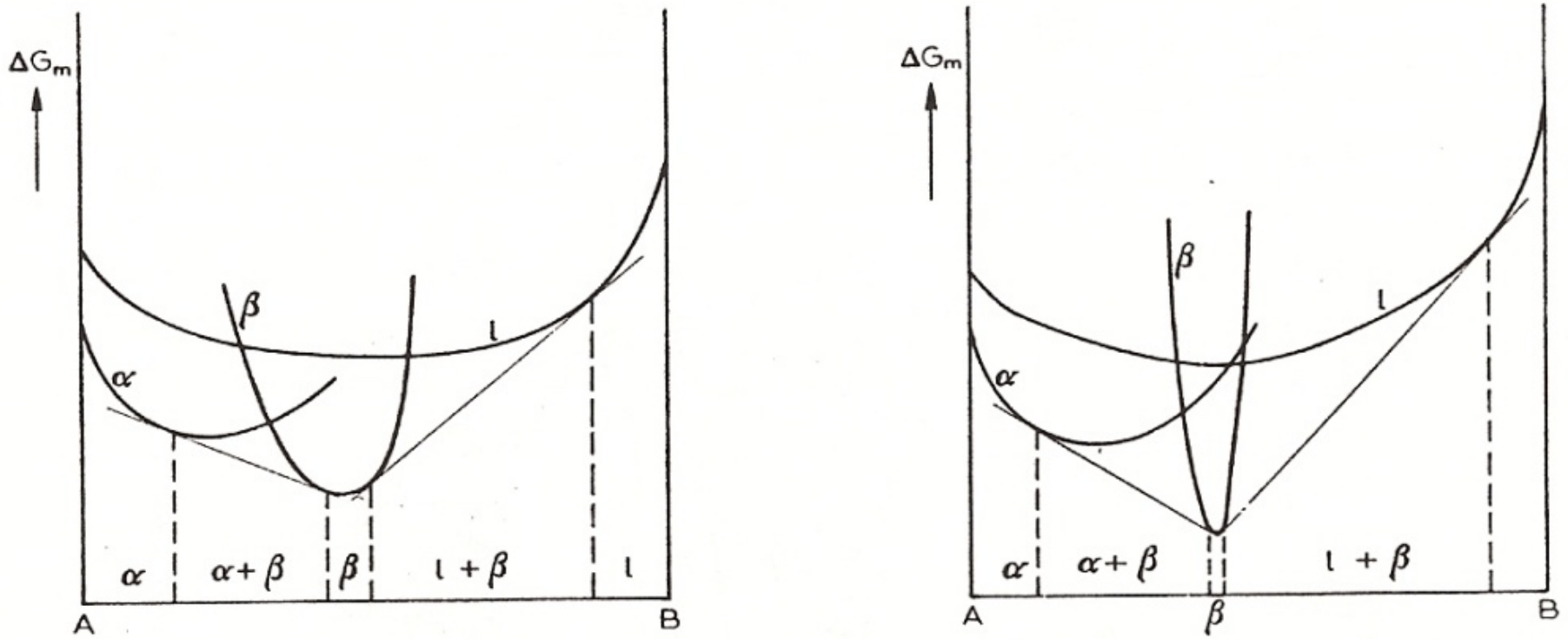

Fig. 70. Decreasing range of stability of an intermediate phase with its increasing stability relative to the termina solid solutions.

4.3.4. Formation of intermediate phases by peritectic reaction

Five successive peritectic reaction

(1)

(2)

(3)

(4)

(5)

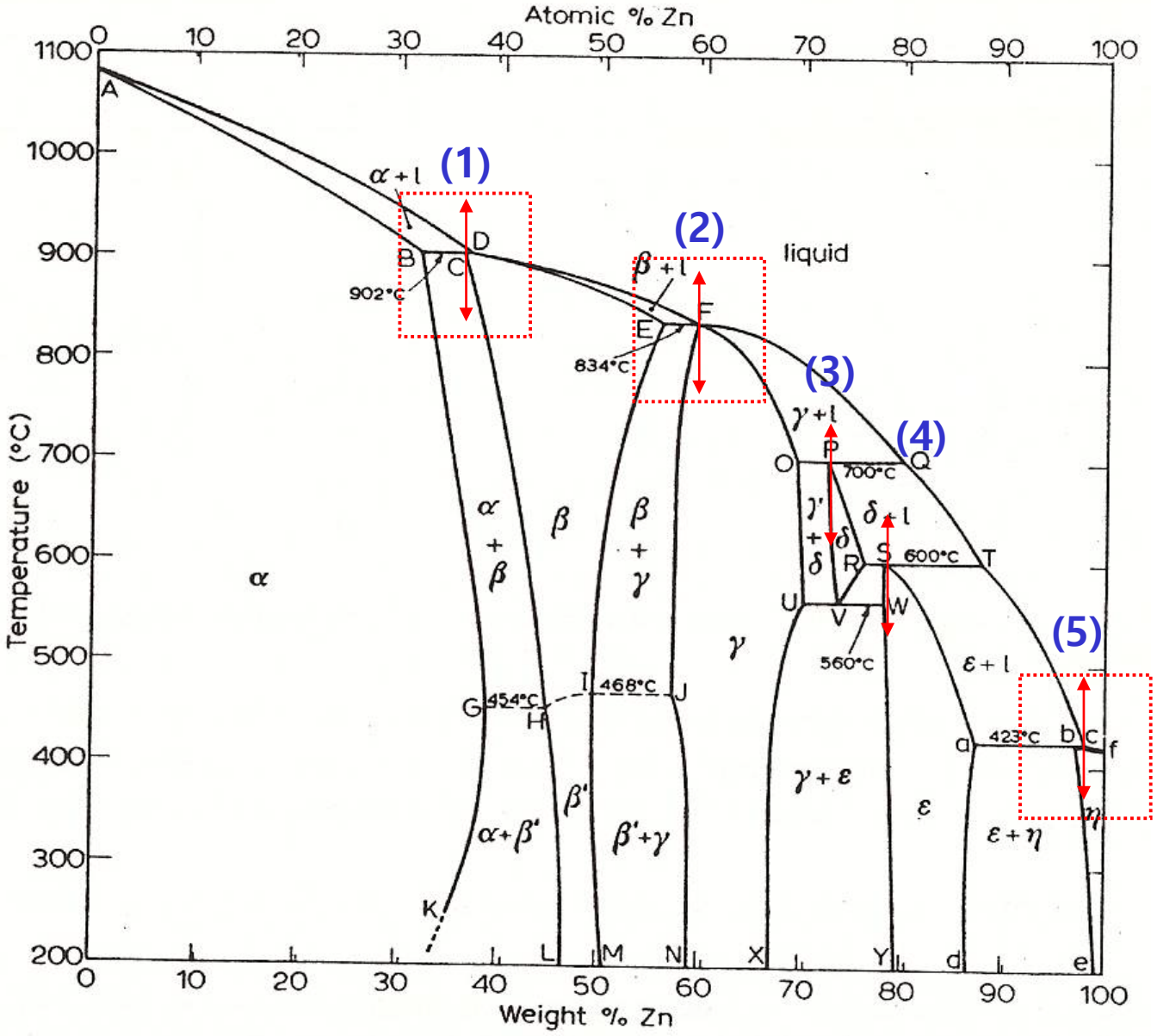

Fig. 71. The Cu–Zn phase diagram. (After G. V. RAYNOR; courtesy Institute of Metals.)

1) Peritectic point virtually coincides with the liquid composition. But, thermodynamically, points P and b is not possible to coincide.

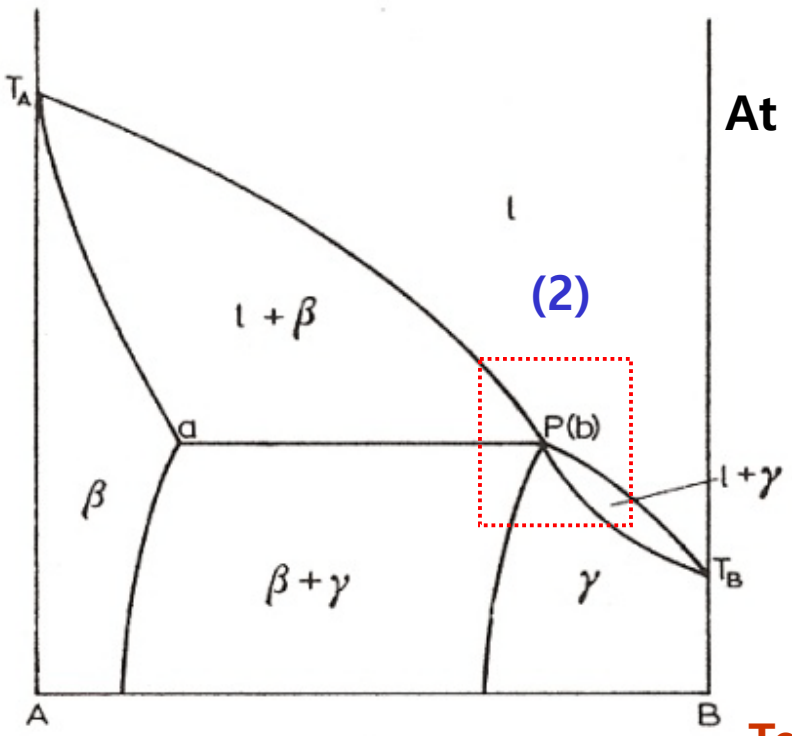

Fig. 72. Limiting case of the peritectic reaction.

At equilibrium, $dG^s = dG^l, \mu_A^S = \mu_A^l, \mu_B^S = \mu_B^l$

$$dG^s = V^s\,dP - S^s\,dT + \mu_A^s\,dX_A^s + \mu_B^s\,dX_B^s$$
$$dG^l = V^l\,dP - S^l\,dT + \mu_A^l\,dX_A^l + \mu_B^l\,dX_B^l.$$

At const P and differentiating with respect to X_A

$$-(S^s - S^l)\,dT = (\mu_A - \mu_B)\,(dX_A^l - dX_A^s).$$

$$(S^S - S^l)\frac{dT}{dX_A} = (\mu_A - \mu_B)\left(\frac{dX_A^S}{dX_A} - \frac{dX_A^l}{dX_A}\right)$$

$$X_A^S = X_A^l \Rightarrow (S^S - S^l)\frac{dT}{dX_A} = 0$$

$$S^S \neq S^l, dT/dX_A = 0$$

Temp. maximum or minimum must be present.

(next page)

Peritectic point and the liquid composition are so close to each other that the experimental techniques used were not able to distinguish them. More refined methods would be expected to produce evidence of a compositional difference these two points ($X_A^S \neq X_A^l$).

The condition for a liquid and a solid phase to have identical compositions is that a temperature maximum or minimum must be present.

From eqn. (102)

$$(S^s - S^l)\frac{dT}{dX_A} = 0.$$

Since $S^s \neq S^l$, then $dT/dX_A = 0$. Thus the condition $X_A^s = X_A^l$ is only associated with $dT/dX_A = 0$, *i.e.* with a minimum or a maximum in the line $T_A T_B$ of Fig. 22. Except for this particular case therefore $X_A^s \neq X_A^l$. There is a difference between the composition of the liquid and solid phase in the general case.

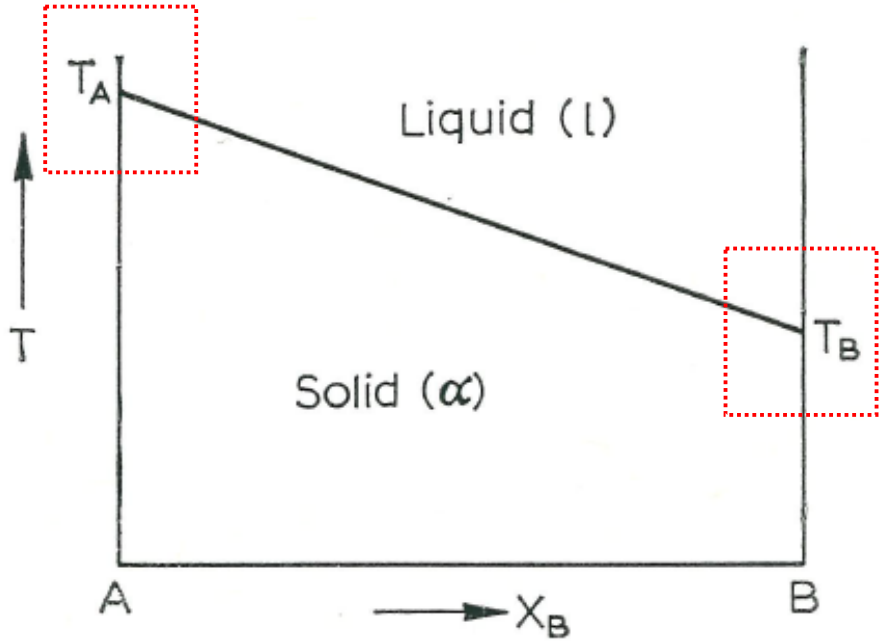

Fig. 22.

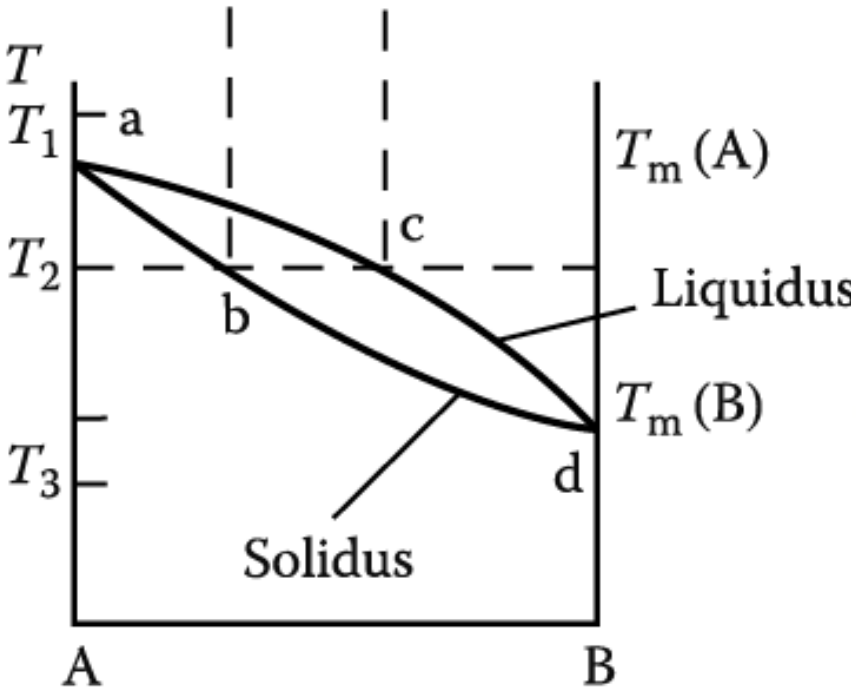

(f)

1) Peritectic point virtually coincides with the liquid composition. But, thermodynamically, points P and b is not possible to coincide.

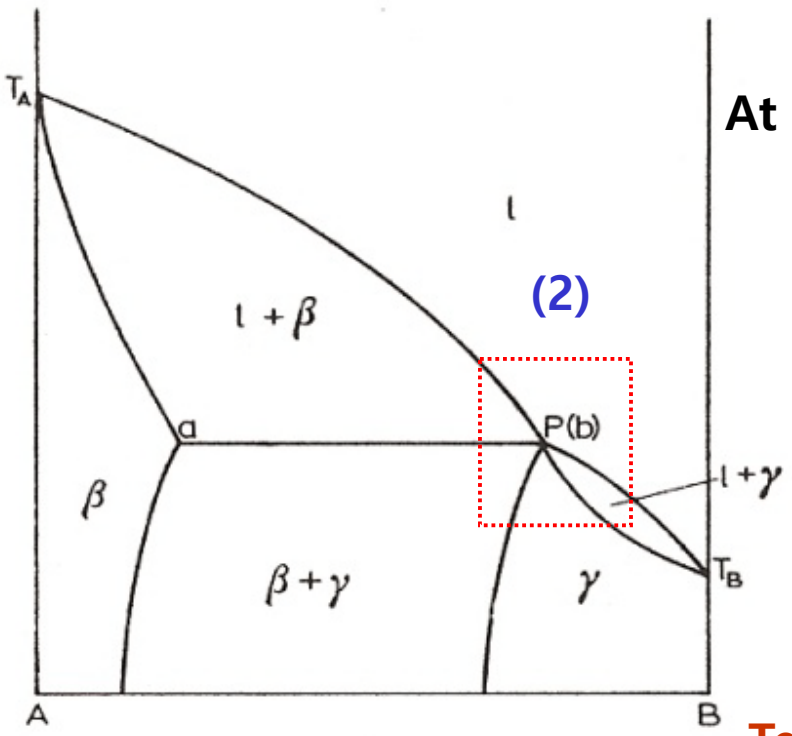

Fig. 72. Limiting case of the peritectic reaction.

At equilibrium, $dG^s = dG^l, \mu_A^S = \mu_A^l, \mu_B^S = \mu_B^l$

$$\mathrm{d}G^s = V^s\,\mathrm{d}P - S^s\,\mathrm{d}T + \mu_\mathrm{A}^s\,\mathrm{d}X_\mathrm{A}^s + \mu_\mathrm{B}^s\,\mathrm{d}X_\mathrm{B}^s$$
$$\mathrm{d}G^l = V^l\,\mathrm{d}P - S^l\,\mathrm{d}T + \mu_\mathrm{A}^l\,\mathrm{d}X_\mathrm{A}^l + \mu_\mathrm{B}^l\,\mathrm{d}X_\mathrm{B}^l.$$

At const P and differentiating with respect to X_A

$$-(S^s - S^l)\,\mathrm{d}T = (\mu_\mathrm{A} - \mu_\mathrm{B})\,(\mathrm{d}X_\mathrm{A}^l - \mathrm{d}X_\mathrm{A}^s).$$

$$(S^S - S^l)\frac{dT}{dX_A} = (\mu_A - \mu_B)\left(\frac{dX_A^S}{dX_A} - \frac{dX_A^l}{dX_A}\right)$$

$$X_A^S = X_A^l \Rightarrow (S^S - S^l)\frac{dT}{dX_A} = 0$$

$$S^S \neq S^l, dT/dX_A = 0$$

Temp. maximum or minimum must be present.

(next page)

Peritectic point and the liquid composition are so close to each other that the experimental techniques used were not able to distinguish them. More refined methods would be expected to produce evidence of a compositional difference these two points ($X_A^S \neq X_A^l$).

2) Decreasing solubility of Zn in Cu with rise in temperature in contrast to the normal decrease in solubility with fall in temperature

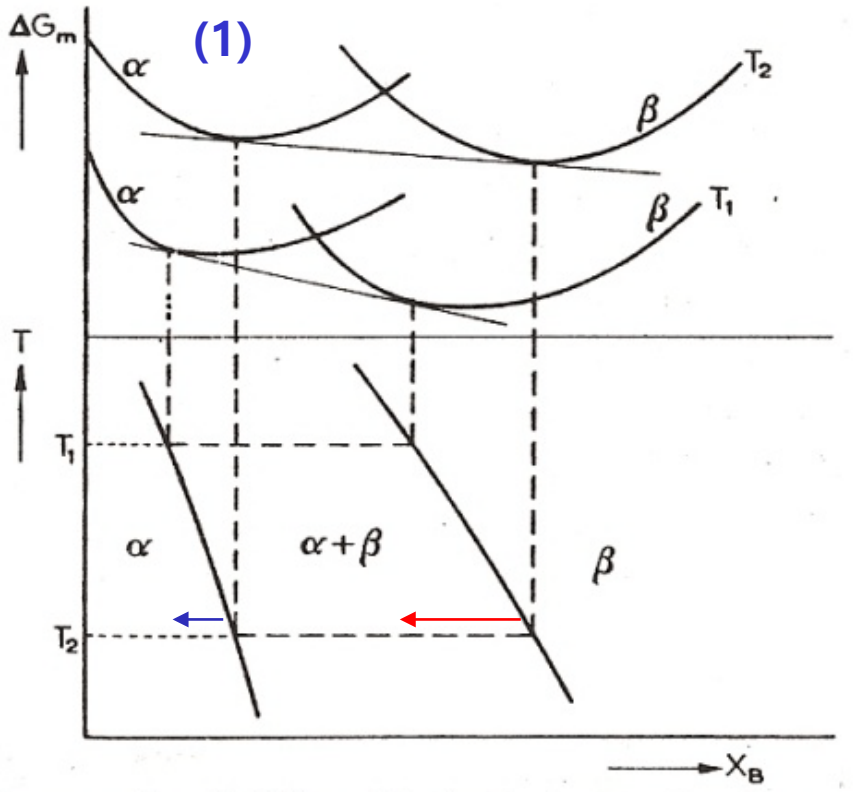

Due to an equilibrium with a disordered intermediate phase (e.g. the β phase above 454 ℃, Fig. 71)

This has been explained as being due to a greater relative movement of the free energy curve of the intermediate phase compared with the α solid solution with rise in temperature.

4.3.5. Non-stoichiometeric compounds

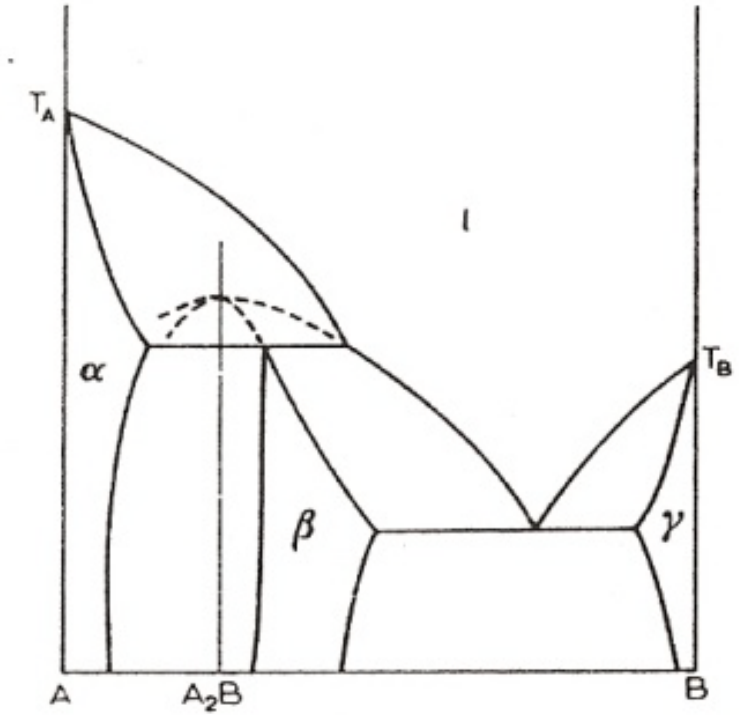

Fig. 74. A non-stoichiometric β phase based on the intermediate phase A_2B.

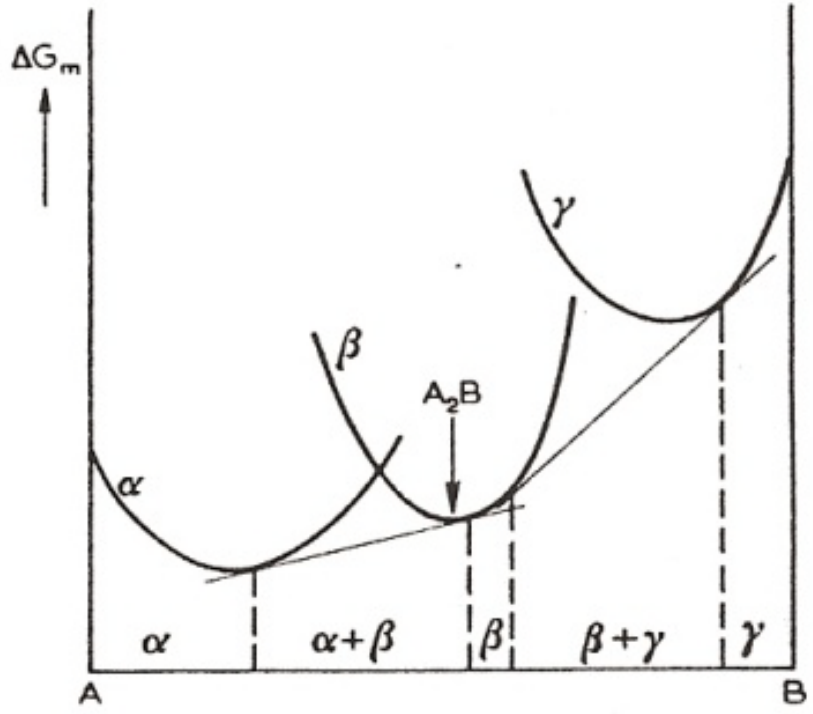

Fig. 75. Use of free energy curves to illustrate the occurrence of non-stoichiometric phases.

4.3.5. Non-stoichiometeric compounds

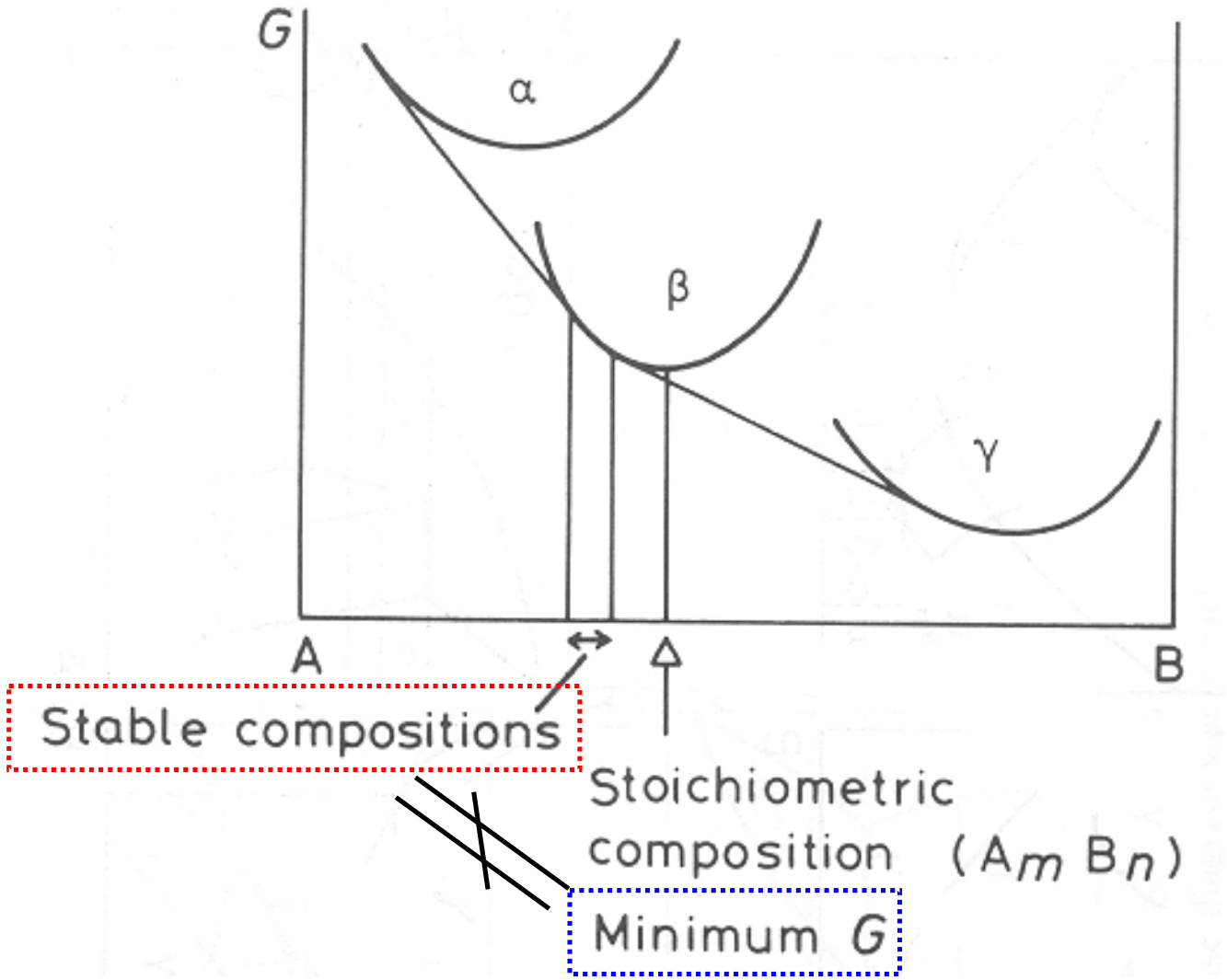

4.3.5. Non-stoichiometeric compounds

θ phase in the Cu-Al system is usually denoted as $CuAl_2$ although the composition $X_{Cu}=1/3$, $X_{Al}=2/3$ is not covered by the θ field on the phase diagram.

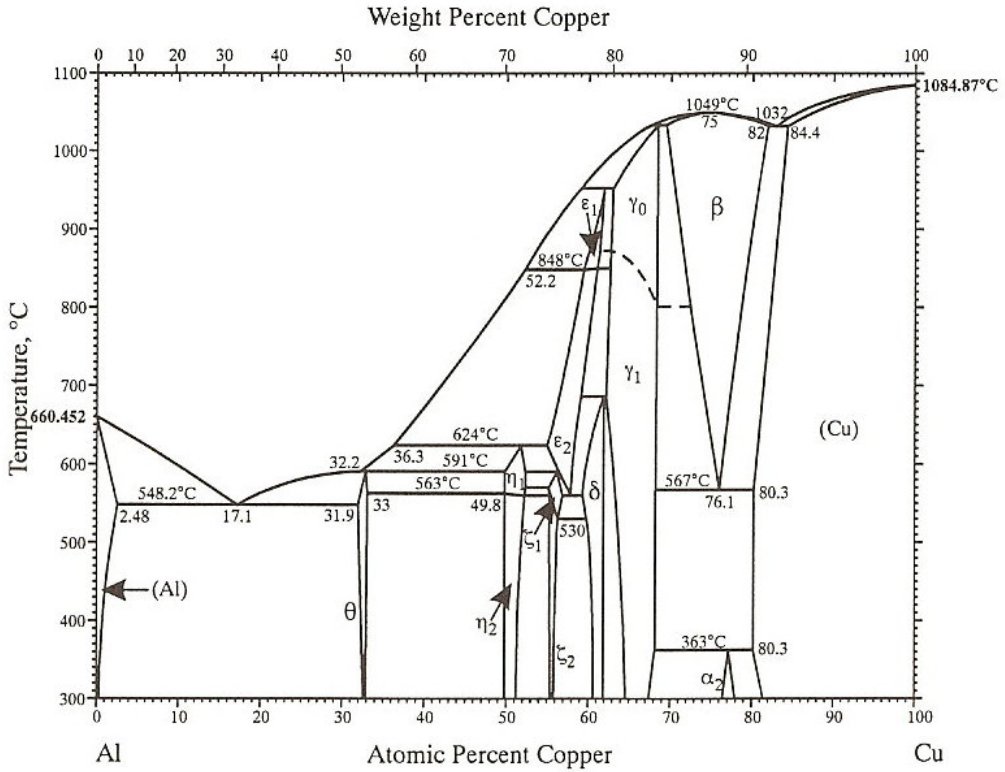

Al-Cu

Al-Cu

Phase	Composition, at.% Cu	Pearson symbol	Space group	Struktur-bericht designation	Prototype
(Al)	0 to 2.48	*cF*4	$Fm\bar{3}m$	*A*1	Cu
θ	31.9 to 33.0	*tI*12	*I*4/*mcm*	*C*16	Al_2Cu
η_1	49.8 to 52.4	*oP*16 or *oC*16	*Pban* or *Cmmm*	…	…
η_2	49.8 to 52.3	*mC*20	*Cm*/2	…	…
ζ_1	55.2 to 56.8	*hP*42	*P*6/*mmm*	…	…
ζ_2	55.2 to 56.3	*m***	…	…	…
ε_1	59.4 to 62.1	*c***	…	…	…
ε_2	55.0 to 61.1	*hP*4	$P6_3/mmc$	$B8_1$	NiAs
δ	59.3 to 61.9	*hR**	$R\bar{3}m$	…	…
γ_0	63 to 68.5	*cI*52	$I\bar{4}3m$	$D8_2$	Cu_5Zn_8
γ_1	62.5 to 68.5	*cP*52	$P\bar{4}3m$	$D8_3$	Al_4Cu_9
β	69.5 to 82	*cI*2	$Im\bar{3}m$	*A*2	W
α_2	76.5 to 78	…	…	…	…
(Cu)	80.3 to 100	*cF*4	$Fm\bar{3}m$	*A*1	Cu

J.L. Murray, *Phase Diagrams of Binary Copper Alloys*, P.R. Subramanian, D.J. Chakrabarti, and D.E. Laughlin, ed., ASM International, Materials Park, OH, 18-42 (1994)

X.L. Liu, I. Ohnuma, R. Kainuma, and K. Ishida, *J. Alloys Compds*, *264*, 201-208 (1998)

Congruent vs Incongruent

Congruent phase transformations: no compositional change associated with transformation

Examples:

- Allotropic phase transformations
- Melting points of pure metals
- Congruent Melting Point

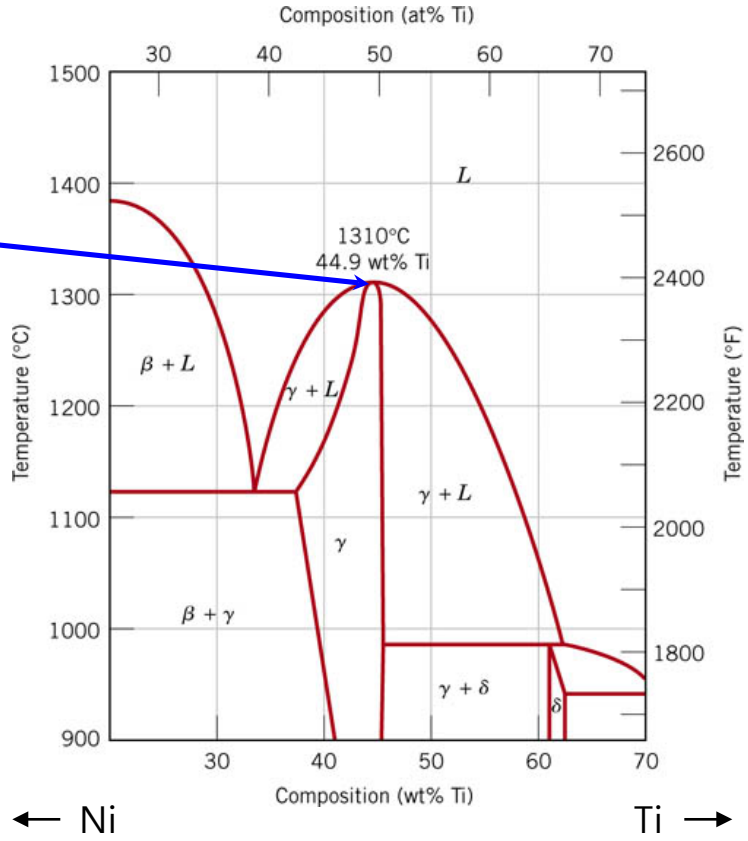

Incongruent phase transformation: at least one phase will experience change in composition

Examples:

- Melting in isomorphous alloys
- Eutectic reactions
- Pertectic Reactions
- Eutectoid reactions

4.4. Congruent transformations

Congruent transformation:

(a) and (b): a melting point minimum, a melting point maximum, and a critical temperature associated with a order-disorder transformation

(c) and (d): formation of an intermediate phase (next page)

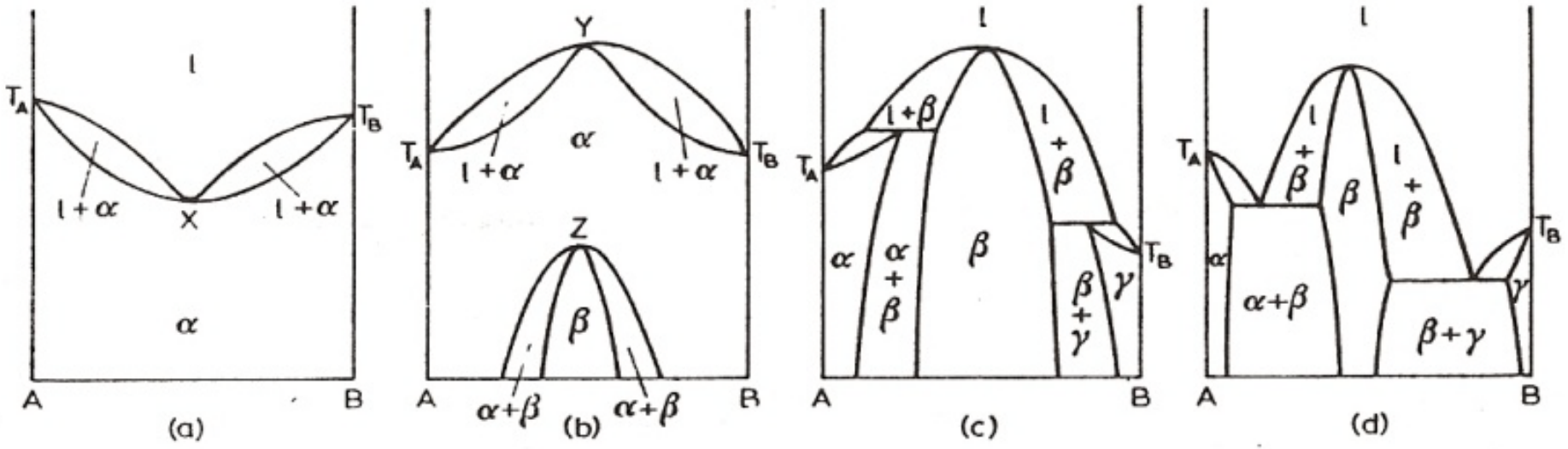

Fig. 76. Examples of congruent transformations.

4.4. Congruent transformations

a. Formation of congruently-melting intermediate phase

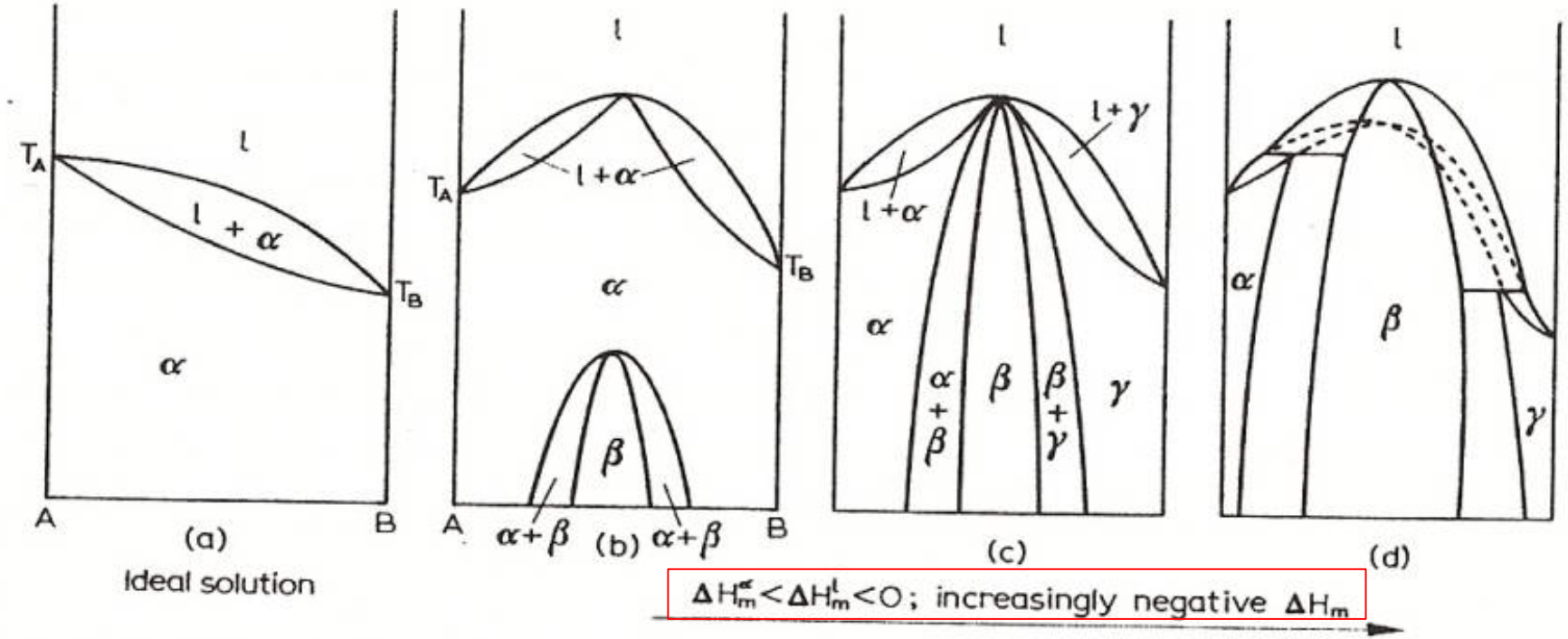

Fig. 77. Effect of increasingly negative departure from ideality in changing the phase diagram from a continuous series of solutions to one containing a congruent intermediate phase.

4.4. Congruent transformations

b. More usual type of congruently-melting intermediate phase

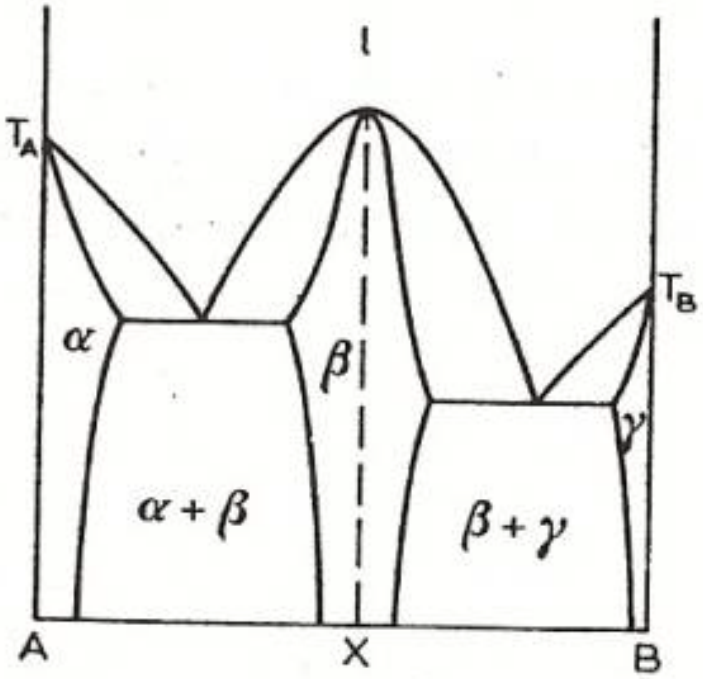

Fig. 78. Phase diagram with a congruent intermediate phase.

→ Partial phase diagram A-X and X-B

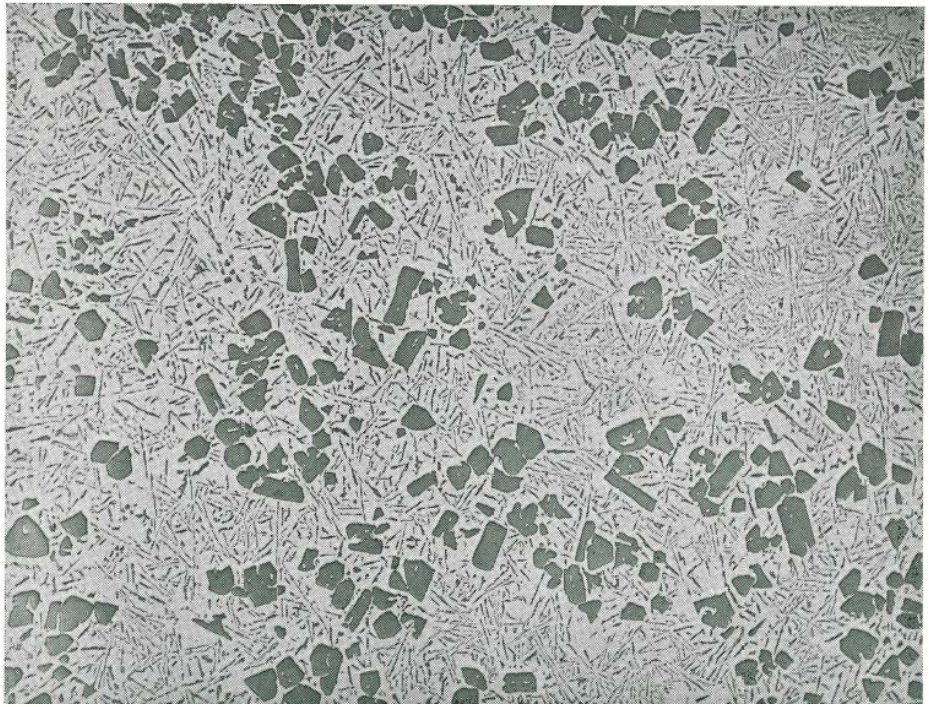

Microstructure of a cast Al-22% Si alloy
showing polyhedra of primary Si in eutectic matrix

: Similar with eutectic alloy system/ primary β phase with well-formed crystal facets (does not form dendrite structure)

In many cases, X = normal valency compound such as Mg_2Si, Mg_2Sn, Mg_2Pb

or Laves phase, particularly stable compounds

b. More usual type of congruently-melting intermediate phase

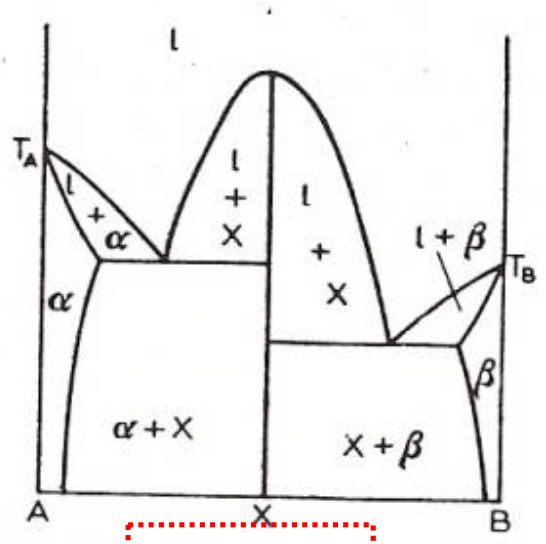

Fig. 79. Limiting case of Fig. 78.

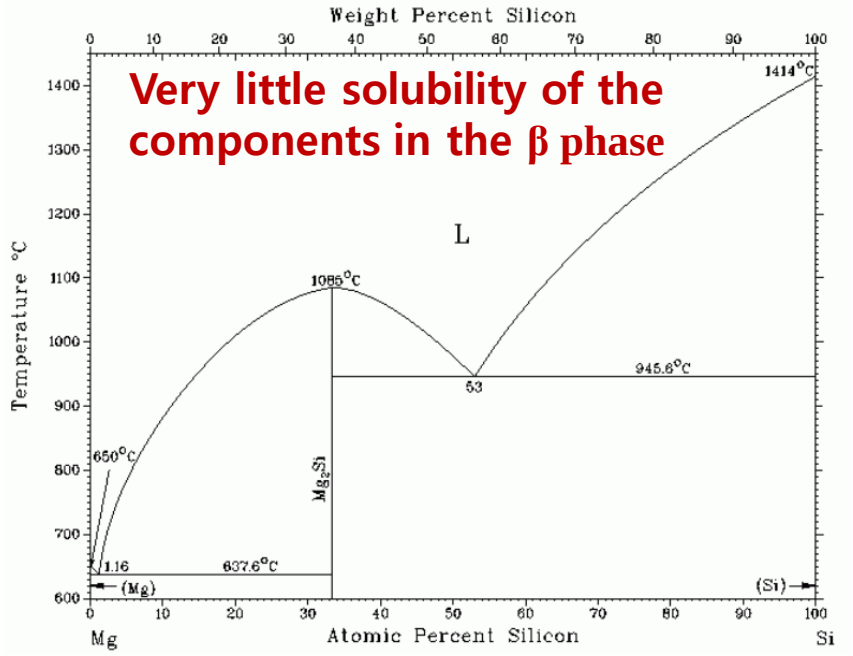

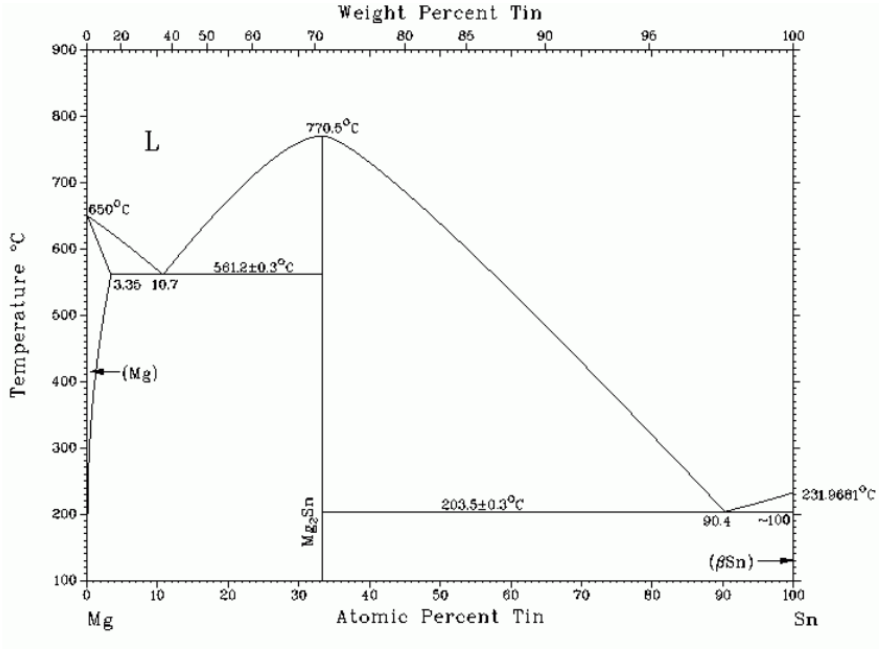

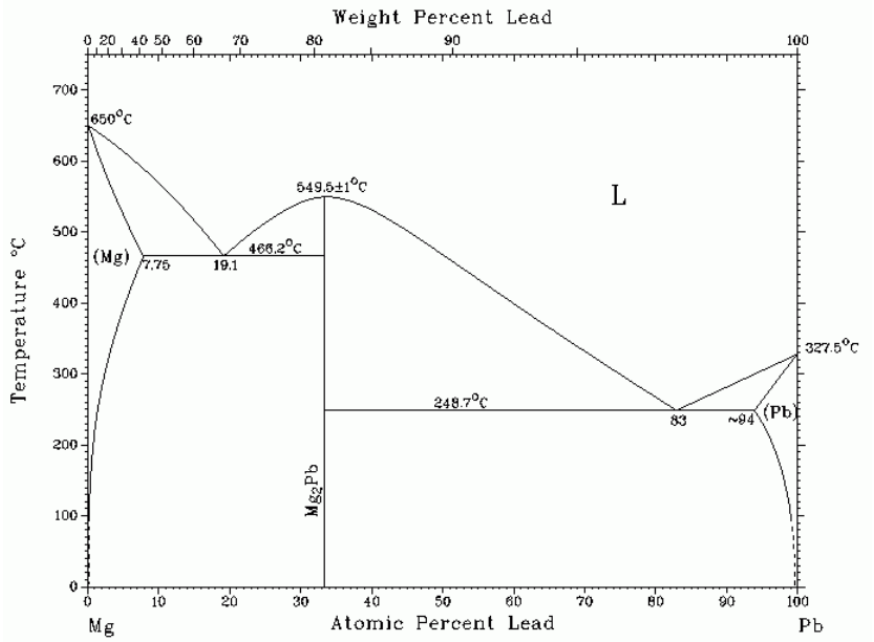

4.4. Congruent transformations

c. Relationship between phase diagrams containing congruent and incongruent intermediate phases

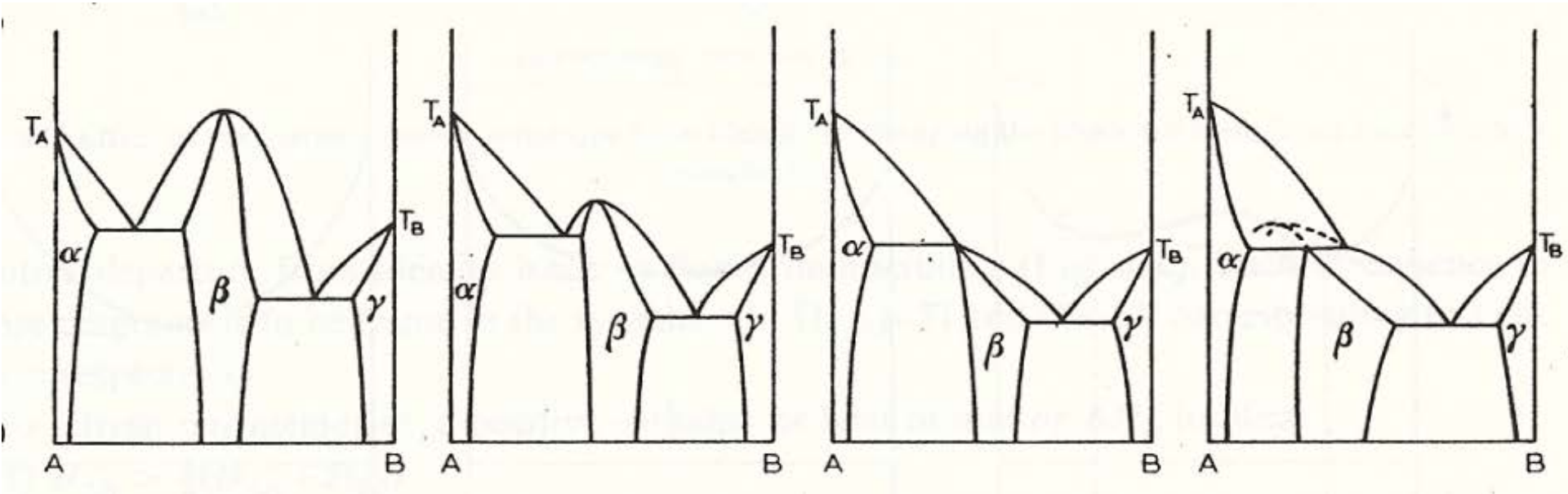

MIDTERM: 23rd April (Friday) 2 PM – 5 PM,

33 Dong 330 & 331 Ho

※ I will post your designated seat in front of the classroom on the day of the test.

Scopes: Text ~ page 117/ Teaching note ~10

and Homeworks